



The importance of water flow for culture of *Dysidea avara* sponges





Promotoren:

prof. dr. ir. R. H. Wijffels,
hoogleraar in de Bioprocestechnologie, Wageningen Universiteit.
prof. dr. ir. J. L. van Leeuwen,
hoogleraar in de Experimentele Zoölogie, Wageningen Universiteit.

Overige leden promotiecommissie:

prof. dr. J. A. J. Verreth, Wageningen Universiteit.
prof. dr. M. J. Uriz, Centro de Estudios Avanzados de Blanes, Spanje.
prof. dr. S. A. Pomponi, Harbor Branch Oceanographic Institution, Verenigde Staten.
prof. dr. P. Aerts, Universiteit Antwerpen, België.

Dit onderzoek is uitgevoerd binnen de onderzoekschool VLAG.





The importance of water flow for culture of *Dysidea avara* sponges

Dominick Mendola

Proefschrift

ter verkrijging van de graad van doctor

op gezag van de rector magnificus

van Wageningen Universiteit,

prof. dr. M. J. Kropff

in het openbaar te verdedigen

op woensdag 9 april 2008

des namiddags te vier uur in de Aula





Dominick Mendola

The importance of water flow for culture of *Dysidea avara* sponges

Ph.D. Thesis Wageningen University, The Netherlands, 2008 – with Dutch and English
Summaries

ISBN: 978-90-8504-908-1





Contents

Chapter 1	Introduction	1
Chapter 2	Aquaculture of three phyla of marine invertebrates to yield Bioactive metabolites: process development and economics	9
Chapter 3	Environmental flow regimes for <i>Dysidea avara</i> sponges . .	39
Chapter 4	Morphology induced flow patterns by <i>Dysidea avara</i> sponges in a flow tank.	55
Chapter 5	Oscular outflow rates for <i>Dysidea avara</i> sponges	75
Chapter 6	Re-plumbing in a Mediterranean sponge	95
Chapter 7	General Discussion and Conclusions	107
	Summary	119
	Samenvatting	123
	Acknowledgements	128
	Training and Supervision Activities	129
	Biography	130





Chapter 1

Introduction to the Thesis





INTRODUCTION TO THE THESIS

The title of this thesis, “*The importance of water flow for the culture of Dysidea avara sponges*” begs two key questions:

- why does man want to culture this sponge, and
- why is water flow important in the culture process?

Dysidea avara is a violet-colored encrusting sponge native to the Mediterranean Sea. It is the natural source of terpenoid compounds avarol and avarone which have shown activity against some of man’s most pernicious ailments, including inflammatory diseases, viral and bacterial infections, and some tumoral cancers. Demand for these compounds as natural products is projected to increase. Aquaculture has been proposed to replace natural collections as a more sustainable method of supply of sponge biomass for natural product extraction. Sponge science fulfills the role of informing sponge aquaculturists on scientific findings related to the culture requisites of these valuable sponges.

For any aquaculture process, *in situ* (in the sea) or *ex situ* (in tanks), water flow past the cultured organisms is of paramount importance for sustaining organism health and vitality. Too much flow and the organisms could be physically harmed, fail to catch their food, or stop growing (and energy resources would be wasted for moving water too quickly through the system). Too little flow and the organisms could be harmed for lack of sufficient exchange of metabolic gases, deteriorating water quality, or access to food. In the case of *ex situ* culture in controlled environment tank systems, too little flow could also harm the metabolic balance of the microorganisms in the bio-filters.

Within the aims of a funded EU CRAFT project, Wageningen University was charged with the investigation of water flow requirements for sponge culture — including *Dysidea avara*. This thesis reports on the findings of those sponge-flow interactions.

Aim and goal of this research

The principal aim of this research was to understand the optimal water flow requirements for the marine sponge *Dysidea avara*, so that flow parameters could be set for *ex situ* culture in tanks, or *in situ* culture in the sea. The ultimate goal was to help insure the success of large-scale aquaculture of the species for obtaining biomass for extraction of its valuable terpenoid natural product avarol.

Research overview

The first phase of the research was directed towards understanding natural flow regimes surrounding individual *Dysidea avara* sponges that were members of a mixed sponge fauna found within a rocky cove on the N. E. coast of Spain. Using SCUBA and employing a 3-D Doppler acoustic velocimeter we recorded bulk current flow in the open water of the cove, and also close to aggregations of sponges on rocky ledges and inside small caves. A heated



thermistor flow sensor was used to record fine-scale flow speed in very close proximity to individual sponges, and outflow velocity from their oscula. Flow velocities and flow regimes were characterized over a year-long period from September, 2005 through October, 2006.

In the laboratory, a special-built flow tank was employed together with laser-illuminated particle tracking velocimetry and high-speed video photography, to visualize and record flow passing over the complex surface morphology of specimens. Oscular outflow velocity and outflow rate were calculated over a range of background flow velocities modelled after nature. The flow tank was also taken to Spain, to compare oscular outflow of freshly-collected wild specimens to that of the tank-reared specimens. From outflow velocities and oscula dimensions, volume outflows were calculated. For specimens that showed over-sized ostia inflow rates were also calculated.

Three-D computational fluid dynamic modeling (CFD) was begun to aid in better understanding fine scale flow around the mm-sized cone-shaped conules which characteristically cover the surface of the sponge. Some preliminary results were obtained which will form the base for future CFD work that will continue past the completion of the thesis project.

Before introducing the Thesis Chapters, I will first give a brief overview of the biology of sponges for the lay reader, and a brief history of flow research in marine biology.

What are sponges...?

Sponges are sessile (*i.e.*, living attached to a substratum) marine and freshwater invertebrate animals with only a cell-level body plan (*e.g.*, they possess no true tissues). An outer epithelial layer of cells, the pinacoderm is separated from the internal cell layer called the choanoderm by the mesohyle, a matrix of amoeboid cells, skeletal elements, and sometimes dispersed or filamentous collagen (called spongin, as in *Dysidea avara*).

The entire sponge body comprises little more than an open hydraulic network of branching inhalant and exhalant canals with flagella-powered cellular pumps in-between. In demosponges (95% of all living species, including *D. avara*) ambient water enters the inhalant canals through a myriad of 5-50 μm -sized inlet ostia spread across the dermal surfaces, and flows through the inhalant canals to the food-filtering choanocytes. It exits via the exhalant canals which lead to one or more mm or larger-size exit holes called oscula or oscules.

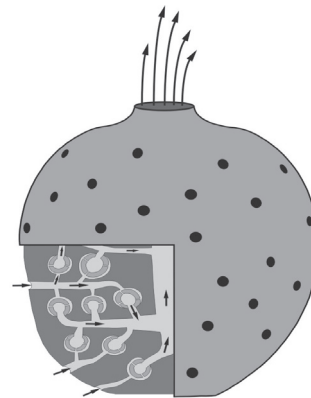


Figure 1. A schematic representation a single osculum sponge with cut-away showing (in order of flow through the aquiferous system): the ostia, inhalant canals, choanocyte chambers, exhalant canals, and finally the osculum. (Drawing not to scale; after original drawing by R. Osinga.)





The system is efficiently designed to pump large amounts of ambient water for filtering-out micrometer-sized food particles such as bacteria, micro-algae and small organic aggregates. The specialized flagellated pumping cells (choanocytes) are arranged 50-200 each into 25-65 μm -dia. spherical or cylindrically-shaped mini-pumping chambers (Bergquist; 1978, Simpson, 1984). It has been estimated that a cubic millimeter of sponge cell mass contains as many as 10 million choanocyte chambers, and with all of its flagella beating simultaneous and continuously, a one kg sponge could pump as much as 23,000 liters of water in a single day (calculated from data of Reiswig, 1974).

Sponges are among the earliest evolved multi-cellular organisms, the Metazoans; with fossil ancestors dating from the pre-cambrian period, some 580 million years in the past (Chia-Wei et al. 1998). Science has so far described approximately 15,000 sponge species, placing all known and fossil species into one of three taxonomic classes within the phylum Porifera. Each taxonomic class is differentiated mainly on the bases of the chemical and fine-scale structure of its inorganic skeletal elements. The Demospongiae class contains 95% of all living sponge species. Members generally have siliceous spicules dispersed in an organic matrix of collagen (some do not, including *Dysidea avara*). It is the dried skeleton of members of the Demospongiae which is the familiar “sponge” for human uses. The Hexactinellida contains the exclusively marine and mostly deep-sea glass sponge with hexactine-formed siliceous skeletal elements. The third class, Calcarea, are also exclusively marine and generally considered the most primitive of living sponges, with all members making a calcareous skeleton from dissolved calcium carbonate.

Most sponges also contain aggregations of various autotrophic and/or heterotrophic sponge-specific symbiotic bacteria which live commensally within the cells of the mesohyl. The symbionts provide nutritional components biosynthesized from dissolved nutrients, and sometimes allelochemicals, exploited by the sponge for defence against would-be predators or competitors vying for precious colonization space.

Sponges reproduce both asexually by budding and fragmentation or gemmules, and/or by sexual means. Sexual reproduction is either as hermaphrodites (where eggs and sperm are released from the same individual and united either internally or externally), or gonochoric (where eggs and sperm are released from different individuals to unite externally in the water column). The fertilized larvae are carried by the ocean currents for periods ranging from a few hours to several days, dependent upon the larvae finding suitable substratum on which to settle and attach. then they metamorphose to begin development of the next sponge colony.

Water flow in marine biological research

Water flow and its importance to the biology and ecology of sponges was first discussed as an important parameter for systematic study by German researcher Ernst Haeckel, in an 1872 manuscript published on his work with freshwater sponges. In 1914, G. H. Parker worked



with sponges from Bermuda and the S. Carolina, USA, and measured oscular outflows using a glass tube placed into sponge oscula. Then in 1923, British naturalist G. P. Bidder published a paper entitled “The Relationship of the form of a Sponge to its Currents.” Bidder’s paper and its fundamentally insightful observations on the relationship between the shape and form of different sponges — and their predictable oscular outflow velocities and volumes — has been cited by literally every modern study of flow, hydrodynamics, feeding and/or clearance rates of sponges.

In the late 1960’s and early 1970s came (literally) a flood of very fundamental field work on flow and its importance to the lives of sponges by Henry M. Reiswig and Steven Vogel. Reiswig’s work was amazingly thorough and expertly detailed, and Vogel’s landmark book “Life in Moving Fluids” has become “The Bible” for any biologist working on fluid flow with terrestrial, aerial and/or aquatic or marine organisms.

This thesis work was supported on the foundational papers put into the literature by these early sponge flow researchers, together with important works of more contemporary bio-fluid-dynamicists such as: H. U. Riisgård, A. R. M. Nowell, P. A. Jumars, and M. K. Denny, among others. Citations to the works by the authors highlighted in this section can be found in the “References Cited” listings at the end of the thesis chapters.

Thesis chapter titles and key questions asked

This thesis is presented in seven chapters, including: this Introduction, five research chapters, and a General Discussion and Conclusions chapter. A summary is provided in both English and Dutch following the last chapter.

Chapter 2

In Chapter 2, “Aquaculture of three phyla of marine invertebrates to yield bioactive metabolites: process developments and economics” presents an overview of processes and economics for in-the-sea aquaculture of three species of marine invertebrates desired for their natural product chemical constituents. The key questions addressed in this review chapter are related to scale-up issues for expanding successful feasibility projects to commercial-scale “*Aquapharms*.” We asked: (1) what are the key cost factors for commercial production for each of the aquacultured products, and, (2) are production costs adequately reimbursed by projected market prices?

Chapter 3

In Chapter 3, “Environmental flow regimes for *Dysidea avara* sponges”, we undertook field research in the natural environment of *Dysidea avara* in the Western Mediterranean Sea. Over a period of 1-year, we conducted underwater experiments at a coastal site in N. E. Spain, using two sophisticated flow-measuring instruments, cameras and flow visualization methods to characterize environmental water flow regimes at three depth sites. The key questions asked



were: (1) what are the characteristics of the natural flow regimes surrounding *D. avara* sponges in nature, and (2) how does the morphology of the sponge change in differing flow regimes?

Chapter 4

For Chapter 4, “Morphology-induced flow patterns by *Dysidea avara* sponges in a flow tank” we took what was learned about flow regimes in nature into the laboratory, and built a flow tank and adapted particle tracking velocimetry as tools to study flow in very close proximity to live specimens. The key questions were: (1) how do

body forms and cm-scale morphological features influence water flow passing around and over individual sponges, and (2) do body forms and cm-scale features aid the sponge in trapping food particles?

Chapter 5

In Chapter 5 “Oscular outflow rates for *Dysidea avara* sponges” we continued the flow tank investigations to quantify oscular outflow velocities and volumes from sponges. The salient questions here had to do with continuity of flow into and out of individuals. We asked: (1) how does oscular outflow vary in relation to ambient (background) flow velocity, and (2) do we see any evidence of induction of flow through the sponge due to background flow?

Chapter 6

In Chapter 6 “Re-plumbing in a Mediterranean sponge” we described the functioning of what we termed “over-sized ostia”, which we observed being formed on the dermal membranes of laboratory-held *Dysidea avara* specimens (and later corroborated for freshly-collected and in situ specimens in Spain). In this research we asked the following questions: (1) what are the inflow velocities and volumes for over-sized inlet structures in relation to oscular outflow velocities and volumes? (2) What is the biological significance of the discovery of over-sized inlets? (3) Are over-sized inlet structures a “peculiarity” of only tank-reared *D. avara* sponges?

Chapter 7, General Discussion and Conclusions

As a compliment to the flow-tank morphology studies undertaken in Chapter 4, we began construction of 3-D computational flow dynamic (CFD) models to help us understand the

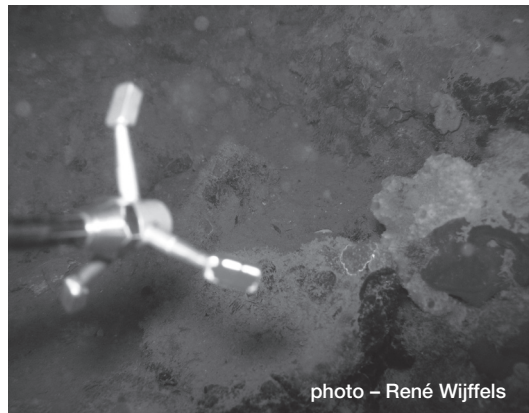


Figure 2. Photo of a *Dysidea avara* sponge ecruled on a rock next to a *Crambe crambe* sponge at study site in N. E. Spain. The instrument is the sender-receiver end of a 3D Doppler velocimeter used during the field portion of this thesis research project.





fluid mechanics within millimeters of a modeled sponge surface under varying background flows. We asked the following questions of the CFD methodology: (1) how do the mm-scale surface conules effect flow over the modeled sponge, and (2) what effect do the conules have on influx rates? Some preliminary CFD results were obtained during the thesis project, however given the (computer) time-intensive nature of applying the method systematically to the questions asked, the CFD modeling work will continue past the completion of this thesis. The reader is directed to the General Discussion and Conclusions in Chapter 7 for insights based on the preliminary CFD results and possible directions for future simulation studies.

REFERENCES CITED

- Bergquist, P. R. 1978. Sponges. Hutchinson & Co. Ltd., London.
- Chia-Wei, L., J-Y. Chen, and T-E. Hua. 1998. Precambrian sponges with cellular structures. *Science*. **279**: 879-881.
- Reiswig, H. M. 1974. Water transport, respiration and energetics of three tropical marine sponges. *J. exp. Mar. Biol. Ecol.* **14**: 231-249.
- Simpson, T. L. 1984. The Cell Biology of Sponges. Springer-Verlag, New York.



Chapter 2

Aquaculture of three phyla of marine invertebrates to yield bioactive metabolites: Process developments and economics

Dominick Mendola^{1, 2*}

¹ CalBioMarine Technologies, Inc., 1001 Capri Road, Encinitas, CA 92024 USA. ² Current address: Bioprocess Engineering Group, Wageningen University, P.O. Box 8129, 6700 EV, Wageningen, The Netherlands

* e-mail: dominick.mendola@wur.nl

Abstract: Large-scale, renewable supplies of chemical constituents derived from marine invertebrates have limited development of potential new natural product-derived drugs. This paper describes the development of two in-sea aquaculture systems designed and engineered for production of large quantities of biomass for two species of marine invertebrates desired for their natural product chemical constituents. The two invertebrates and their products were: (1) the cosmopolitan, arborescent ectoproct (bryozoan) *Bugula neritina* (Phylum Ectoprocta) for its anticancer chemical constituent bryostatin 1; and (2) *Ecteinascidia turbinate* (Phylum Chordata; Sub-Phylum Tunicata) the source of anticancer ecteinascidin 743. For the third invertebrate Phylum Porifera, and its representative sponge *Acanthella cavernosa* (source of the anti-parasitic and anti-infective kalihinols) in-sea systems were not developed in favor of controlled environment tank culture systems. For the bryozoan and tunicate, projected economics for commercial-scale in-sea production proved cost effective. This was in contrast to the controlled environment sponge culture tank system which did not prove to be economical due to inherent slow growth and low natural product yields in culture. A non-destructive method for “milking” natural product chemicals from sponges was tested and is described.

Key words: *natural products, marine invertebrates, aquaculture methods, economics*



INTRODUCTION

Marine invertebrate natural product discoveries

The first marine invertebrate-derived natural product compounds, spongothymidine and spongouridine, were isolated from the Caribbean sponge *Tethya crypta* in the early-mid 1950s (Bergmann and Feeney, 1950, 1951; Bergmann and Burke, 1955). Since those first discoveries greater than 12,000 novel chemical compounds having been isolated from marine sources (all phyla) and more than 300 patents involving marine compounds having been issued (Faulkner, 2001, Kerr and Kerr, 1999).

In 1969, Cytosar (Ara-C) a potent antitumor analog of one of the *Tethya crypta* compounds was approved in the USA as the first marine derived drug. It was followed in 1981 by approval in the USA of two more *Tethya crypta* compound analogs, Acyclovir and Vidarabine (Ara-A), both antiviral agents. Then in Dec. 2004 Prialt® (zinc onotide) an analog of a naturally-occurring peptide from the marine mollusk *Conus magus* won market approval in the USA and in Europe for treatment of intractable neuropathic pain. And most recently (Dec. 2007), Yondelis® (ecteinascidin 743) an anticancer agent isolated from the colonial ascidian *Ecteinascidia turbinata* (Caribbean and Mediterranean) was awarded marketing approvals in the USA and in Europe (David J. Newman, NCI/USA pers. comm.). Additionally, one marine anti-inflammatory compound, pseudopterosin C from the Caribbean soft coral *Pseudoptero-gorgia elisabethae*, has been marketed since the early 1990s as an additive for a line of high-end cosmetics (Look *et al.* 1986). Many more marine-derived compounds have since entered or are now entering human clinical trials for a variety of human disease indications. So finally after more than 50 years of discovery and development it can be said the “tide is turning” for marine drugs, with a future that promises to be even brighter (Anonymous, 2001, Fusitani, 2000, Jaspars, 1999, Newman *et al.* 2000, Newman and Cragg, 2004, Newman and Cragg, 2007). [See addendum following this chapter for an update on the clinical and/or commercial progress for bryostatin 1, ecteinascidin 743 and zinc onotide.]

Low chemical yields: Impediments to progress

Given that marine natural product compounds are for the most part secondary metabolites, natural product yields are commonly in the 10^{-4} to 10^{-6} % range on a wet-weight basis, and sometimes even lower titers are found. At these low chemical titres, accurate and reliable detection methods can themselves become an impediment to progress. Also, with such low yields it can take literally kilo-tonnes of freshly-harvested biomass material (laboriously handled then extracted and purified in relatively small batches) to produce sufficient quantities of compound to support a successful pre-clinical and clinical development program. In addition to inherent low natural product yields, many other technical and logistical problems have challenged marine natural product researchers. In a yr-2000 review, the late Scripps



Institution of Oceanography marine chemistry pioneer D. J. Faulkner presented a capsulated history of some of the problems which beset the development of a number of major discoveries in marine natural products. Dr. Faulkner also offered his unique perspective on the probable causes and reasons why many of the major discoveries and programs ended short of approval to become new commercial drugs (Faulkner, 2000).

Aside from the cases where a facile and economical chemical synthesis can be developed, many invertebrate derived compounds will require alternative supply technologies if they are to advance in development past their initial discovery and chemical elucidations. For invertebrate-derived compounds, the environmental consequences of large-scale natural collections of these often rare and sparsely distributed organisms stand out as a major impediment to new drug development. Therefore, more environmentally-benign technologies must be developed for guaranteeing a reliable, renewable and cost-effective source of supply (Rouhi, 1995).

Marine pharmaceutical aquaculture: An alternative supply technology

In the mid 1980's, as commercial aquaculture for marine and freshwater food species was advancing in practice worldwide, a natural question was asked: can commercial aquaculture methods for food species, such as fish, invertebrates, and macrophytes be applied for the culture of non-food species desired for their natural product chemical constituents? Our extensive experience with a variety of food aquaculture species led us to conclude that indeed it might be possible to "grow drugs from the sea."

As with any food specie candidate, criteria for initiating aquaculture trials with a new invertebrate desired for its natural product chemical constituent begins with access to the knowledge base of published scientific reports on its biology, natural history, reproductive biology and life cycles, food requirements and environmental requisites. Also important is knowledge of its inherent growth rate and productivity in the ocean, and information on its distribution and abundance. In any case, feasibility studies must be performed to test whether or not the organism can be considered for scaled-up growth trials leading eventually to development of a commercially viable aquacultural production system.

The ability to observe the organism in its natural habitat in the ocean (*i.e.* using SCUBA-assisted diving, submersibles, or underwater video surveillance) is of paramount importance, since only by observing the organism in its natural setting can the aquaculturist gain clues to its behavior, which will be vital for designing an aquaculture methodology optimized for the growth requisites of that particular organism. For sessile invertebrates such as sponges, bryozoans, and ascidians one might not at first think much could be learned from their "behavior" in the field, however this is not the case. Careful and close observations of any organism in its natural surroundings can yield valuable clues for the eventual design and operation of an aquaculture methodology and apparatus to best serve the needs of the organism for survival, growth and overall productivity.



The challenges can be monumental and progress can at times be excruciatingly slow, but with persistence and continual “tinkering” with the culture system and protocols, success can come for even the most temperamental of organisms. For the most difficult species it may not be possible to bring them into culture, or it could take literally years of concerted effort for achieve even a modest level of successes. In these difficult cases a cost/benefit analysis completed as part of the feasibility study may prove the effort to be unwarranted. However, once one representative of a class of organisms has been successfully brought into culture, the methods and protocols used can, in most cases, be applied to other members of the same class of organisms, speeding the progress of the second effort towards fruition.

Given the high level of risk and uncertainty in this new area of endeavor, aquaculture is rightly seen as an almost last-resort technology for underpinning the continued development of new marine natural product discoveries. In some cases aquaculture may be the only alternative currently available, notwithstanding the eventual development of more desirable production options such as: chemical synthesis, fermentation of the source bacterium (*e.g.* symbiont), or transfer of the requisite genetic encoding DNA taken from the source organism into a more salubrious transgenic microorganism for fermentation of the desire natural product.

This paper presents results from the development of tank culture and in-sea aquaculture methods for representatives of three phyla of marine invertebrates [Ectoprocta, Chordata, (Sub-Phylum Tunicata) and Porifera] whose natural product chemical constituents are [or were at one time] desired as potential new human drug candidates. Results of grow-out trials for biomass and drug production are presented in three case studies, as are summary costs for scale-up to commercial-sized “Aquapharms”, and calculated biomass and drug-equivalent production costs.

CASE I: ECTOPROCTA – *BUGULA NERITINA*

Materials and Methods

During the years 1990-1994, laboratory facilities for larval settlement experiments and small-scale growth trials were maintained on the shore of Aqua Hedionda lagoon located 55-km north of San Diego, CA. From 1994 to the present, a larval settling facility has been maintained on the ocean pier of the UCSD Scripps Institution of Oceanography (SIO) located in La Jolla, CA. USA. Wild stock of *B. n.* to support the aquaculture projects was collected from various near-shore rock reefs in Southern California, USA. Aquaculture facilities for tank culture experiments were located on the shore of Agua Hedionda lagoon in San Diego County. Facilities included a small indoor laboratory for analytical work, and an outdoor greenhouse which housed large and small tank arrays employed for growth trials [Fig. 1]. At SIO, all work was done in collaboration with Professor Margo G. Haygood and her laboratory





The culture strategy conceived for *Bugula neritina* (“*B. n.*”) was based upon settlement of large numbers of larvae from wild-collected “broodstock” onto artificial substrata (*e.g.* perforated plastic plates), followed by grow out to maturity in tanks on-shore or attached to an engineered structure submerged in the ocean [Fig. 2]. The culture protocol included a pre-growth period of from 3-6 weeks conducted in on-shore “raceway” tanks followed by in-the-sea grow out on the structure lasting from 4-22 months depending on the goals of the individual trials. To obtain a harvest at the end of a growth trial, culture panels (= plates) were removed from the structure by the SIO divers and returned to the deck of the pier for harvesting of the biomass which had grown onto the surfaces of the plates.

CHAPTER 2 | 13

were used in conjunction with small tanks for the initial growth studies, and larger plates were used in larger tanks for scaled-up growth trials. The larger plates were also used on the undersea structure for the in-sea growth trials. The 2.5-mm diameter perforations allowed passage of water currents through the plates, and by design, provided mini-refuges within the perforations for the newly settled larvae (100 microns diameter). Two 10-cm diameter holes were cut into each of the 0.6-sq. m. culture plates to relieve any pressure that might be imposed on the plates from the force of the ocean current once the plates were covered with *B.*

n. colonies. These “weep holes” helped to assure that the plates would not be torn loose from the undersea structure or fractured during passage of storms.

The largest of the on-shore pre-growout tanks held 4,500 L of 0.2 micron-filtered natural seawater, and could accommodate 20 large culture plates [Fig. 3]. Within the 4,500 L tanks a “racetrack”-type water circulation pattern was set into motion around a centrally-placed divider panel by directing the incoming fresh seawater pipe in the desired direction of flow. The influent flow rate was maintained at 8-10 L/min. for 16-18 hrs/day, 7-days per week. Water exited the tank via a single 6-cm diameter screened overflow pipe. The influent stream was stopped for 6-8 hrs/day for feeding of the *B. n.* colonies. Top-to-bottom water circulation within the tanks was maintained using a number of perforated air bars that were placed on the bottom of the tank parallel to the long dimension [Fig. 4].

An array of 85 L clear plastic “Sun-Tube” algal culture tanks was set-up within the greenhouse for culture of a variety of micro algal strains to provide live food for the cultured *B. n.* colonies. Microencapsulated and other micro-particulate “artificial” food components were mixed together with the live algal cells to make up the standard diet which was used for all in-tank growth trials. Before feeding, the algal cells were “washed” from the F/2 media used for their culture, by employing a tangential flow filtration apparatus. The tanks were fed

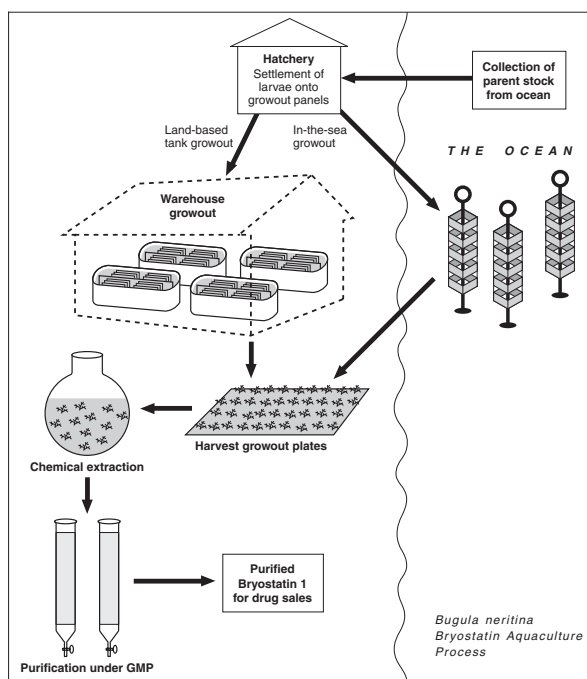


Figure 2. Process flow schematic drawing for the in-sea aquaculture process for *B. neritina* and bryostatin 1 production.



Figure 3. One of two 4,500 L fiberglass prototype raceway tanks for aquaculture of *B. neritina*, located within a nearshore greenhouse culture facility, Carlsbad, California. Technician is feeding one of various cultured micro-algal species grown in the “Sun-Tubes” at the left of the raceway.

on a volume basis at the rate of 1,000- 4,000 algal cells/ml of tank volume per feeding. Usually only one feeding per day was accomplished, however for some trials the cell concentration was doubled (*e.g.* from 2,000-8,000 cells/ml) to test the effect of an overabundance of feed on productivity. Zooid gut content analyses using light microscopy were performed to assess the variety of food-types consumed, and whether or not they were digested during the relatively short throughput time (*i.e.* 20 minutes).

In-sea grow out trials were conducted using a steel-framed buoyant structure measuring 1 meter square by 7 meters in length [Fig. 5]. The structure could accommodate 20 of the 0.6 sq. m. culture plates, leaving each alternate bay along each side of the structure open to provide for water circulation. The plates were attached to the undersea structure by divers. The mooring site was located 1,000 m offshore of the SIO pier in approximately 40 m of water. The structure was buoyed at the 16-m depth contour from a 1,800 kg. anchor placed on the ocean floor. A 90 cm. diameter hollow steel float provided floatation. A 2 cm. diameter braided polypropylene line with heavy galvanized steel shackles and large galvanized marine-rated

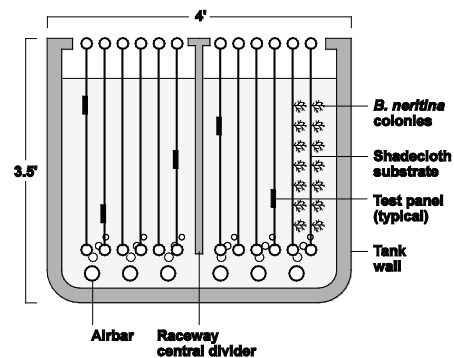


Figure 4. Schematic drawing of a cross section of one of the 4,500 L fiberglass raceway tanks for aquaculture of *B. neritina*.



swivels connected the anchor to the structure and the structure to the float. The structure incorporated fixed-pitch propellers at either end that allowed for rotation of the structure in the ambient ocean current.

Tank and in-sea grow out trials were conducted for varying periods of time over 6 years. In general, grow out trials in the 4,500 L tanks lasted from 20-32 weeks. Two completed in-sea growth trials lasted 4.5 mos. and 22 months respectively. Other sea trials were begun but aborted for reasons mostly having to do with poor growth resultant from warm El Niño currents (see results). At the termination of a growth trial, the culture plates with the mature cultured colonies attached were removed from the tanks or from the undersea structure and carried into the laboratory or onto the pier for harvest. The cultured colonies were removed from the culture plates with the aid of wood scrapers, cleaned of fouling organisms and debris, and placed on perforated plates to drain before weighing and freezing. Weights and allied culture and environmental data were recorded in laboratory notebooks and then transferred to a computer database.

Results and Discussion

It was a fortunate consequence of fate that bryostatin 1 would be discovered from the most studied of all marine invertebrates, *Bugula neritina*. The first natural history description was published in 1758 by the British Museum of Natural History in the treatise “*Systema Naturae*”



Figure 5. Launching of the 7-m long prototype in-sea aquaculture structure from the pier at UCSD Scripps Institution of Oceanography, La Jolla, California. Picture shows new, grey perforated pvc-plastic culture panels, large floatation sphere, and fixed-pitch propellers located within both ends of the structure.



written by the father of taxonomy, Caroli Linnaei. In the intervening 250 years, hundreds of scientific papers on every aspect of the biology, natural history, reproduction and larval biology of the organism have been published. From this great base of scientific information much was learned to establish a strategy and protocols for aquaculture of the organism.

Another fortunate aspect is that *B. n.* is commonly found (if not sparsely distributed) from sites in northern Baja California, upwards into California (USA), ranging from San Diego to San Francisco. For the aquaculture work, field populations for *in situ* study and collection of starter-stock for the growth trials were available throughout most months of the years of the project. Populations are found growing from holdfasts attached to rock reefs and jetties in relatively shallow water (8-15 m), and on the undersides of boats, docks and pier pilings. Using SCUBA and small craft, collection of sufficient live material for conducting the trials was a relatively easy task.

From work done by our collaborators at SIO it is now known that the species consists of two genetically distinct strains or chemotypes, which are separated in the environment along temperature and depth contours [Davidson and Haygood, 1999]. Both chemotypes produce bryostatins, however only the deep, cold-adapted strain produces bryostatin 1. “Bryo-1” is the only chemical congener of the bryostatin family of 19 different molecules which is being tested in human clinical trials. For learning purposes ahead of the actual controlled growth trials, it was found that either the deep or the shallow populations could be used as starter stock for provision of larvae. However, in order to determine the magnitude of bryostatin 1 natural product yields in the controlled growth trials, only deep-type broodstock was used.

On average 1 kg of sexually-mature deep-adapted *Bugula neritina* colonies produced in the range of 1,000-8,000 larvae for settlement. In comparison, the shallow populations routinely produced in the range of 100,000-300,000 larvae for the same quantity of biomass, and over a shorter period of time as well. For the aquaculturist it was a pity that the shallow type does not produce bryostatin 1, which would have obviated the need for such large quantities of broodstock to start the aquaculture process. The shallow-type does produce bryostatins, but a suite of chemical congeners known as “minor” bryostatins, none of which have as yet been tested in human clinical trials.

In normal years, wild populations of *B. n.* (both shallow and deep-types) produce copious quantities of larvae in two peaks of abundance, the first during the spring and the second during the fall months. Exceptions to this rule are during the years when unseasonably warm El Niño coastal currents reach northward into S. California from S. America. In El Niño years the normal bi-modal abundance of gravid *B. n.* colonies is severely disrupted, since the colonies are fairly intolerant to ambient water temperatures above about 21°C., and they can die off *en masse*.



***Bugula neritina* growth trials: Tanks**

During the years 1992 through 1994, eight (8) separate grow-out trials were completed using the pair of 4,500 L raceway tanks installed in the Agua Hedionda greenhouse facility. Grow-out trial periods ranged from 3 to 22 weeks duration. The shorter trials (3-8 weeks) were all aborted for various reasons and none yielded greater than 25 grams biomass per square meter of substrate surface area. The biomass productivity for the longer trials (21.5 & 22 weeks, $n = 10$ samples) averaged only 154 grams wet biomass per square meter of culture substratum harvested (range: 65.4 - 615.4 g/m²). In severe contrast to these meager results, the biomass productivity for a 10-week growth trial using the small 10 L aquaria averaged 3,728 grams wet biomass per square meter of culture substratum harvested (range: 2,752 - 4,810 g/m², $n = 6$). For the small tank growth trials run over a longer period of time (29.5 weeks, $n=3$) the average biomass productivity was similarly high at 2,090 grams wet biomass per meter of culture substratum harvested (range: 831 - 4,237 g/m²).

It is obvious from these widely disparate results that some form of tank effect was most likely in-play, allowing the *B. n.* colonies being cultured in the smaller tanks to grow much, much better than those in the larger tanks. Although the exact causal factors for this tank-effect were never discovered nor enumerated, we theorized (based partly on results obtained from an allied flow rate versus feeding/growth study; NSF- III-9361806, A. B. Leonard, P. I.) that the micro-flow regimes in close proximity to the cultured colonies in the small 10 L tanks were more conducive for capture of food particles and successful feeding and growth of the cultured *Bugula* colonies, than were the micro-flow regimes in close proximity to the cultured colonies in the larger 4,500 L raceway tanks. The results of the NSF study showed that successful feeding and the best colony growth occurred within a relatively narrow range of flow speeds termed the “medium flow regime” (30.5–36.3 mm/s). In the experiments, flow speeds were very accurately measured using a very small heated thermistor flow sensor placed into the micro-environment surrounding the ringlet of tentacles of the feeding zooids. The zooids had settled onto small perforated PVC test panels which were placed into position within the working sections of one of three precisely-engineered and fabricated 20 L acrylic plastic flow chambers.

***Bryostatin* content in tank-cultured biomass**

Bryostatin 1 content of tank-harvested biomass for the twelve (12) grow-out trials completed (4 small-tank trials and 8 large-tank trials) ranged from not detectable (n.d.) to 14.2 µg per gram dry weight of harvested biomass (ave. 7.5 µg per gram dry weight). This average and range was deemed to be acceptable for these first tank culture experiments, when viewed in comparison to bryostatin 1 yields from wild-collected samples (ave. 16.9 µg per gram dry weight).

However, due to unresolved tank-effect factors which limited production in the 4,500 L



tanks in this study, a commercial-scale build-out based on even larger-sized tanks was projected to not be economical. Extrapolating the small-tank culture results (which showed very good per unit-area yields) to a commercial-scale build-out was also deemed to be uneconomical, due to the astronomically large number of small tanks that would be required to meet production goals, antogether with the large labor component which would be required to tend and clean each of the small tank units on a year-around basis.

Projected economics: Bugula neritina tank culture system

Although the tank culture results were somewhat disappointing, economics for two sizes of *Aquapharm* modules based on use of large closed-system tanks were projected to be 25,000 kg/yr and 50,000 kg/yr biomass wet-weight, respectively. At the nominal bryostatin 1 titers obtained in the prototype tank culture trials (8.1 micrograms per gram dry weight, dry weight = 20% of wet weight) the two modules would be capable of producing 41 grams and 81 grams of bryostatin 1 per year, respectively. Construction costs for the 50,000 kg/yr module would total \$7.5 million U.S., and \$4.2 million for the 25,000 kg/yr module. The largest single cost item (accounting for approximately half of the total construction costs in each case) was for the biomass drug extraction and purification sub-system, which would have to be built to GMP (Good Manufacturing Practice) standards - accounting for the extreme expense. The remainder of capital costs were for the large aquaculture tanks (66 and 33 each, respectively) and for the supporting aquaculture sub-systems. For these cost projections, the two “tank-pharms” were housed under well-engineered greenhouse-type buildings, which would be much more cost effective in California, than tilt-up cement wall warehouse-type structures (which would need to incorporate built-in skylights and overhead lighting for culture of the micro-algal foodstuffs required for the cultured *Bugula* colonies).

Start-up costs for 2-years (during which time there would be no bryostatin output from the farms) would amount to \$3.8 million for the larger, and \$2.8 million for the smaller farm modules. Steady-state operations costs would amount to \$2.4 million per year for the larger module and \$1.5 million per year for the smaller module. For generating these cost models, capital costs were amortized to zero during a 7-year projected life of the farm, and no costs for use of capital were included in the calculation.

The bottom line biomass production costs for the two modules shows a slight economy of scale for the larger module (\$48/kg vs. \$51/kg wet-weight), which is not significant for the assumptions made in the model. Projected costs for biomass produced from either of the two modules (not final drug costs) were in the range of \$29,500-\$31,300 per gram of bryostatin 1-equivalent. This calculation assumed no chemical conversion of bryostatin 2 to bryostatin 1. (*Note:* In 1991, an efficient (*ca.* 70% yield) laboratory-scale semi-synthetic chemical conversion of bryostatin 2-1 was reported by Professor G. R. Pettit - the discoverer of bryostatin, and his colleagues at Arizona State University (Pettit, 1991). Given that bryostatin



2:1 ratios are approximately 1:1 in both aquacultured and wild-collected biomass, employing a scaled-up process modeled after Dr. Pettit's protocols would yield additional bryostatin 1 from the harvested biomass at a yet-to-be-determined production efficiency and cost.

***Bugula neritina* in-sea aquaculture trials**

During the years in which the in-sea aquaculture trials were conducted (1994-1998), Southern California experienced El Niño warm ocean current events in 3 of the 5 years. During one in-sea trial conducted in 1994-95, a lens of warm El Niño water (22-25°C.) blanketed the entire Southern California Bight region down to the 16-m. depth contour. In that year all of the cultured colonies on the structure died, causing the trial to be aborted. Nearly all of the naturally-occurring colonies in the Bight died-back as well, leaving only the “root-stock” (rhizomes) of the decimated colonies for beginning new growth in the next “normal” season.

As a consequence of El Niño, only two in-sea aquaculture trials were completed during the years 1994-1998. The first completed trial was started in the fall of 1995, and was terminated after 4.6 months total growth period (*e.g.*, 3-6 weeks in the shore tanks, and 13-16 weeks at sea for the various batches of settled growth plates). During that trial the mean depth of the culture panels on the undersea structure was 11.5 meters. Growth and biomass productivity was very good on the 6 growth plates harvested, producing an average biomass yield of 2.88 kg/m² of culture plate area over the 19 week growth period (note: although biomass was harvested from both sides of the plates, the calculation for biomass yield is based on the surface area of only one side of the plate, *i.e.*, 0.6 m²). Bryostatin 1 production for the first growth trial averaged 7.44 µg per gram d. w. with a range of n.d. - 13.6 µg per gram dry weight of biomass analyzed (n = 18). By comparison, the average tissue concentration from 98 wild samples of deep-type *B. neritina* collected from S. California waters during the years 1990-1997 was 16.9 µg per gram dry weight, range = n.d.- 60.8 µg per gram dry weight.

The results from the second, much longer growth trial were even more impressive. After 22 months in the ocean, two 0.6 m² culture plates were harvested from the structure and 5 samples taken for chemical analyses. The average biomass yield for each of the harvested panels was a massive 6.0 kg/m² (same assumptions as above for calculating yield per unit plate area). This was over twice the per-area yield of the first 4.6-month grow-out trial. The average bryostatin 1 concentration of harvested biomass for this longer growth trial was 13.1 µg per gram dry weight (n = 5), with a range of 10.5 – 16.1 µg per gram dry weight. The average concentration achieved is very close to the natural biomass average of 16.9 µg per gram dry weight referenced above.

Both in-tank and in-sea growth trials were relatively efficient in terms of drug yield per unit of broodstock used. Using these data, and projecting forward to a commercial-scale *Aquapharm* (design productivity = 100 grams bryostatin 1 per year), approximately 25,000



kg. of wild colonies would be required to provide the huge quantities of larvae needed to meet production goals. However, it is important to remember that the broodstock colonies themselves would yield bryostatin 1 from chemical extraction after they had spent all of their larvae for the aquaculture operations. This additional yield of 35 grams of bryostatin 1 from broodstock, when added to the 100 gram production target, would boost total drug production from the *Aquapharm* to 135 grams per year. On a per unit wet-weight basis, the in-sea aquaculture trials produced an equivalent yield of 5.4 mg/kg wet weight of bryostatin 1. This aquaculture yield can be favorably compared to an average drug yield from wild-collected *Bugula neritina* biomass of only 1.4 mg/kg wet weight, giving aquaculture an almost 4-fold drug yield increase over wild-collections to achieve the same production goals.

Productivity for a single 7-m-long, 20-panel aquaculture structure is illustrated in Figure 6. The figure includes a projection of the number leukemia patients treatable using the bryostatin 1 produced from just one in-sea structure harvested after a 1-year grow out period. Dose per patient is based upon regimens administered in NCI-monitored Phase II clinical trials in the USA. Assumptions are made that the biomass productivity per unit area of culture plates is the same for all 20 culture plates at harvest (namely, 2.8 kg/m²) and that the bryostatin 1 content of harvested biomass is the same as that observed for the second, 22 month in-sea growth trial (e. g. 13.1 µg per gram d.w.) - even though no data is available for a grow out trial of 12 months duration. If the 22 month grow out period observed in our second growth trial is used instead of the 12 month assumption, then the number of patients treated would be halved, e.g. 60 patients per year.

Projecting forward to a commercial-scale *Aquapharm* capable of producing 100-grams of bryostatin 1 per year (the expected yearly demand after 3 years of market penetration) we calculate that 200 individual structures of larger size than the prototype (i.e., 72 culture panels vs. 20 of the prototype) would be required. This level of natural product yield assumes using no semi-synthetic chemical conversion of bryostatin 2 to bryostatin 1, which has been demonstrated at an efficient yield level (Pettit, G. R., 1991). It remains to be seen whether or not the State of California permitting agencies would

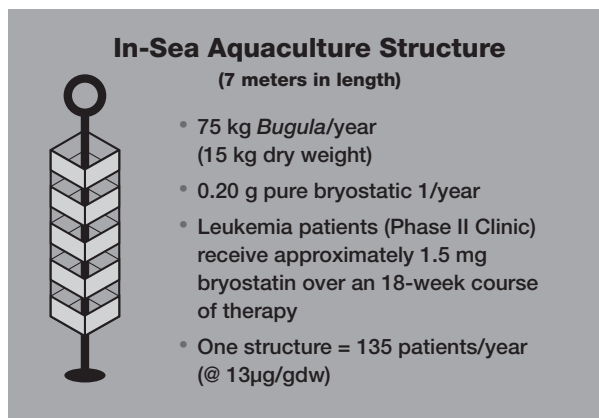


Figure 6. Cartoon illustrating biomass and natural product (bryostatin 1) yields from a single 20-panel undersea structure used for aquaculture of *Bugula neritina* in California waters.



allow such an ambitious undersea build-out, given the inherent risks and potential negative environmental impacts of such an aggressive undersea construction project. However, with almost 500 miles of the California's coastline suitable for culture of *Bugula neritina* (e.g., the region coincident with the natural distribution of *B. n.*) placement of 200 relatively small undersea structures throughout this zone, would diminish local environmental impacts tremendously, and therefore it is conceivable that State permitting agencies would allow the development of a "distributed" *Bugula neritina* "Aquapharm", especially in light of the projected human benefits of the project.

Projected economics: *Bugula neritina* in-sea culture system

The oceanographic, aquacultural engineering and logistical challenges incumbent in the task of building, placing and maintaining 200 structures in the ocean on a continuous basis for a 5-7 year period are monumental – if not within the state-of-the-art. Nonetheless, capital cost projections and economics for operations have been carefully and thoroughly compiled in anticipation of a possible real-world need to support future commercial sales of bryostatin 1. Presentation of the entire set of results is outside the scope of this paper; however a summary capsulation will serve. Construction costs for all capital facilities (250 ea., 72-panel in-sea structures, plus 2 complete on-shore fully-equipped hatchery buildings, plus permitting, land costs and construction management, etc. is approximately \$13 million. Start-up costs amount to approximately \$2.5 million, and steady-state operating costs for years 3-7 average approximately \$3 million per year. Summary costs for biomass productivity only, amortized over the 7-yr. projected life of the facilities, are in the range of \$50,000 to \$60,000 per gram of drug-equivalent biomass (not final drug costs which would include costs for extraction, purification, formulation, packaging, marketing, etc.). In addition, neither capital recovery nor interest paid on any loans or borrowed funds have been factored into the calculation – it is simply just "biomass production costs."

CASE 2: CHORDATA (SUB-PHYLUM TUNICATA) *ECTEINASCIDIA* TURBINATA

Materials and Methods

Aquaculture trials for the "Mangrove Tunicate" *Ecteinascidia turbinata* ("*E. t.*") were conducted during the years 1996-2000, using leased facilities at the Keys Marine Laboratory (a facility of the State of Florida Department of Agriculture and Consumer Services). The laboratory is located on Long Key, approximately 120 km southwest of Miami, Florida (Lat. 24°47'N. Long. 080°50'W.). The *E. t.* culture laboratory was outfitted indoors with three, 250 L polyethylene larval settlement and grow-out tanks, and out-of-doors with six, 300 L poly-tanks. All tanks were plumbed to receive filtered ambient seawater on a flow-through basis. The effluent from each tank overflowed by gravity into a receiver pipe then back into Florida Bay.



A small algal culture unit in the laboratory supplied live algal food stocks, which were supplemented with “artificial” food stocks similar to those described for *B. n.* The captive colonies were fed twice daily for 6-8 hrs, with the influent flow to the tanks turned off. Internal water circulation was maintained in each of the tanks on a constant, 24-hour/day-basis using ceramic air-stones fed by a compressed air pump. Before leaving the laboratory each day the technician would return the influent flow to each tank and turn-off the room lights. Each morning, the flow would again be turned-off to each tank, and the feeding cycle repeated, 7-days per week, throughout the experiment.

For collecting broodstock and placing of the lab-settled ropes onto the undersea culture units, the project was served by two small boats. A 3.5-m rubber boat with motor was used for collecting in ultra-shallow inlets and channels; and a larger 8-m craft served for offshore placement of lab-settled ropes and for tending two grow out arrays in the ocean. The two ocean-side grow out sites (1,000 sq. m.) were located approximately 1,000 m seaward from the southeastern-most point of Long Key, in water of approximately 4-6 m in depth. The bayside site was located the same distance offshore northwest of Long Key in the opposite direction. The ocean bottom on the bayside site was covered in a deep layer of fine silt, whereas the ocean-side site was covered in white coralline sand of from 5-40 cm-thick (over ancient coral bedrock). A few living coral outcroppings were sparsely distributed about the ocean-side site, whereas the bayside site had no outcroppings visible above the deep silt layer.

The culture scheme conceived for *E. t.* was essentially the same as that developed for *B. n.* Gravid, mature “broodstock” colonies of *E. t.* were collected from nature and placed into 50 L broodstock holding tanks [Fig. 7]. The larvae (which are at first phototrophic upon release from the parent zooids) were attracted to the higher light levels at the water surface of the tank. There (and by virtue of a constant flow of water provided into and thence out of the broodstock tank) the larvae were be carried over a pvc-pipe weir into a settling tank below. The bottom and two opposite sides of the settling tank were covered with very closely spaced lengths of 1.25 cm-diameter, black polyethylene rope. Since the normal behavior for larvae

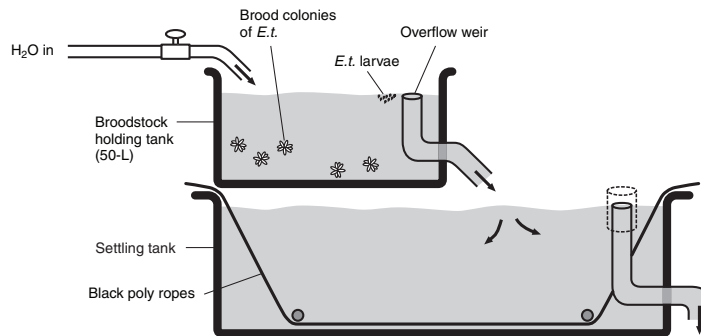


Figure 7. Schematic drawing of the dual-tank system used for settling larvae of *Ecteinascidia turbinata* onto polyethylene ropes for grow out in tanks or in the ocean.



in the wild is to seek out shadowy protected places in which to settle, the shade provided by the tightly-packed black-colored ropes (in contrast to the highly translucent tank walls) attracted most, if not all, of the larvae entering the settling tanks to settle onto the black poly-ropes rather than onto the interior tank surfaces. After settlement each competent larva metamorphosed into a fully-functional *E. t.* zooid, and began to feed and grow. Asexually budding of the first zooid produced the second, third and so forth zooids until a viable, small-sized colony of cloned zooids was formed from each settled larva.

Following a period of from 4-6 weeks of “pre-growing” in the laboratory tanks, the settled poly-ropes with the small *E. t.* colonies attached were transferred to the in-sea grow out structures. The in sea culture modules depicted in [Figure 8] were constructed from 2.5-cm-diameter PVC pipe, and coated with antifouling paint of the type commonly used for fiberglass boat hulls. Each unit was constructed with short legs on basal anchor plates which raised the culture units off of the ocean bottom about 30 cm. Multiple modules were placed on the oceanside station, whereas the bayside station was equipped with only a single rope-lattice-type module and no PVC modules.

A few growth trials were conducted in saltwater-filled, land-locked sand “barrow pits” to gauge their suitability for *E. t.* aquaculture. Some of the barrow pits were connected to the ocean through narrow channels, while others received new water only through the porosity of the coral rock base of the islands. Since the borrow pits were often very deep, growth studies were conducted from floating rafts on the surface, with the test units lowered to a depth of 1.5 m.

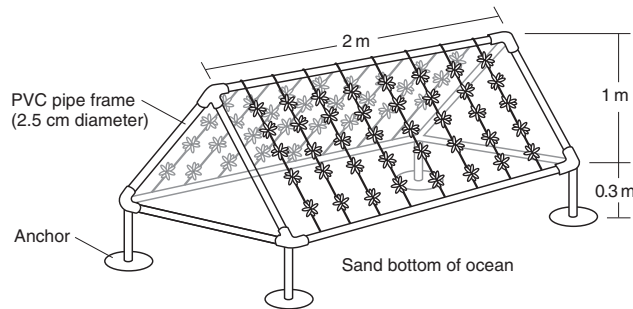


Figure 8. Schematic drawing of a pvc-pipe structure used for grow out of *Ecteinascidia turbinate* in the ocean. In practice each structure was stocked with ten 1.5-m black poly. culture ropes.

Results and Discussion

Broodstock collections, larval settlement and grow-out

Gravid colonies of *E. t.* were relatively easy to find in each month of the year, except for July and August when ambient seawater temperatures could reach 30-34°C. In the winter months of December and January water temperatures would be at their lowest of the year (15-16°C). Colonies could be found in the winter, but the individual zooids of those colonies were small and not gravid. In the early spring, when seawater temperatures reached 18-20°C, zooids would begin to become gravid with brooded larvae. In the peak months for gravid colonies





(April-June, water temp. 28-30°C) single zooids could have as many as 10 larvae in their ovaries at various stages of development. An average colony-of-the-year would generally have from 100-200 zooids growing from a common basal mass of stolon material attached to the substratum. For colonies that had been growing on the same substratum for year-after-year, huge masses of stolon and zooids could be found, some containing upwards of 2,000-3,000 individual zooids.

Sampling was done under permits from the State of Florida. Terms of the permits specified that no more than 50% of any colony visited could be sampled, and no part of the natural substratum could be taken. Since most of the colonies encountered were attached to submerged roots of mangrove trees (a protected genus in Florida) it took considerable agility with a sharp pair of fine-point scissors to remove a sample of zooids without braking off a piece of the mangrove root. Only 30 kg of wild broodstock were collected over the entire 5-yr project, while approximately 1,800 kgs were produced through the aquaculture (*e.g.*, average 60 kg per kg of broodstock collected).

Over the entire project, settlement success for all larvae introduced into the tanks was greater than 98%. This remarkable figure attests to the precociousness of *E. t.* larvae, and a strong biological imperative to settle. The physical design of the tank system also contributed positively to the preferential settlement of larvae onto the black-colored ropes. Once settled the zooids grew and budded sister zooids rapidly. Within 30-45 days most of the ropes were adequately covered with zooids to insure that the *E. t.* colonies would grow faster than any fouling organisms (mostly sponges and other tunicate species) that might fortuitously settle onto the bare rope areas once the ropes were placed into the ocean. In the ocean the starter colonies grew rapidly through asexual budding to cover an entire 1.2-meter rope in as short as 35 days. However, the average full-coverage time for all seasons of the year was 45-50 days. Biomass production averaged 400 grams ww/m-rope (range, 200-1,200 grams ww) attained in 45-90 days in the sea. The average crop cycle period was 60 days (*e.g.* 6 cycles per year) yielding an average biomass productivity per rope per year of 1,200 grams wet weight.

Using 1,200 grams/rope/yr and extrapolating to a fully-stocked hectare of undersea ET “*Aquapharm*” we obtain a projected yield of 16,000 kg/hectare/yr wet weight tunicate biomass. Using ecteinascidin tissue concentrations in the range of 1.0 to 8.6 mg/kg wet weight ET-743 + ET-729, natural product drug yields per hectare of ocean bottom in aquaculture would be in the range of 16 to 138 grams/yr. (*Note:* ET-729 was not easily separated from ET-743 in the chemical analysis procedure used. The observed ratio of the two chemical congeners was approximately 1:1 ET-743 to ET-729.)

Some of the better barrow pit grow-outs attained yields and crop periods similar to those from the sea-bottom culture units (350-500 grams in 35-45 days). However, for one of the land-locked barrow pits, relatively poor growth was attained. It was suspected that the poor



growth in that pit was due to a combination of low concentrations of food organisms in the water column, and detrimental dissolved gases such as H_2S (noticed via nasal detection) most likely emanating from decomposing organic matter on the bottom of the non-flushed barrow pit. For the barrow pits with open connections to the ocean, these limitations were not seen.

Given that barrow pit culture would require no putting-to-sea in boats or diving, barrow pit culture could offer significant cost saving in operational simplicity over sea bottom culture. Costs for divers, diving insurance, boat operations, premiums for workman's compensation (for divers and boat operators) would be eliminated if not significantly reduced. A number of well-flushed vately-owned barrow pits were discovered in the mid-to-lower Florida Keys, to potentially produce (if business arrangements and permits could be obtained) upwards of 30,000 kg of biomass per year on floating raft culture units (ET-743+729 drug yields would be in the range of 30-258 grams per year).

High survival rates, almost no fouling or predation, and no costs expended going to sea, were seen collectively to be a great advantage for tank culture. However, time to maturity for in-tank crops in these grow out trials was much longer than for those in the ocean. On average full coverage of the rope culture units took from 90-120 days in the tanks vs. 60-90 days for in-sea culture. Biomass yields also averaged 50% in tanks than that obtained from the in-sea growouts. When extrapolated to a full-sized commercial farm, tanks grow outs did not at first appear to be economical compared to ocean or barrow pit grow outs. However, if losses to ocean or barrow pit sites from a direct hit by a hurricane were factored into the equation, tank system costs become competitive. First-hand experience on this project in 1995 with hurricane Irene illustrates the point. The category 4 hurricane passed directly over the project's ocean growout site with apparent great force (including a reported 3 m. tidal surge). Two days after the storm had passed a dive inspection trip to the site found no trace of any of the culture units. The site was completely void of any of our man-man structures (save one 4-bag cement anchor and 1 m of heavy rope) and was now covered by 20-30 cm of clean, white, fine sand.

Economic projections: *Ecteinascidia* aquaculture

A detailed cost analysis was completed for building and managing an *E. t.* biomass production facility located in the mid-Florida Keys. Target production goals were set in the range of 10-30 MT tunicate biomass per year, over a 5-year period. If capital costs were absorbed and amortized totally within the 5-year project term, overall costs for biomass production raised to \$52/kg (frozen) f.o.b. the farm gate. If capital was handled in another way (e.g. written off as an R&D costs over a longer period of time, and/or as a component of a larger, corporate profit/loss statement, overall production costs were lowered into the range of \$21.00/kg for the first year's production, reducing to \$14.46 by the fifth year of operations. Drug equivalent costs based on these projections were in the range of \$3,800 to \$14,000 U.S. per gram of ET-743 (assumed no chemical conversion of the congener ET-729 to ET-743).



CASE 3: PORIFERA – *ACANTHELLA CAVERNOSA*

Materials and methods

Sponges for the culture and stress induction experiments were collected from the Mbengga Lagoon of the Fijian archipelago. Collection was accomplished using SCUBA during two collection expeditions (1992 & 1994). When collecting, the basal pieces of each sponge specimen (where it was attached to the native reef) was left intact to allow for re-growth after cutting of sponge “explants” for the aquaculture experiments. Explants were held underwater at a near-shore reef on wire-mesh racks for the duration of each of the two 2-week dive expeditions, and retrieved on the last day for packing and shipping via air-freight to California. Transit time totaled 24 hrs from packing in Fiji to arrival in California.

A closed-circuit aquaculture tank system [Fig. 9] was set-up at the CalBioMarine laboratory in Carlsbad, CA to hold the Fijian sponges for aquaculture and for the chemical induction trials. The system allowed for both group holding as well as for individual holding (small tank arrays for individual holding are not depicted in the drawing). Experiments were performed to test for growth, the effects of supplemental feeding, and the effects of applied severe stress factors on natural product content over time.

A volume displacement device was fabricated which allowed for very accurate measurements of added sponge tissue (*e.g.* growth) for each cohort over the time period of the trials. Water quality measurements for NH_4 , NO_2 , DO, pH, salinity, and turbidity were made at regular intervals throughout the trials to assure that the water quality remained within acceptable ranges. Temperature was controlled in the range 27-31°C, using a titanium

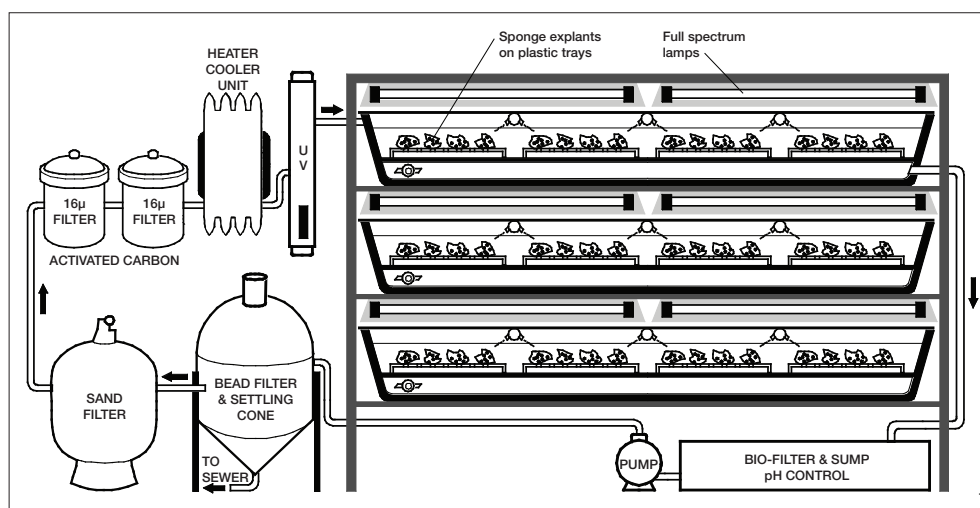


Figure 9. Schematic drawing showing components of the closed-cycle aquaculture system used for growth and natural product induction trials with *Acanthella cavernosa* (marine sponges). Note: 7 L small tank arrays not shown.



exchanger heater/chiller unit and thermostat. Light levels were measured with a LICOR underwater light sensor and meter. Evaporation lowered the system water level, so reverse osmosis-produced freshwater was added weekly to make up for any volume losses.

All sponges in all trials were fed a standard diet mix consisting of live micro algae, lyophilized bacteria, microencapsulated and powdered foodstuffs (designed for use in marine shellfish hatcheries). Daily feeding quantities were adjusted to raise the level of residual food particles in the culture system to within the range of 5,000-10,000 particles/ml (measured using a particle counter), and thus particle counts varied from day-to-day. Feeding periods were 6 hrs/day for 6 days/week. A filter by-pass loop installed in the system plumbing allowed for re-circulation of food-laden culture water during the daily feeding periods. After feeding and throughout the remainder of each day (*e.g.* 18 hrs.) the filter by-pass was closed re-directing the overflow of the tanks through the series of particulate and biological filters. For the tanks that were to receive extra feed in the trial, the inlet water stream to those tanks was first turned-off then the extra ration was poured directly into the tanks.

A 7-month acclimatization period was allowed before the stress treatment trials were begun. Not all sponge explants acclimatized well to the system. Those that did not were removed, weighed and frozen for subsequent determination of natural product content as systems controls. Following the stress induction experiments, extra sponges not included in the experiments were kept in the system for an additional 10 months, before all were sacrificed for natural product chemical determinations. To normalize for live tissue to skeleton ratio, sub-samples were preserved for total protein measurements (against a standard curve of Bovine Gamma Globulin). Protein measurements were performed using a Bio-Rad Protein Assay kit. Chemical determinations for kalihinol content (*e.g.*, levels of the 3 major metabolites in the family of kalihinanes) were conducted for the field-collected baseline samples and for the cultured sponge samples.

Stress induction experiments

Sample preparation

After the initial 7-month acclimatization period in the aquaculture tank system, 40 sponges were selected for the stress experiments. Each selected sponge was sampled for starting (or initial) kalihinane content by bisecting the sponge (held underwater within its holding tank) along its mid-sagittal plane using a scalpel blade. Samples “A” (one-half of each sponge) were preserved for chemical analysis for “T = 0” at the start of the experiment. Samples “B” (the other half of each sponge = treatment half) were left attached to its original plastic plaque, which was placed onto the coral gravel substratum in each of the 40 treatment aquaria to await commencement of the stress induction experiments.

Experiment 1: Light and damage

Three treatments were used in this experiment which ran for 30 days total: 1) tissue damage (multiple shallow scalpel cuts applied to the dorsal surface of the sponge, at the beginning of



the trial and after 2 weeks); 2) high illumination (min. 280 micro-mol quanta $\text{m}^2 \text{s}^{-1}$ irradiance from heat-shielded halogen lamps). Background light levels were < 50 micro-mol quanta $\text{m}^2 \text{s}^{-1}$ irradiance); and 3) tissue damage plus high illumination in combination.

Experiment 2: Cellular expression

Thirty-two sponges were selected for this experiment, 16 selected at random were compressed using moderate finger pressure (gloved hand) while being held out of water and above a collection beaker. Squeezing pressure was normalized as best could be done by muscle memory of the treatment person and only until orange-colored cellular material was expressed into a collection beaker. The remaining 16 sponges in this experiment were untreated controls. Treatment sponges were squeezed twice, once at the beginning and again after 2 weeks. The experiment was terminated after 1 month when all treatment sponges were first documented, then preserved for natural product (kalihinane) determinations.

Experiment 3: Light treatment

Five treatment sponges illuminated with strong light (min. 280 micro-mol quanta $\text{m}^2 \text{s}^{-1}$ irradiance from heat-shielded halogen lamps) for 12 hours per day. Five additional sponges were aggregated as a group into a single 7 L aquarium and incubated in total darkness (black plastic-shielded aquarium). The experiment was concluded after 7-days and the sponges were first documented and preserved for chemistry determinations.

Experiment 4: Chemical induction

Five sponges were cut with dissecting scissors into small fragments and placed in the same aquarium with 5 undamaged sponges, for 2 periods of 5 hrs. over an interval of 4-days. The undamaged sponges were physically separated from the dissected sponge fragments and from each other within the aquarium. The dissected fragments (“Source” tissue) were pooled at the end of the experiment for chemical determinations of the aggregate lot. The 5 undamaged (“Target” tissue) were each extracted separately for individual chemical determinations of natural product content. The controls from Experiment 2 also served as controls for this experiment.

Data analysis

After evaluation of the initial chemical data sets, we elected to report chemical yields as total “FD” fraction weight, since this organic fraction (“Fraction D”) was found to contain all of the kalihinanes present the sponge tissues, with the 3 major kalihinols comprising on average 77% of the “FD” fraction. The FD weight was found to be a reliable predictor of kalihinol yield ($r^2 = 0.841$, $P = < 0.00001$).

For analysis of experimental treatment effects, “FD” weight was normalized to sponge protein content and also to dry weight. For analysis of culture system effects (baseline vs. initial samples from the culture system) “FD” weight was normalized to dry weight only, since protein content was not performed on the field-preserved baseline samples.



Graphical analysis was used for visualizing and reporting results and statistics. Since exploratory data analysis indicated no significant positive treatment effects, a formal numerical data analysis (*e.g.* by ANOVA and *a posteriori* tests) was unnecessary. We did perform one *a priori* comparison of means (Baseline “FD” weights compared to “Initial” samples). Because the sample sizes were small and unequal, a standard bootstrapped equivalent of the *t*-test was used.

Results and Discussion

Sponge aquaculture and natural product induction experiments

Field collections, shipping and overall explant survival were very successful: 81% survival after 7 months in the culture system. Baseline sponge total chemical content for the 3 major kalihinanes was $0.48\% \pm 0.007$ (average \pm 1 SD d.w.). The “FD” fraction averaged approximately 1.5% of the sponge dry weight.

After an initial refractory period where most of the surviving sponges lost cellular material, > 70% of the cohorts began to add new cellular material (*e.g.* grow), and they continued to add new cell mass throughout the initial 7-month pre-experimental period. However none of the sponges ever regained their original size during the 7-month pre-experimental period.

Total kalihinane and “FD” content (relative to dry wt. sponge) increased for all sponges over the 7-month holding period [Figs. 10, 11]. The observed increase in “FD” extract weight was found to be statistically significant ($P < 0.0000001$ by bootstrapped comparison of means). However, in the absence of protein normalization data for the baseline samples

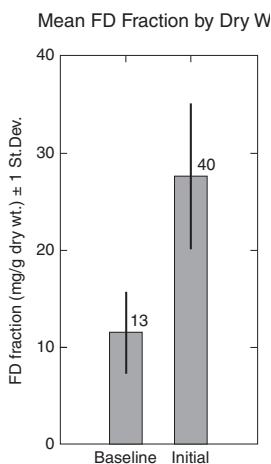


Figure 10. Weight of organic “FD” (kalihinane-containing) fraction of Baseline and Initial sponge samples from experiment 1 (light and damage) \pm 1 standard deviation, normalized to sponge dry weight (mg/g). Numbers above histograms refer to number of samples analyzed.

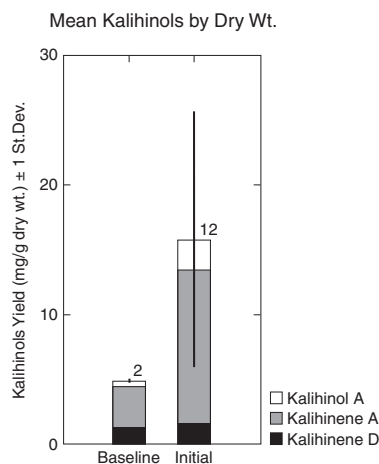


Figure 11. Mean of major kalihinol content by HPLC of Baseline and Initial samples from experiment 1 (light and damage \pm 1 standard deviation), normalized to sponge dry weight (mg/g). Numbers above histograms refer to number of samples analyzed.





(an unfortunate oversight of the experimental design) we could not be certain whether the observed increase reflected a net gain of kalihinanes or merely a condensation of cellular materials due to loss of inorganic skeletal materials.

It was theorized that application of stress inducing treatments chronically over time, would induce the sponges (and/or any natural product-producing symbionts) to biosynthesize more natural product compounds than is normally seen, as a chemical defense against the applied stress factor. However, none of the experimental treatments were found to increase kalihinol yields with any statistical validity [Figs. 12, 13]. In experiment 4, the “Target/Source” trial, some effect of damaged source sponges on secondary natural product induction in the target sponge explants was shown [Fig. 13].

Albeit, for this single trial experiment the standard deviation of the measured effect in the target sponges overshadowed completely the observed differences between the source and target explants. For the light and damage experiments (experiments 1, 3 & 4) kalihinol yields tended to decrease for all specimens chemically analyzed. Pair-wise before/after comparisons for the individual sponges clearly indicate that the kalihinol decrease was consistent and pervasive [Figs. 14, 15, 16]. Protein content of sponges before and after conclusion of the experiments showed no significant differences, so therefore the decrease in kalihinol content represented a net loss of natural products, not merely a loss of live cellular material.

For the squeezed sponge experiments (cellular expression) the total collective yield of

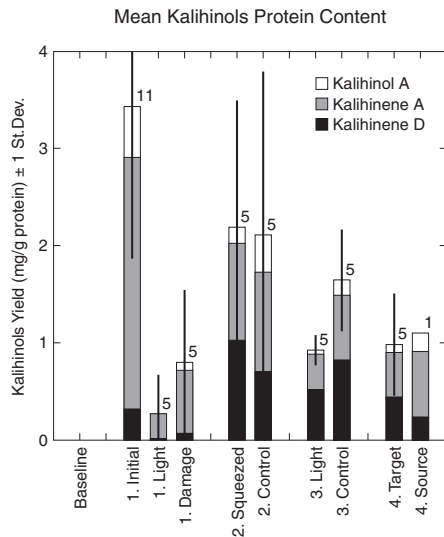


Figure 12. Kalihinol content by HPLC of experimental sponges from experiments 1- 4 ± 1 SD normalized to sponge protein content (mg/mg). The number of samples analyzed is marked above histograms.

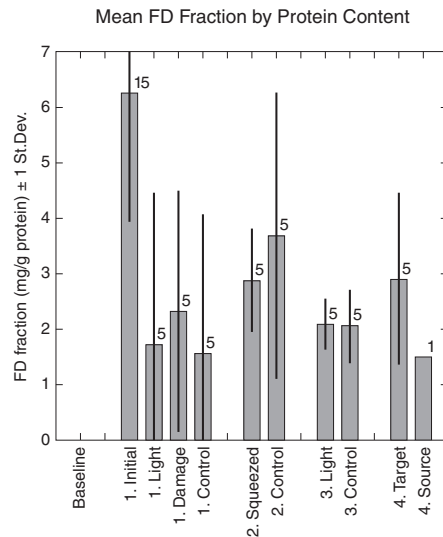


Figure 13. Weight of the organic “FD” (kalihinane-containing) fraction of experimental sponges from experiments 1- 4 (± 1 SD) normalized to sponge protein content (mg /mg). The number of samples analyzed is marked above histograms.

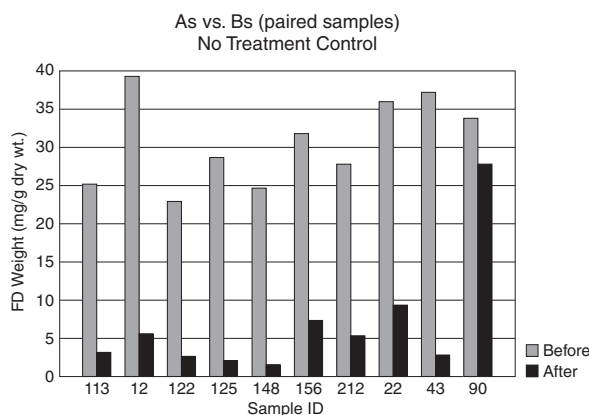


Figure 14. Before-after comparison of the organic “FD” (kalihinane-containing) fraction content (mg./g. dry weight) of sponges from the no treatment control of experiment 1. Each pair of bars represents samples taken from the same sponge.

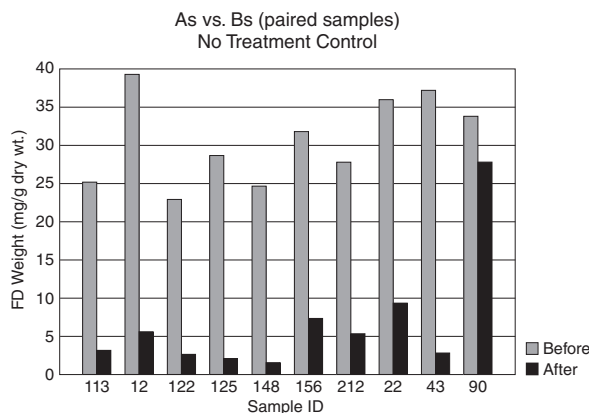


Figure 15. Before-after comparison of the organic “FD” (kalihinane-containing) fraction content (mg/g dry weight) of sponges from the high light treatment protocol of experiment 1 (high light only). Each pair of bars represents samples taken from the same sponge.

kalihinols from the 16 treatment sponges (9.8 grams total dry weight) after two squeezings separated by a period of 2 weeks was 0.027 mg. While this yield was small compared to the whole-sponge extracts (0.01% of the total major kalihinols present in the 16 specimens), it is important to note that cellular expression (squeezing) had no apparent negative effect on the levels of kalihinols in the squeezed sponges. The expressed sponges rapidly recovered after each treatment with no apparent loss of condition (visual observations) or kalihinol content. When normalized to dry weight of sponge the squeezed samples averaged 21.7 mg/g whereas the controls averaged 17.2 mg/g. When normalized to protein content the squeezed samples averaged 2.17 mg/g and the controls 2.10 mg/g.



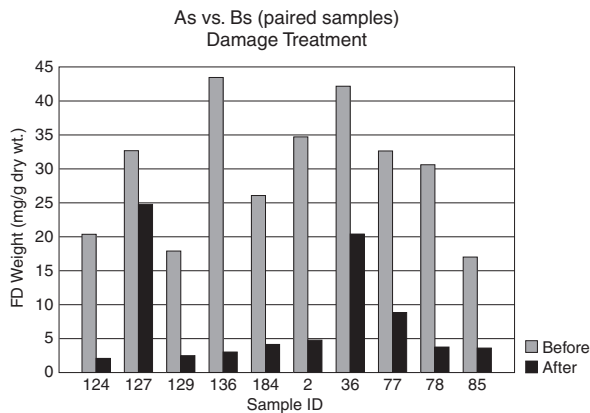


Figure 16. Before-after comparison of the organic “FD” (kalihinane-containing) fraction content (mg/g dry weight) of sponges from the tissue damage treatment protocol of experiment 1 (tissue damage only). Each pair of bars represents samples taken from the same sponge.

CONCLUSIONS

Case 1: *ectoprocta* – *Bugula neritina*

At present there exists no economical chemical synthesis for bryostatin 1, nor is there a completed microbial fermentation, native or transgenic (see Hale *et al.* 2002 for an excellent and complete review of the chemistry and biology of the bryostatins). Therefore by default if not by its merits, in-sea aquaculture as demonstrated in this study remains as the only environmentally prudent option for provision of large-scale (*ca.* 100 grams/yr) supplies of bryostatin 1. However, given the large capital and start-up expenses and the relatively high risk of implementing a commercial scheme such as projected from these results, it remains to be seen if the pharmaceutical company wishing to market the drug will embrace and support this technology. A cost/benefit analysis could tip the scales in favor of aquaculture, since projected revenues from worldwide sales of what promises to be a blockbuster new adjuvant therapy for cancer and immune-compromised diseases are potentially huge.

Case 2: *Chordata (Sub-Phylum Tunicata)* – *Ecteinascidia turbinata*

The *E. t.* aquaculture project was overall technically very successful, and with a financial proposal in-hand the project went looking for a market. It was known that the sole company in the world to hold marketing rights for the drug ET-743 was PharmaMar, S.A., of Madrid, Spain. It was also known that PharmaMar had been developing their own *E. t.* aquaculture operations in the Mediterranean Sea during the same period CalBioMarine was developing its project in the Florida Keys. At that time the PharmaMar project was producing approximately 40 MT per year of biomass. Through discussion, CalBioMarine learned that PharmaMar’s then current production costs were significantly below CalBioMarine’s projections for a



scaled-up project in the Florida Keys. After much discussion and efforts towards trimming the Florida production costs to a bare minimum, no business deal was made, owing mostly to the fact that CalBioMarine could not guarantee a future price for its *E. t.* biomass in a range acceptable to PharmaMar. This outcome was in concert with the often echoed result from other U. S. domestic (food species) aquaculture operations, namely, that an aquaculture enterprise built and operated on USA soil will have a difficult time competing economically with projects for the same species located in countries with lower labor, land, and other fixed costs. For the Florida *E. t.* aquaculture project, the largest cost components of production were for labor and labor-related insurance premiums (workers compensation insurance). Thus as a final result, CalBioMarine's Florida aquaculture project was priced out of the world market for *E. t.* biomass and drug.

Case 3: porifera – *Acanthella cavernosa*

Although the results from the stress induction experiments varied wildly, these experiments showed some trends that should be explored in better controlled follow-on experiments. The project results did identify a novel non-destructive incremental harvesting method for sponge natural products (at least for species such as *Acanthella cavernosa* that are sturdy enough to survive the treatment). It was concluded that the cellular expression method (termed “sponge milking”) could be applied to other sturdy sponges whose natural products might enter development as potential drugs in the future. In those cases, the method could be applied to supply small quantities of natural product for pre-clinical testing and evaluation without destroying the collection of live sponges taken from the environment and held in an aquaculture system. The critical questions remaining to be answered with respect to the sponge milking method were: 1) what is the maximum possible harvest intensity?, 2) would partial dissociation of the non-cellular portion of the mesohyl (via incubation in Ca, Mg-free seawater) before harvest treatment enable more efficient cellular expression?, and 3) what is the optimum combination of harvest intensity and frequency of cellular expression? However for the kalihinols, these questions are somewhat moot, since the compounds were dropped from development by the pharmaceutical company that owned the rights to them, and there was [is] no further call or need for either wild-collected or aquacultured samples of the sponge for natural product development.

General Conclusions

It can be generally concluded from these results that marine pharmaceutical aquaculture (especially in-sea aquaculture) for certain species and phyla of marine invertebrates is now a feasible and manageable technology that can be scaled to meet – at least in part, the needs for clinical and/or commercial drug supplies. Cost effectiveness for two species, *Bugula neritina* and *Ecteinascidia turbinata* has been proven from the results of these experiments. In the case of *Ecteinascidia turbinata*, in-sea and in-pond aquaculture (practiced by others)



has already provided drug for supporting human clinical trials for hundreds of cancer patients in Europe (PharmaMar, S.A., pers. comm.).

Aquaculture should be investigated for new marine invertebrate species being developed for their natural products, especially where alternative supply technologies such as chemical synthesis or fermentation have been ruled-out for lack of feasibility or cost effectiveness. In-sea aquaculture (when practiced responsibly and with an underpinning of expertise in oceanographic engineering, and a full understanding of the marine ecology of the region) should not deplete natural populations of source organisms, nor substantially or irreversibly damage the undersea environment.

More work needs to be done to optimize controlled-environment tank culture systems for invertebrate culture and natural product yields, since in the end, land-based systems present the lowest overall risk, the greatest possibility for controlled production and sustained growth, and the lowest environmental impact, when compared to open-sea systems which are all subject to the unpredictable vagaries of nature and the possibility for environmental degradation.

ACKNOWLEDGEMENTS

The CalBioMarine development team was composed of talented marine biologists, aquaculturists, marine natural product chemists, diver/collectors, microbiologists, and technicians. Key CalBioMarine employees who contributed to the development of the culture systems and protocols were: Alexander B. Leonard, Ph.D., John R. M. Chisholm, Ph.D., Janice E. Thompson, Ph.D., Barbara J. Javor, Ph.D., Carolyn J. Sheehan, B.S., and Guy N. Rothwell, P.E (California); and Erich Bartels, B.S. and Claudine Bartels, M.S. (Florida Keys).

Academic collaborators from nine different universities, oceanographic research institutions, natural history museums, and marine aquariums contributed expertise and services not available in-house at CalBioMarine. Ron McConnaughey and his staff of student and professional divers and small boat operators at UCSD/SIO/MBRD must be collectively commended and acknowledged for their unwavering service to the in-sea *Bugula neritina* culture project. Kristi Paulson Mendola provided the line art drawings and figure illustrations for this paper.

Financial support was provided through the Small Business Innovation Research grants and contract programs of the following U.S. government agencies: The National Cancer Institute (NCI) (*Bugula neritina* aquaculture projects); the Department of Agriculture (*Ecteinascidia* aquaculture project); The National Science Foundation (*Acanthella* aquaculture and *Bugula* flow/growth projects); and the Department of Commerce, NOAA, National Coastal Resources Research and Development Institute (*Bugula* in-sea aquaculture).

The NCI / Natural Products Branch, with funding provided by the Bristol-Myers Squibb Company (and through the NCI's contractor SAIC-Frederick, chemistry group leader Mary Koleck, Ph.D.) provided for the chemical analyses of bryostatin content of both wild-collected



and aquacultured *Bugula neritina* biomass. Chemical analyses of cultured and wild-collected *Ecteinascidia turbinata* biomass were conducted by Professor Russell G. Kerr and his students in the Department of Chemistry at the Boca Raton campus of Florida Atlantic University (Dr. Kerr's students also contributed as technicians on the Phase I feasibility project). Comparison data for ecteinascidin natural product content from wild-collected *E. t.* colonies from Long Key, FL. was provided by Dr. Amy Wright of Harbor Branch Oceanographic Institution in Florida. All chemistry for determination of natural product content of sponge biomass was performed by Professor Phillip O. Crews and his laboratory personnel at the University of California, Santa Cruz, Department of Chemistry and Biochemistry.

REFERENCES CITED

- (Anonymous). 2001. Marine Biology in the Twenty-First Century. Nat. Acad. Sci., NRC/OSB (USA):1-7.
- Bergmann, W., and R. J. Feeney. 1950. Isolation of new thymine pentoside from sponges. *J. Am. Chem. Soc.* **72**: 2809-2810.
- Bergmann, W., and R. J. Feeney. 1951. Marine products. XXXII. The nucleosides of sponges I. *J. Org. Chem.* **16**: 981-987.
- Bergmann, W., and D. C. Burke. 1955. Marine products. XXXIX. The nucleosides of sponges. III. Spongothymidine and spongouridine. *J. Org. Chem.* **20**: 1501-1507.
- Davidson, S. K., and M. G. Haygood. 1999. *Biol. Bull.* **196**: 273-280.
- Faulkner, D. J. 2000. *Ant. van Leeu.* **77**: 135-145.
- Faulkner, D. J. 2001 *Nat. Prod. Rpts.* **18**: 1-49.
- Fusetani, N. (ed). 2000. Drugs from the Sea. Karger, Basel. Pp. 1-5.
- Hale, K. J., M. G. Hummersone, S. Manaviazar, and M. Frigerio. 2002. *Nat. Prod. Rpts.* **19**: 413-453.
- Jaspars, M. 1999. Chemistry & Industry (GB) (Jan.): 51-55.
- Kerr, R. G., and S. S. Kerr. 1999. *Exp. Opin. Ther. Patents* **9**(9): 1207-1222.
- Look, S. A., W. Fenical, G. K. Matsumoto, and J. Clardy. 1986. The pseudopterosins: a new class of antiinflammatory and analgesic diterpene pentosides from the marine sea whip *Pseudopterogorgia elisabethae* (Octocorallia). *J. Org. Chem.* **51**: 5140-5145.
- Newman, D. J., G. M. Cragg, and K. M. Snader. 2000. The influence of natural products upon drug discovery. *Nat. Prod. Rpts.* **17**: 215-234.
- Newman, D. J. and G. M. Cragg. 2004. Advanced preclinical and clinical trials of natural products and related compounds from marine sources. *Curr. Med. Chem.* **11**: 1693-1713.
- Newman, D. J., and G. M. Cragg. 2007. Natural products as sources of new drugs over the last 25 years. *J. Nat. Prod.* **70**: 461-477.
- Pettit, G. R., D. Sengupta, and C. L. Herald. 1991. *Can. J. Chem.* **69**: 856-860.
- Rouhi, M. A. 1995. *Chem. & Eng. News* (USA). Nov. Pp. 42-44.

Note: The Introduction to this thesis chapter was up-dated and modified from the originally published version, which can be accessed from the literature as:

Mendola, D. 2003. Aquaculture of three phyla of marine invertebrates to yield bioactive metabolites: Process developments and economics. *Biomol. Eng.* **20**: 441-458.





ADDENDUM TO CHAPTER 2

The three marine invertebrate-derived compounds referenced in the Introduction to this chapter [bryostatin 1, ET-743 (trabectedin /Yondelis®), and Ziconitide / Prialt®] have each progressed in human clinical trials since the original publication of this chapter in 2003. Yondelis® and Prialt® have both been approved as commercial drugs in Europe and pending commercial approvals soon in the USA. The foregoing is a brief update on the clinical progress, new drug approvals, and raw material sourcing for these three compounds.

Bryostatin 1

Bryostatin 1 is antitumor polyketide macrolactone from the cosmopolitan, temperate, arborescent bryozoan, *Bugula neritina*. Since entering the clinic in the early 1990s, bryostatin 1 has been used in over 80 human clinical trials against a wide variety of cancers, both as a single agent with limited success, and with higher efficacy in combination with other anticancer agents (fludarabine, paclitaxel, vincristine, and cisplatin). As of December, 2007, there are four Phase I and eight Phase II human clinical trials for cancer indications underway in the USA, all sponsored by the National Cancer Institute.

Clinical supplies have come from two 18,000 kg collections of natural biomass from the California coast (total yield: 36 grams GMP bryostatin 1). Synthesis of biologically active simplified analogs is currently being investigated by two groups (Wender, 2006; Trost, 2007). Also under investigation is heterologous expression of the putative gene cluster isolated from an identified putative symbiont *Candidatus Endobugula sertula* to produce a hypothetical precursor base structural material, bryostatin 0 (Sudek *et al.* 2007). From this base molecule, the authors propose that bryostatin 1 could be made using additional biosynthetic genes identified for expression of the functionally obligatory C-20 substituents (given that the C-7 substituents have been shown to be irrelevant for pharmaceutical activity).

Ecteinascidin 743

Ecteinascidin 743 (trabectedin/Yondelis®) is antitumor tetrahydroisoquinoline alkaloid from *Ecteinascidia turbinata* (Ascidian, colonial); Caribbean and Mediterranean. The compound entered human clinical trials in the early 1990s (sponsor-licensee, PharmaMar S.A., ES) as a single agent treatment against soft tissue sarcomas, and later as a combination therapy with carboplatin against ovarian cancer, and with liposomal doxorubicin against breast cancer. In Sept. 2007, the European Commission authorized PharmaMar to commercialize Yondelis® in the 27 countries of the EU for patients suffering from advanced soft tissue sarcoma when standard treatments have failed. In Dec., 2007 it was released and became available in Germany and in the U. K.; and on Dec. 31, 2007 it was approved for release in Spain. In the USA the drug is being tested in Phase III trials for ovarian, non-small cell lung, and prostate cancer



by PharmaMar together with their licensee Johnson & Johnson (Ortho Biotech division), and in the EU in (by PharmaMar) in Phase II trials for breast cancer. Additionally, early trials are also underway by the National Cancer Institute (USA) for potential use in the treatment of advanced, persistent or recurrent uterine leiomyosarcomas and solid tumors.

Initial supplies for early-stage clinical trials came from large-scale aquaculture of the source ascidian on racks at three locations in the Western Mediterranean Sea [developed by PharmaMar max. biomass yield in 2004, 100 MT (Mendola *et al.* 2006)]. Later clinical supplies were produced by PharmaMar through a semi-synthesis from cyanosafracin-B, an antibiotic produced via fermentation of the source bacterium *Pseudomonas fluorescens* (Menchaca *et al.* 2003). This same process has been scaled-up to produce supplies of Yondelis® for both the USA and EU commercial sales.

Ziconitide/Prialt®

Ziconitide / Prialt® is a synthetic equivalent of a naturally occurring peptide found in the marine snail *Conus magus*. The drug (an N-type calcium channel blocker) was launched in the USA in 2005 by Elan Pharmaceuticals, and in 2006 in the U. K. and in Germany by Eisai Pharmaceuticals for management of severe, chronic pain. Sales in 2005 were \$6M USD; 2006, \$12 M USD; and 2007, \$8.2 M USD (through 3rd Qtr.); (source: David J. Newman, NCI/USA, Pers. comm.).

Addendum: Personal communication sources

David J. Newman, D. Phil. Chief, Natural Products Branch, National Cancer Institute, Frederick, MD, USA. (verbal information, printed data, and other published and un-published materials in pre-print form.)

Addendum: References cited

- Menchaca, R., V. Martinez, A. Rodríguez, N. Rodríguez, M. Flores, P. Gallego, I. Manzanares, and C. Cuevas. 2003. Synthesis of the natural ecteinascidins (ET-729, ET-743, ET-759B, ET-736, ET-637, ET-594) from cyanosafracin-B. *J. Org. Chem.* **68**: 8859-8866.
- Mendola, D., S. A. Naranjo Lozano, A. R. Duckworth, and R. Osinga. 2006. The Promise of Aquaculture for Delivering Sustainable Supplies of New Drugs from the Sea: Examples from in-Sea and Tank-Based Invertebrate Culture Projects from Around the World. In: Proksch, P. and W.E.G. Müller (eds). *Frontiers in Marine Biotechnology*. Horizon Bioscience, Norfolk, England.
- Sudek, S., N. B. Lopanik, L. E. Waggoner, M. Hildebrand, C. Anderson, H. Liu, A. Patel, D. H. Sherman, and M. G. Haygood. 2007. Identification of the putative bryostatin polyketide synthase gene cluster from “*Candidatus Endobugula sertula*”, the uncultivated microbial symbiont of the marine bryozoan *Bugula neritina*. *J. Nat. Prod.* **70**: 67-74.
- Trost, B. M., H. Yang, O. R. Thiel, A. J. Frontier, and C. S. Brindle. 2007. Synthesis of a ring-expanded bryostatin analogue. *J. Am. Chem. Soc.* **129**: 2206-2207.
- Wender, P. A., J. C. Horan, and V. A. Verma. 2006. Total synthesis and initial biological evaluation of new B-ring modified bryostatin analogs. *Org. Lett.* **8**: 5299-5302.





Chapter 3 Environmental flow regimes for *Dysidea avara* sponges

Dominick Mendola^{1,3}, Sonia de Caralt^{1,2}, Maria J. Uriz²,
Fred van den End¹, Johan L. van Leeuwen³, René H. Wijffels^{1*}

¹Wageningen University, NL, Food & Bioprocess Engineering Group;

²CSIC Centre for Advanced Studies, Blanes (Girona) Spain; ³Wageningen University, NL, Experimental Zoology Group *e-mail: rene.wijffels@wur.nl

Abstract: Water flow regimes were characterized over a one-year period for a shallow rocky sublittoral environment in the Northwestern Mediterranean where *Dysidea avara* sponges are particularly abundant. 3-D Doppler current velocities at 8-10 m depths ranged from 5-15 cm/s over most seasons, occasionally spiking to 30-66 cm/s. A thermistor flow sensor was used to map flow fields in close proximity (≈ 2 cm) to individual sponges at 4.5, 8.8, and 14.3 meter depths. These “proximal flows” averaged 1.6 cm/s in calm seas and 5.9 cm/s during storm, when the highest proximal flow (32.9 cm/s) was recorded next to a sponge at the shallowest station. Proximal flows diminished exponentially with depth, averaging $2.6 \text{ cm/s} \pm 0.15 \text{ SE}$ over the entire study. Flow visualization studies showed oscillatory flow (0.20-0.33 Hz) was the most common regime around individual sponges. Sponges at the 4.5 m site maintained a compact morphology with large oscula year-around despite only seasonally high flows. Sponges at 8.8 m were more erect with large oscula on tall protuberances. At the lowest flow 14.3 m site sponges were more branched, heavily conulated, with small oscula. The relationship between sponge morphology and ambient flow regime is discussed.

Key words: water flow, sponge morphology, flow tank, *Dysidea avara*





INTRODUCTION

Dysidea avara (Schmidt, 1862), a violet-colored, encrusting and heavily conulated dictyoceratid sponge, is known from mostly sciaphilic microhabitats of the rocky sublittoral Mediterranean to 80 m depths (Uriz *et al.* 1992). It is the natural source of avarol and related metabolites which have shown anti-tumoral, anti-bacterial, anti-viral, and anti-inflammatory activities (Müller *et al.* 1986, Minale *et al.* 1974, Uriz *et al.* 1996). Avarol as the natural product is currently being tested on humans in Germany as an additive to a skin cream for treating psoriasis (Pietschmann *et al.* 2004). Early clinical results have been promising and projections for an expanded market have begged the question of a sustainable source of supply. Aquaculture for the production of drugs from sponges has been reviewed by Battershill and Page (1996), and aquaculture of *Dysidea avara* (both *in situ* and *ex situ*) has been proposed and preliminarily investigated (Sipkema *et al.* 2005). Recently Bannister *et al.* (2007) identified hydrodynamic features of the environment as key parameters for selecting suitable sites for bath sponge aquaculture on the Great Barrier Reef in Australia.

Bidder (1923) was the first to relate the general morphology of a sponge to environmental flow and oscular output. Bell and Barnes (2000), and Bell *et al.* (2002a, 2002b, 2006) studied the influences of bathymetry and flow on morphology and distribution of a number of sponge species. They showed more massive and encrusting forms dominated in high-energy sites, whereas arborescent forms dominated at low current sites. Riedl (1977) working with colonial cnidarians and sponges also showed that as depth increased morphology changed from more compact forms at the surface to more erect, taller, plumate forms in the deeper zones. Pronzato *et al.* (1998) studied morphological adaptations of three species of the genus *Spongia* along an 80 m submerged vertical cliff and found distinct morphological differences which could be separated by depth, *i.e.*, differences in ambient flow speeds.

Palumbi (1984, 1986) studied acclimation, body plan limitations and morphological changes of *Halichondria panicea* in relation to varying flow regimes within a large coastal inlet in Alaska. He found individuals at the entrance of the inlet (higher flows) had thicker colonies and added skeletal mass (*i.e.*, spicules) as a means of resisting stronger wave forces. Kaandorp (1999) studied the relationship between water flow and the form (degree of compactness) of the sponge *Haliclona oculata*, a hydrozoan, and a hard coral using an algorithmic method, and found increasingly more compact morphologies along a gradient of exposure to water movement.

Barthel (1991) presented relevant data on the influence of differing flow regimes on the growth form of the cosmopolitan sponge *Halichondria panicea*. In a sub-tidal oscillating flow regime the form was thickly encrusting globosc, whereas at a sheltered “cave-like” setting the sponge formed long slender, partly anastomosing branches extending upward from a relatively small base. Meroz-Fine *et al.* (2005) studied changes in morphology and

physiology of *Tetilla* sp. sponges in the E. Mediterranean in relation to light, depth, and water flow from differing habitats. They found tide-pool-inhabiting sponges (higher wave forces) had significantly larger body volume and more skeletal silica than did cohorts inhabiting sub-tidal caves, or a nearby 30 m site. Transplants from the deeper (calmer) site to a shallow (turbulent) site significantly increased spicule content to match the shallow-living individuals. Hill and Hill (2002) looked at morphological plasticity in a tropical sponge in relation to wave energy and predation pressures. They found that treatments in higher wave force habitats or those challenged with artificial predation increased their spicule density as a means of defense against the potentially damaging forces of high wave energy or increased levels of predation.

The overall aim of our research is to design tank systems to culture *Dysidea avara* for the production of avarol. Sponges are notoriously sensitive organisms that are difficult to culture *ex situ* (Sipkema *et al.* 2005). So far we have not been successful in our attempts to grow *Dysidea avara* in tanks. Effects of food quality and quantity gave unsatisfactory results in growth experiments (Sipkema *et al.* 2006). During collections of *Dysidea avara* it became apparent that the flow regime we applied in our tanks differed from the natural regime. We immediately noticed that *Dysidea* was usually present in habitats protected from strong currents. In addition, we noticed different morphologies at different sites, which we suspected were related to local flow conditions. We planned to do flow-tank experiments to study the interaction of flow and particle uptake by the sponges. Therefore, we would need to know natural flow conditions to set starting parameters in the flow-tank. Hence, the need for comprehensive field studies was indicated.

The specific aim of this research was to measure flow regimes within a rocky sublittoral cove on the N. E. coast of Spain, where *Dysidea avara* was known to be more abundant and attain larger size than from other similar environments nearby. Bulk current flow and flow in very close proximity to individual sponges in both calm and stormy seas would be determined at different depths where sponges showed different morphologies.

MATERIALS AND METHODS

Site selection, sponge selection, identification and sampling periods

Field studies were conducted in N. E. Spain on the Costa Brava in the vicinity of L'Escala, Girona, at Punta del Romani (PR) and within the Cala Illa Mateua (CIM) cove [GPS coordinates: 42°06.863' N, 003°10.116' E]. Five field trips were conducted: 26-30 September, 2005; 3-30 March, 29 May-2 June, 25-28 July, and 27-31 October, in 2006. The sublittoral rocky plateaus of the point, with its many small caves, tunnels and rocky overhangs provided ideal habitats for the sponges. Using SCUBA, study sites were selected at three depths just west of the point: Site A, at 4.5-5.5 meter depths; Site B, 8.8 meters; and Site C, 14.3 meters.



Each of the sites comprised two subsites (“main” and “annex”) located in close proximity to one another which were *a priori* differentiated as distinct flow microhabitats.

Site A: The shallowest site was located closest to the shore and in the lee of the point. The A-main site at 5.5 m was located in a “mini-cave” where many healthy *Dysidea avara* sponges were found. The A-annex site was located within a small cleft in the rock at 4.5 m depth where a number of small, but healthy-appearing *D. avara* were found. A total of 6 sponges were selected (3 at each subsite).

Site B: The intermediate depth 8.8 m B-site was the least exposed of the three sites studied. It was located at the base of a steep, west-facing rock wall and protected from the west by giant boulders and from the east and south by steep rock walls. Three large sponges were selected from inside a mini-cave (B-main subsite) on the west-facing wall, and three from a B-annex subsite at the same depth but on an exposed rock shelf just outside of the mini-cave. Adjacent to the mini-cave and just before the south wall a large tunnel connected to a large vertical tube which opened into shallower water.

Site C: The deepest of the three study sites (14.3 m) was the furthest from the shore and the protection of the submarine portions of the point. Given that wave forces diminish exponentially with depth and in proportion to wave length (Sverdrup *et al.* 1961) protection for the sponges at Site C came by virtue of their depth, not rock cover. The C-annex subsite was located a bit closer to the lowest rock shelves of the point, but still at 14.3 m depth, so potentially the annex sponges could receive some protection from the rocks – especially in an easterly sea. The sampled sponges (3 main and 3 annex) were found encrusting on large rocks which were mostly buried in sand. The maximum depth visited at Site C was 15.1 m, the deepest range for *Dysidea avara* sponges within the study cove.

3-D Doppler velocimeter

Bulk current flows within the cove were measured using a 16-MHz MicroADV acoustic Doppler velocimeter (Sontek, San Diego, CA, USA). The “ADV” measures the velocity of moving water by the Doppler principle, where the frequency of sound at a receiver is shifted from the transmitted frequency in proportion to the speed of the water moving through an acoustical sampling volume located 5 cm below the sender transducer. From signals received from a triangular array of receivers, water velocity vectors in three directional components (XYZ Cartesian) were recorded. By vector addition the resultant flow speed (V_{net}) was computed and displayed on X-Y coordinates in relation to time. A “relative signal strength” (RSS) output signal was recorded as an indirect measure of the particle density in the sampled water mass, used as an indication of relative turbidity.

The ADV was deployed onto the sea bottom from an inflatable diver-towed mini-raft and affixed to a sturdy steel tripod placed on the sea bottom. Recordings were made at each of the three depth sites for varying periods (usually for no less than 3 h). In operation, raw flow

data was transmitted up the cable connecting the ADV to its signal processing electronics housed on the inflatable. The analog signal (900 MHz) was radioed directly to a shore-based computer in real-time.

Thermistor flow sensor and recorder

An advanced thermistor flow sensor and recorder was specially-designed and built to measure water flow speeds in close proximity to individual sponges. The principle of operation is based on the rate of heat removed from a submerged, electrically-heated thermistor (temperature sensitive electrical resistor) which is related to the speed of the water mass moving past it (Reiswig 1971, 1974, Vogel 1977). The non-directional flow probe comprised a 0.9 mm diameter glass-bead-covered thermistor silicone-sealed onto the distal end of a 2 mm diameter stainless steel tube. The electrical connections ran down the core of the tube and connected to a 1.5 m-long electrical cable connecting the probe to the recorder. A second ambient temperature compensation thermistor was molded onto the outside of the recorder case. An LCD screen under a clear plastic lid showed the flow-related meter readings and magnet-operated function buttons.

The thermistor probe was calibrated in a commercial tow-tank (Delft Hydraulics, NL) but only through a limited range of 0.17-13 cm/s. For speeds in excess of 13 cm/s calibration relied upon the wider-ranged temperature response curve of the thermistor which was stored onto firmware of the instrument's circuitry. Before each measurement the stored temperature response curve was electronically referenced to recalibrate the probe to the ambient temperature. We estimated measurement errors increased from $\pm 2\%$ at the lowest speeds to approximately $\pm 15\%$ at the highest speeds encountered in this study.

The measurement protocol in the field called for recording a series of individual flow speeds at 4 different placements of the probe around the periphery, and 2 placements over the top of a sponge all within 10-15 minutes. Flow was measured approximately 2 mm from the surface of the sponge and within 2-4 cm of the local substratum (such measurements are termed "proximal flow speeds", or "proximal flows" throughout paper). At the underwater site, a lead-weighted, tri-footed stainless steel platform served as a stable mount for holding the thermistor probe, which was attached to a length of flexible aluminum rod. The rod was shaped and bent to position the thermistor at the exact spot next to the sponge where the flow measurement was to be made. The set-up during a typical field measurement is shown in Fig. 1.

Flow visualization

Water flow regimes around individual sponges were visualized using an array of mini-flags made of thin strips of fluorescent orange surveyor's tape pinned onto a sponge. The flags rotated freely on the pins and waved in response to the slightest water movement. A companion method employed milky suspensions of micrometer-sized white latex particles

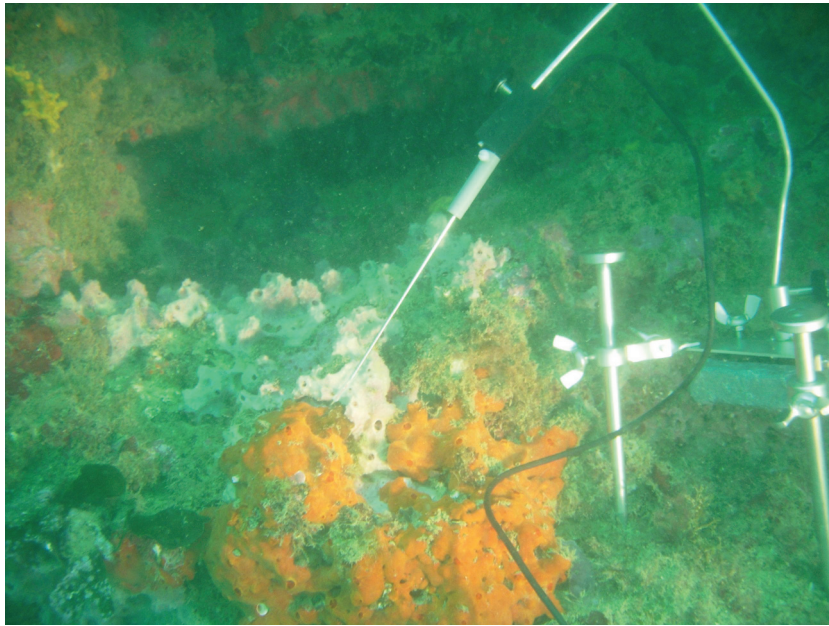


Figure 1. Set-up for proximal flow measurements with the thermistor probe and probe stabilizer platform, positioned around purple *Dysidea avara* specimen. (Note: orange colored sponge in foreground is *Crambe crambe*.)

aspirated over a sponge from a syringe. The current-induced motions of the flags and latex clouds were recorded as short video movies on a Nikon® Cool-Pix 5200 camera.

RESULTS

Weather and sea conditions

Mild weather conditions and calm seas prevailed during the Sept. 2005, and March, July, and Oct. 2006 sampling periods. Underwater visibility during these calm periods was 10-15 m. During the May-June, 2006 field-trip, strong “Tramuntana” winds (Beaufort scale 5-6) blew towards the study site from across the Gulf of Roses with swells and breaking waves cresting to 1-2 meters. Underwater visibility during this storm was 3-4 m, attributable to entrained bottom sediments and air from the sea surface.

Bulk current profiles (ADV recordings)

Calm Seas: 3-D Doppler flow profiles were recorded from inside the mini-cave at the A-main site (5.5 m) in Sept., 2005. Recording showed oscillating flows with a maximum amplitude of approx. ± 12 cm/s and periodicity of 12-20 cpm (0.20-0.33 Hz). The smallest component of the 3-axis recording (± 2 cm/s) was in the “Z” direction, *i.e.*, the up/down flow component with respect to the water surface.



During calm seas on 3/06, the resultant flow speed (V_{net}) of the bulk current flow recorded at 4 different placements along a 50 m transect crossing the 10-12 m depth contours ranged from 3-13 cm/s. During summer (7/06) at 8.8 m near Site B, and for the first 0.75 h of recording, V_{net} ranged from 5-30 cm/s with only a few surges to 50-66 cm/s. For the remaining 1.75 h, V_{net} reduced to the 5-10 cm/s range with a few surges to 15-20 cm/s. RSS spiked at 25-30 dB after passage of peak flows and thereafter reduced to the 0-5 dB range with only a few spikes reaching 15-20 dB levels. V_{net} at 9 m (close to Site B) during the fall sampling period (10/06) was in the range of 3-13 cm/s for the entire 3-h recording. RSS was very high (55-60 dB) indicating a heavy load of particulate matter in the water column. All ADV recordings during calm seas could be characterized as oscillating flows with 3-5 second periodicity.

Stormy Seas: Despite the very stormy sea surface generated by the seasonal Tramuntana winds of early summer, V_{net} at 9.3 m (close to Site B) remained in the low range of 3-8 cm/s for most of the three hour recording period. Two broad, jagged peaks reaching 25-30 dB on the RSS trace indicated medium-to-high particulate matter content in the water column, most likely due to entrained bottom sediments. However, in general throughout the recording RSS levels were low (4-7 dB) indicating low particulate content in the water column.

Proximal flows around individual sponges

Figures 2, 3, & 4 display all proximal flow measurements made at each of the three depth/sites over the entire 7-month study period.

Site A: Sponges at the shallowest site experienced the highest speed and the widest range of proximal flows: (March-Oct) average = 4.0 cm/s \pm 0.3 SE, range 0.4-32.9 cm/s (Fig. 2). During the storm of 1 June, sponge A-1 at the shallowest 4.5 m A-annex subsite experienced the highest proximal flows of any sponge: average = 19.0 cm/s \pm 6.2 SE, range 7.4-32.9 cm/s. Four days after the full strength of the storm had passed proximal flows around this same sponge reduced to average = 4.7 cm/s \pm 2.0 SE, range 1.9-12.4 cm/s, and in calm seas sponge A-1 experienced flows in the range of 0.4-4.0 cm/s.

Site B: The 7-month (March through Oct.) average flow speed at the intermediate depth site was 2.3 cm/s \pm 0.1

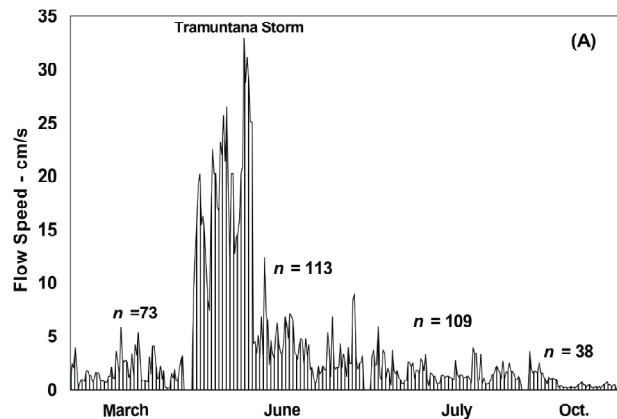


Figure 2. Proximal flows at the 4.5 m Site A, March through October 2006. The Tramuntana storm period of late May-early June is labeled, as are the number of measures for each of the field-trips.

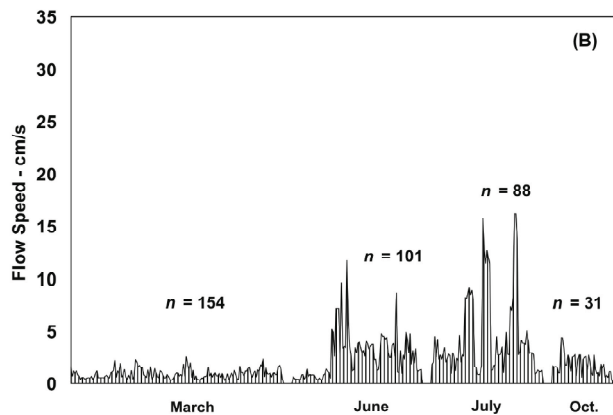


Figure 3. Proximal flows at the 8.8 m Site B, March through October 2006. The number of measures for each of the field-trips are shown above the corresponding month.

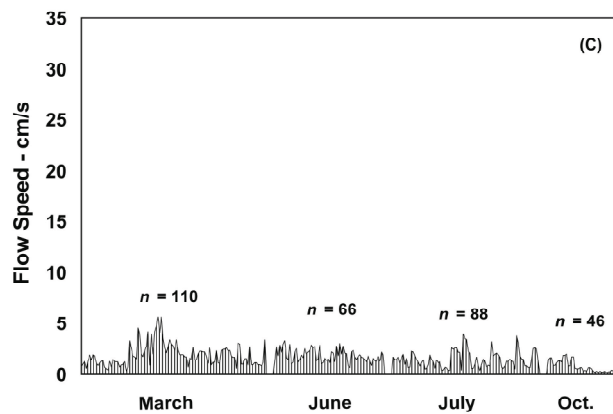


Figure 4. Proximal flows at the 14.3 m Site C, March through October 2006. The number of measures for each of the field-trips are shown above the corresponding month.

SE, range 0.3-16.3 cm/s (Fig. 3). On 5 June, after the full force of the Tramuntana storm had passed sponge B-6 (B-annex subsite) experienced the highest flows recorded at the B site (7 measures > 5 cm/s, one measure 11.8 cm/s). Less expected were the high flows recorded for the same sponge in calm seas on 25 July (6 measures > 7 cm/s, highest, 16.3 cm/s).

Site C: The 7-month (March through Oct.) average flow speed at the deepest of the three sites was $1.6 \text{ cm/s} \pm 0.05 \text{ SE}$, range 0.2-5.67 cm/s (Fig. 4).

Figure 5 presents results of 1,015 thermistor flow-sensor measurements made in close proximity (i.e., ≈ 2 cm of the sponge surface) to 15 *Dysidea avara* sponges (5 each from Sites A, B, and C) over the four field-trips in 2006. The overall average proximal flow speed for all depths, sea conditions and seasons was $2.6 \text{ cm/s} \pm 0.15 \text{ SE}$. In calm seas the average flow was only $1.6 \text{ cm/s} \pm 0.03 \text{ SE}$. In stormy seas the average proximal flow was $5.9 \text{ cm/s} \pm 1.7 \text{ SE}$. Proximal flows followed the expected distribution (decreasing exponentially with depth)



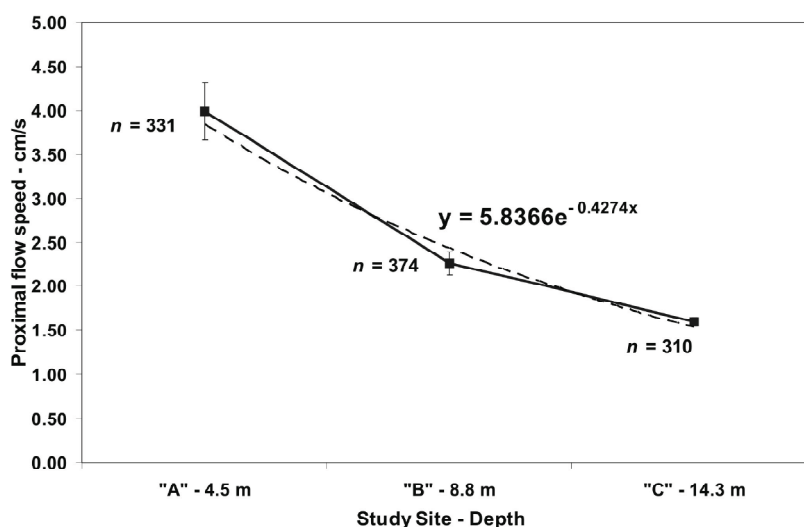


Figure 5. Proximal flows (cm/s) measured close to *Dysidea avara* sponges in relation depth and site from March to October 2006. Error bars show ± 1 standard error of the means (the very small error bars for the C-site data are not visible). The dashed trendline shows a best-fit exponential equation to the mean data points at each depth.

with the highest flows and greatest variability recorded at the shallowest site, followed by the intermediate site, with the deepest site showing the lowest proximal flow speeds and the smallest variation. Flows at the three depths differed significantly from each another (single factor ANOVA $P = < 0.001$).

Flow visualization

Fifty-seven, 1-2 minute movies were made of flow regimes around individual sponges. The results showed that the most prevalent flow regime at all depths and at all times of year was oscillatory, *i.e.* back-and-forth flow over and around a sponge in a more or less horizontal plane, with smaller magnitude vertical flow components overlain. The range of periodicity of the oscillation was timed at 12-20 cpm (0.20 Hz-0.33 Hz). The residence time of a given mass of water hovering and lingering over a particular sponge was timed at 0.75-1.5 minutes depending on oscillation frequency.

Sponge morphotypes

Figure 6 (a, b, c) show the distinctive sponge morphotype predominating at each of the three main depth sites. Site A sponges (4-5 m depths, Fig. 6a) were in-general smaller, more compact, and more thinly-incrusting than the sponges at either of the other two sites. Site A sponges generally possessed smaller oscula than did Site B sponges, however most specimens possessed a few larger oscula placed on raised but not conspicuously elevated protuberances.

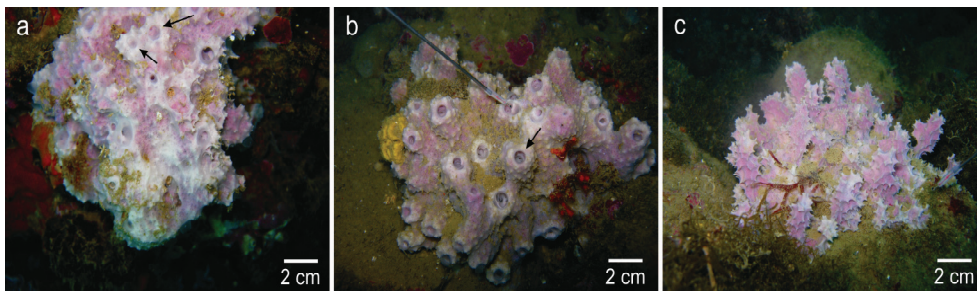


Figure 6. Typical morphotypes of *Dysidea avara* sponges from the three depth sites. (a) Site A, 4.5 m; arrows point to oscula on two short, connected protuberances; (b) Site B, 8.8 m; arrow points to large osculum on tall protuberance; note: thermistor probe positioned over very large osculum; (c) Site C, 14.3 m; thermistor probe is seen positioned near base of sponge and to the right in photo. Note: buildup of organic matter on the substratum between the erect, heavily-conulated “fingers” of this specimen.

The sponges located under the protected overhang of the mini-cave of the B-main subsite (Fig. 6b) exhibited more erect and massive body forms than did sponges from either sites A or C. Sponges at the B-main subsite had large oscula (up to 10 mm diameter) each located at the apex of a thick protuberance rising 3-5 cm above the mean body surface. B-annex subsite sponges were of a more flattened morphotype than those inside the mini-cave, but they also possessed elevated, thick protuberances with large terminal oscula.

Sponges at Site C (Fig. 6c) were always distinctly erect, heavily branched and heavily conulated with conspicuously small oscula not placed at the highest extremities of their branches.

Oscula of the sponges were not open in all cases. In high flow conditions (*e.g.* during the Tramuntana storm in early June) oscula exposed to these higher flow conditions were closed. An example of such an event is shown in Fig. 7. This is a sponge at Site B, the oscula on the front side are exposed to high flow conditions and are closed, while oscula at the backside are protected against flow (facing the wall of the cave) and are open.

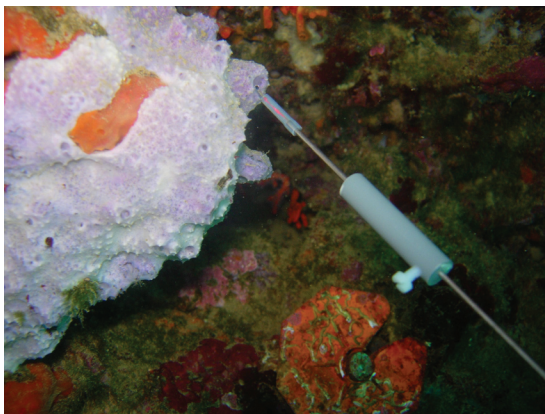


Figure 7. Sponge at Site B, with thermistor probe placed above an osculum. The left side of the sponge shows oscula that are facing the unprotected opening of the “mini-cave” and are exposed to higher flow conditions. The right side of the sponge is facing the rear cave wall where there is less flow; and the oscula are open.



DISCUSSION

Proximal vs. vicinity flow regimes

We found mean proximal flows around individual sponges were quite low, ranging from 1.6 cm/s to 4.0 cm/s (except during infrequent storms). Our use of two complimentary flow measuring instruments showed us the local bulk ocean current velocity (which averaged 10–12 cm/s over the course of our study) is significantly higher than the flow very close to the sponges. Our findings agree with classical physical oceanographical works which instruct that water velocity near the bottom in the shallow sublittoral zone will be much lower than the bulk current velocity in the local water column (Hiscock, 1983, Nowell and Jumars, 1984, Sverdrup *et al.* 1961).

Flow visualization studies

Under the influence of surface waves, the near-bottom flow regime in the shallow sublittoral is mostly oscillatory (Bascom, 1964; Hiscock, 1983; Nowell and Jumars, 1984). Our results confirmed this axiom, and showed that a given water mass in an oscillating regime hovered and lingered over an individual sponge for a longer period than would a water mass transported by unidirectional flow of the same mean velocity. As each oscillation passed through the near zero velocity cross-over point the slightly heavier than water latex particles (mimics of natural planktonic food) sank a bit closer towards the surface of the sponge. The morphology of the sponge then came into play acting to further extract momentum from the moving water mass and increase the particle settling rate (as was demonstrated in modeling studies for various classes of benthic organisms by Abelson *et al.* 1993).

From published studies on sponge fluid mechanics (Riisgård *et al.* 1993, and Vogel, 1977, 1994) we know that the micrometer-sized ostia take-in food particles under a slight negative pressure generated by the pumping action of the choanocytes driving water out of the oscula. Based on our field observations (supported by the findings of others who studied the consequences of oscillatory flow and particle capture for other benthic invertebrates and macrophytes, *e.g.* Denny *et al.* 1985; Hunter, 1989; Koehl, 1982; Leonard *et al.* 1988), we initiated flow-tank and computer modeling studies to test the hypothesis that an oscillatory flow regime worked together with sponge morphology to enhance food particle inflow rates in *Dysidea avara* (to be submitted).

Sponge body forms and water flow regimes

From results of modeling studies Denny *et al.* (1985) and Denny (1994) concluded that the mechanical limits of strength of tissues dictate that benthic invertebrates are smaller in size in wave-swept zones than their cohorts from deeper more protected zones. In a more recent study, Denny (2006) calculated safety factors against breakage for a number of organisms



living in the wave-swept environment, and concluded that there was a significant amount of “over-design” (or adaptation) in body plans to cope with the extreme forces under which these organisms normally live. Koehl (1999), following on the original work of Alexander (1981) on distribution of strengths and stresses in populations of animals, proposed the concept of ‘environmental stress factor’ which she suggests is an ‘age- and *season-dependent* safety factor.’

When compared to sponges from the deeper B and C sites, the more compact Site A sponges support the theoretical models of these authors. The smaller, more rounded and compacted body shapes of the A-site sponges can be considered an adaptation to their seasonal exposure to the large forces generated by storm-driven waves. The intermediate depth B-main sponges were the largest of all sponges surveyed. They possessed the tallest protuberances with the largest terminal oscula. Their shape is correlated with the generally low flows found within their protected mini-cave habitat, and is supported by the concept that oscula placed high on protuberances help insure maximum separation of ejected metabolic wastes and new oxygenated water and food particles entering the ostia at the surface of the sponge (Vogel, 1977, 1994).

Also interesting for the B-site overall, are the intermediate-level proximal flows (7-16 cm/s) recorded during the June and July study periods (Fig. 3). This relative high range (in the context of our results) could be explained by the “alley-like” bathymetry of the B-site and the presence of the large through-tunnel, which together acted to funnel wave energy back and forth through the rather narrow walled site and up-and-back through the tunnel, increasing local flows — especially for the more-exposed B-annex sponges.

C-main and C-annex sponges showed the same highly-branched and heavily conulated body forms, reflecting the generally low flow regimes found throughout the C-site. Their tall, scalloped-edged, finger-like processes together with the occurrence of many small oscula could be viewed as adaptations to increased levels of sedimentation (Jackson, 1979, Bell and Barnes, 2000). Although Site C sponges were never observed to be smothered with sediment (which is mostly larger-grained sand in this zone), we did commonly see layers of fine organic matter built-up on the substratum spaces between the finger-like processes of C-site sponges (visible in Fig. 6 c). Associated with this organic matter are large populations of microorganisms, which together with ultra-fine organic particles could become food for the sponge whenever portions of the trapped debris were re-suspended and thereafter settled-out onto the ostial fields of the sponge.

Anatomical adaptations to high flow

Dysidea avara is not supported by a stiff silicious skeleton as are other species known from stronger flow regimes (Palumbi, 1986, Bell and Barnes, 2000). Its skeleton is composed of criss-crossing spongin fibers. Considering its relatively fragile body type one might conclude

this sponge runs the risk of being torn apart by high wave forces such as those encountered seasonally at our Site A.

However, *Dysidea* exhibits three behaviors and/or anatomical adaptations which contribute to its ability to colonize and survive in high-flow environments. First is its habit of taking-up sand grains and other inorganic particles to stiffen primary skeletal fibers (Teragawa, 1986). Second is its ability to grow into a compact drag-reducing body form in high-flow regimes. And the third is its tensile structure body plan (Otto, 1962) first demonstrated by Teragawa (1985) with *Dysidea etheria*, when she showed that the surface membrane was under constant tension while the membrane-supporting main skeletal fibers were in constant compression.

Thus the entire *Dysidea* body plan allows the organism to bend, flex and deform under the influence of the forces imparted by waves. We observed such adaptive flexing, bending and vibrating of the Site A sponges during the early-summer Tramuntana storm as they resisted the potentially damaging forces of the waves.

CONCLUSIONS

We have shown that at one rocky coastal site on the Northwestern Mediterranean coast, *Dysidea avara* sponges live primarily in low, oscillating flow microhabitats afforded protection by rock cover and/or depth. The sponge adjusts and adapts its body plan to the prevailing flow regime attaining a variety of morphotypes found at differing depths and flow microhabitats.

These findings have implications for *in situ* ecological studies of feeding, growth and behavior of sponges in general. Moreover, the information gained should help aquaculturists set or select optimal flow regimes for tank or in-sea cultures of *Dysidea avara* for natural product production.

Proximate flows are low (< 5 cm/s). In our culture tanks flow is generally higher (e.g., Khalesi *et al.* 2007, worked with flows in the range of 3-20 cm/s). For successful *ex situ* cultivation the flow conditions need to be adapted to conditions found in nature. It was clearly demonstrated that variations in the low flow observed in the field resulted in different morphologies of the sponges. The consequence of different flow regimes and morphologies will be further studied in our laboratory using a flow tank and particle tracking velocimetry. Results from these studies will provide us the flow information needed to design culture tanks suitable for effective production of avarol from *Dysidea avara*.

ACKNOWLEDGEMENTS

This study was financially supported by EU Project No. 017800. We acknowledge diving assistance of Marieke Koopmans, Marzia Sidri, and Detmer Sipkema. We thank the Fentons for their gracious generosity in providing their seaside villa at Cala Illa Mateua for use as our



dive expedition headquarters. We thank Hans Meijer of the WUR/ATV electronics shop for his innovative design and fabrication of the thermistor and 3-D Doppler instrument packages, and Jos van den Boogaart WUR/EZO for facilitating the calibration tows of the thermistor probe, and help with graphics for the manuscript.

REFERENCES CITED

- Abelson, A., T. Miloh, Y. Loya. 1993. Flow patterns induced by substrata and body morphologies of benthic organisms, and their role in determining availability of food particles. *Limnol. Oceanogr.* **38**: 1116-1124.
- Alexander, R. McN. 1981. Factors of safety in the structure of animals. *Sci. Prog.* **67**: 109-130.
- Bannister, R. J., R. Brinkman, C. Wolf, C. Battershill, and R. de Nys. 2007. The distribution and abundance of dictyoceratid sponges in relation to hydrodynamic features: identifying candidates and environmental conditions for sponge aquaculture. *Mar. and Fresh. Res.* **58**: 624-633.
- Barthel, D. 1991. Influence of different current regimes on the growth form of *Halichondria panicea* Pallas. In: J. Reitner and H. Keupp (Eds.) *Fossil and Recent Sponges*. Springer-Verlag, Berlin, Heidelberg.
- Battershill, C. N. and M. J. Page. 1996. Sponge aquaculture for drug production. *Aquaculture Update* **16**: 5-6.
- Bascom, W. 1964. *Waves and beaches. The dynamics of the ocean surface*. Doubleday & Co., New York.
- Bell, J. J., and D. K. A. Barnes. 2000. The influence of bathymetry and flow regime upon the morphology of sublittoral sponge communities. *J. Mar. Biol. Assoc. U.K.* **80**: 707-718.
- Bell, J. J., D. K. A. Barnes, and C. Shaw. 2002a. Branching dynamics of two species of arborescent demosponge: the effect of flow regime and bathymetry. *J. Mar. Biol. Ass. U.K.* **82**: 279-294.
- Bell, J. J., D. K. A. Barnes, J. R. T. Turner. 2002b. The importance of micro and macro morphological variation in the adaptation of a sublittoral demosponge to current extremes. *Mar. Biol.* **140**: 75-81.
- Bell, J. J., *et al.* 2006. Morphological monitoring of subtidal sponge assemblages. *Mar. Ecol. Prog. Ser.* **311**: 79-91.
- Bidder, G. P. 1923. The relation of the form of a sponge to its currents. *Quart. J. Microscop. Soc.* **67**: 292-323.
- Denny, M. W. 1994. Extreme drag forces and the survival of wind and water-swept organisms. *J. exp. Biol.* **194**: 97-115.
- Denny, M. W. 2006. Ocean waves, nearshore ecology, and natural selection. *Aqua. Ecol.* **40**: 439-461.
- Denny, M. W., T. L. Daniel, and M. A. R. Koehl. 1985. Mechanical limits to size in wave-swept organisms. *Ecol. Monogr.* **55**: 69-102.
- Hill, M. S., and A. L. Hill. 2002. Morphological plasticity in the tropical sponge *Anthosigmella varians*: responses to predators and wave energy. *Biol. Bull.* **1202**: 86-95.
- Hiscock, K. 1983. *Water Movement*. In: Earll & Erwin (eds.) *Sublittoral Ecology*. Clarendon Press, Oxford.
- Hunter, T. 1989. Suspension feeding in oscillatory flow: the effect of colony morphology and flow regime on plankton capture by the hydroid *Obelia longissima*. *Biol. Bull.* **176**: 41-49.
- Jackson, J. B. C. 1979. Morphological strategies of sessile animals. In: *Systematics Association Special Volume No. 11*, pp. 499-555, "Biology and Systematics of Colonial Organisms", G. Larwood and B.R. Roser (eds.). Academic Press, London and New York.
- Kaandorp, J. A. 1999. Morphological analysis of growth forms of branching marine sessile organisms along environmental gradients. *Mar. Biol.* **134**: 295-306.

- Khalesi M. K., H. H. Beefink, and R. H. Wijffels 2007. Flow-dependent growth in the zooxanthellate soft coral *Simularia flexibilis*. *J. Exp. Mar. Biol. Ecol.* **351**: 106-113.
- Koehl, M. A. R. 1982. The interaction of moving water and sessile organisms. *Sci. Amer.* **247**: 124-132.
- Koehl, M. A. R. 1999. Ecological biomechanics of benthic organisms: life history, mechanical design and temporal patterns of mechanical stress. *J. Exp. Biol.* **202**: 3469-3476.
- Leonard, A. B., J. R. Strickler, and N. D. Holland. 1988. Effects of current speed on filtration during suspension feeding in *Oligometra serripinna* (Echinodermata Crinoidea). *Mar. Bio.* **97**: 111-125.
- Meroz-Fine, E., S. Shefer, and M. Ilan. 2005. Changes in morphology and physiology of an East Mediterranean sponge in different habitats. *Mar. Biol.* **147**: 243-250.
- Minale, L., R. Riccio, and G. Sodano. 1974. Avarol, a novel sesquiterpenoid hydroquinone with a rearranged drimane skeleton from the sponge *Dysidea avara*. *Tet. Lett.* **38**: 3401-3404.
- Müller W. E. G., A. Maidhof, R. K. Zahn, H. C. Schröder, M. J. Gasic, D. Heidemann, A. Bernd, B. Kurelec, E. Eich, and G. Sibert. 1985. Potent antileukemic activity of the novel cytostatic agent avarone and its analogues *in vitro* and *in vivo*. *Cancer Research* **45**: 4822-4827.
- Otto, Frei (ed.). 1962. Tensile Structures. Vols. 1 & 2. M. I. T. Press, Cambridge and London.
- Nowell, A. R. M., and P. A. Jumars. 1984. Flow environments of aquatic benthos. *Annu. Rev. Ecol. Syst.* **15**: 303-28.
- Palumbi, S. R. 1984. Tactics of acclimation: morphological changes of sponges in an unpredictable environment. *Science*. **225**: 1478-1480.
- Palumbi, S. R. 1986. How body plans limit acclimation: responses of a demosponge to wave force. *Ecol.* **67**: 208-214.
- Pietschmann, R., M. Shatton, and W. Schatton. 2004. EU patent number EP1391197. Application number: EP20030016673 20030801. Munich, DE.
- Pronzato, R., G. Bavestrello, and C. Cerrano. 1998. Morpho-functional adaptations of three species of Spongia (Porifera, Demospongiae) from a Mediterranean vertical cliff. *Bull. Mar. Sci.* **63**: 317-328.
- Reiswig, H. M. 1971. *In situ* pumping activities of tropical Demospongiae. *Mar. Biol.* **9**: 38-50.
- Reiswig, H. M. 1974. Water transport, respiration and energetics of three tropical marine sponges. *J. Exp. Mar. Biol. Ecol.* **14**: 231-249.
- Riedl, R. 1977. Water Movement. In: O. Kinne (ed). Marine Ecology. John Wiley & Sons, Chichester.
- Riisgård, H. U., S. Thomassen, H. Jakobsen, J. M. Weeks, P. S. Larsen. 1993. Suspension feeding in marine sponges *Halichondria panicea* and *Haliclona urceolus*: effects of temperature on filtration rate and energy cost of pumping. *Mar. Ecol. Prog. Ser.* **96**: 177-188.
- Sipkema, D., R. Osinga, W. Schatton, D. Mendola, J. Tramper, and R. H. Wijffels. 2005. Large-scale production of pharmaceuticals by marine sponges: sea, cell or synthesis? *Biotechnol. Bioeng.* **90**: 201-222.
- Sipkema, D., N. A. M. Yosef., M. Adamczewski, R. Osinga, D. Mendola, J. Tramper, and R. H. Wijffels. 2006. Hypothesized kinetic models for describing growth of globular and encrusting demosponges. *Marine Biotechnol.* **8**: 40-51.
- Sverdrup, H. V., M. V. Johnson, and R. H. Fleming. 1961. The Oceans, Their Physics, Chemistry and General Biology. Prentice-Hall, Englewood, N. J. [tenth printing] Pp. 518, 519, 585.
- Teragawa, C. K. 1985. Mechanical function and regulation of the skeletal network in *Dysidea*. In: New Perspectives in Sponge Biology. Ed. K. Rützler. Third Internat. Conf. on Biol. of Sponges. Woods Hole, MA, USA. Smithsonian Institution Press, Washington, D.C. Pp. 252-258.
- Teragawa, C. K. 1986. Particle transport and incorporation during skeleton formation in a keratose sponge: *Dysidea etheria*. *Biol. Bull.* **170**: 321-334.
- Uriz, M. J., D. Rosell, and D. Martin. 1992. The sponge population of the Cabrera archipelago (Balearic Islands): Characteristics, distribution and abundance of the most representative species. PSZN I: *Mar. Ecol.* **113**: 101-117.



- Uriz, M. J., X. Turon, J. Galera, and J. M. Tur. 1996. New light on the cell location of avarol within the sponge *Dysidea avara* (Dendroceratida). *Cell Tissue Res.* **285**: 519-527.
- Vogel, S. 1977. Current-induced flow through living sponges in nature. *Proc. Natl. Acad. Sci.* **74**: 2069-2071.
- Vogel, S. 1994. *Life in Moving Fluids*. 2nd ed. Princeton University Press, Princeton, N. J.



Chapter 4 Morphology induced flow patterns by *Dysidea avara* sponges in a flow tank

D. Mendola^{1,2}, J. G. M. van den Boogaart², R. H. Wijffels¹, J. L. van Leeuwen^{2*}

¹Bioprocess Engineering Group, ²Experimental Zoology Group, Wageningen University, P.O. Box 8129, 6700 EV, Wageningen, The Netherlands * e-mail: johan.vanleeuwen@wur.nl

Abstract: We studied how whole body shape and cm-scale morphological features (protuberances) of the marine sponge *Dysidea avara* affected local flow-fields around live specimens in a flow tank. Flow speeds were varied from 0 to ≈ 13 cm/s in both uni-directional and oscillating modes modeled after natural flow regimes. High-speed video and particle-tracking velocimetry (PTV) was used to calculate particle velocities, streamlines and vorticity in 2-D. We observed regions of lowered velocity, higher vorticity and local vortices close to the sponge. Morphology-induced flow patterns varied greatly between specimens and experiments, were highly ephemeral in nature, and difficult to predict. Results illustrated the high degree of complexity of 3-D flow-fields surrounding complex-shaped sponges, even when placed into a laminar flow stream in a flow tank. We hypothesized that the complex morphology of this species acted to redirect fluid momentum and passage of potential food-sized particles over the sponge, sometimes causing particles to become trapped within lower velocity water masses between protuberances, becoming more available for influx and ingestion. Due to laser light scattering and low particle abundance close to the sponge, PTV methods could not resolve flow effects within 0.5 mm of the sponge surface. Therefore, we could not study possible flow modulating effects of the 0.3-1.6 mm cone-shaped conules. We propose that CFD would be a good tool for studying such fine-scale flow effects, as well as sensitivity of net influx to variations in surface features.

Key words: sponge, flow tank, morphology, flow patterns, particle capture





INTRODUCTION

Dysidea avara (Schmidt, 1862) is a keratose, encrusting marine sponge known from the rocky sublittoral Mediterranean to at least 55 m depths (Uriz *et al.* 1992). It is most often found in sheltered low-oscillating flow (0-10 cm/s) environments. However, some individuals do settle and survive to adult size in protected near-surface habitats where seasonally high flows occur (Mendola *et al.* 2007a). The sponge often shows a plethora of finger-like protuberances each capped by an osculum. Covering its entire dermal surface (including the protuberances) are small (0.3-1.6 mm) cone-shaped protrusions called conules, formed from up-lifting of the dermal membrane by the primary skeletal fibers (Teragawa, 1985). The sponge is desired by man for its valuable bioactive secondary metabolites avarol and avarone (Müller *et al.* 1986, Minale *et al.* 1974, Uriz *et al.* 1996). Aquaculture has been proposed (Sipkema *et al.* 2005) for obtaining supplies of the sponge and its metabolites, as a sustainable alternative to exploitive natural collections.

The *effects of flow on morphology of sponges* is dealt with almost exclusively in the literature in an environmental context, where sponge shape and species distributions are related to differences in environmental water flow regimes (*e.g.* Bell *et al.* 2000, 2002a, 2002b). The reverse theme, the *effects of morphology on flow* has been less often discussed.

Witte *et al.* (1997) studied the effects of sponge (*Thenia abyssorum*) shape on local flow and food particle capture using a 3-D Doppler velocimeter mounted above a flume. Boundary layers above and behind two, small (dead) specimens were disturbed by the shape and size of the sponges, with the influence extending 14 cm down-stream and several cm on either side of the largest of the two specimens. Turbulence intensity rose from 20% in front to 160% behind the specimens, where “leeward deceleration of the flow occurred.” The authors proposed that vortex-aided particle deceleration and downward particle motion on the leeward side of test specimens aided food particle capture in this deepwater Norwegian sponge.

Abelson *et al.* (1993) also looked at the role of body morphology in determining the availability of food particles for sessile marine invertebrates. A fluid dynamic model was developed on the supposition that benthic organisms with differing “slenderness ratios” (SR; height-to-width) would encounter particles with differing nutritional and mechanical characteristics. Results showed the low (< 0.05) SR-ratio group would be exposed to more particles of larger size, while the high (> 1.0) SR-ratio group would experience a flux of more particles of smaller size (*e.g.* $< 2 \mu\text{m}$). Also discussed was a possible complimentary role for “wake trapping”, *i.e.*, the effect of eddies generated by morphology on the behavior of particles entrained in the flow-stream. Although the authors suggested morphology-induced eddies would increase the local concentration of particles, unfortunately no data were presented for such eddy-trapping effects. They also expected that substrate (abiotic) morphology should play a crucial role in particle flux and availability (*and we suggest the*



morphology of neighboring benthos as well) but no data were presented to support such effects.

The primary aim of this research was to study the effects of surface morphological features of *Dysidea avara* sponges on flow passing over live specimens in a flow tank. Our hypothesis was that the complex morphology of this species acted to redirect fluid momentum and passage of potential food-sized particles over the sponge, sometimes causing food particles to become trapped within lower velocity water masses between protuberances, and between inter-conule “mini-valleys” where they would become more available for influx and ingestion by the sponge.

MATERIALS AND METHODS

Specimen collection and maintenance

Nine, small-size (15-50 cm³) *Dysidea avara* specimens were collected at 9-12 m depth on pieces of native rock from the L’Escala region in N.E. Spain. Specimens were transported to The Netherlands (NL) and maintained in a 550 liter aquarium with bio-filtration over a period of 3-months. Sponges were fed twice daily with marine broths made from fish and shrimps, and/or manufactured shellfish diets (INVE, Belgium CAR-1 & SELCO), and 3-4 times per week with cultured micro-algae (*Phaeodactylum tricornutum*, *Nannochloropsis* sp.); total starting concentrations 2×10^5 to 3×10^5 particles/ml.

Flow-tank set-up in the laboratory

A 7.5 liter Perspex plastic laminar flow tank (Fig. 1) was specially-built for flow tracing experiments with live *Dysidea avara* sponges, within the normal range of flow velocities found around individual sponges in nature (*i.e.*, zero-13 cm/s). The horizontal, vertically-recirculating water path was controlled by a DC motor-driven paddlewheel connected to a regulated DC power supply, reversing relay and timer. This arrangement allowed for unidirectional or bidirectional oscillatory flows over a pre-set frequency range of 0.1-1.0 Hz. The working section of the flow tank (18 cm x 12 cm x 6 cm) was isolated from the bulk volume of the flow-stream by two banks of flow straighteners made from formed blocks of thin-walled polypropylene straws, each with an internal diameter of 5.7 mm. The upper limit for maintaining laminar flow within the working section (without a sponge sample in-place) was approximately 13 cm/s (in either direction), however non-laminar flows at higher velocities could be produced.

Flow tank set-up in the field

A second flow-tank and PTV set-up was installed for a 1-week period in a temporary laboratory assembled near the collection site in Spain. The intent was to test for any difference in behavior and/or performance between freshly-collected, and longer-term laboratory-reared sponges.



Unfiltered natural seawater at ambient temperature/salinity was used for the Spain set-up, with only added glass beads for flow tracing (no algae). Of 12 freshly-collected sponges, 7 were pumping sufficiently to be used as subjects either in the 7.5 l flow tank and/or in a larger 20 l capacity flow tank. We recorded 193 flow experiments in Spain, 10 of which used oscillating background flow regimes; the remainder used unidirectional flow regimes.

Particle velocity measurements

Prior to commencing flow-tracing experiments the flow tank was filled with 30 μm sand-filtered seawater taken from the sponge holding tank. The flow tank was seeded with either cultured microalgae (*Nanochloropsis* sp., 3–4 μm dia., or *Isochrysis galbana*, 6–8 μm sickle-shaped rods) or pre-soaked 0.5–6.0 μm dia., hollow, and nearly neutrally buoyant glass beads (J. J. Bos, NL) to attain a particle density of *ca.* 100,000 particles/ml. Particle density was checked regularly and kept at *ca.* 100,000 particles/ml. The particles were required to reflect laser light for tracing particle paths over, into (ostia) and out of (oscula) of the live sponge specimens.

A laser light sheet (0.5 mm width) was projected downward into the flow tank from an Excel 2300 laser solidly mounted onto a cement wall behind the tank. A high-speed (50–500 fps) video set-up employed a Redlake® Motionopro 10,000 digital camera back coupled to a Nikon® 105/1:2.8 lens and 50 mm extension ring, all mounted on a sturdy tripod. The camera lens was oriented perpendicular to the vertical light sheet by arranging its front surface as close to parallel with the laser light sheet as visually possible. Images were captured onto a PC using Redlake's Midas Player® software and analyzed using Matlab® with embedded sub-routines. Routines written in MatLab® were used to compute velocity vectors from tracked particles locations and to produce interpolated vector plots on an equidistant 0.5 mm x 0.5 mm grid, using three sequential video frames.

Flow-tracing experiments were run periodically over a 3-month period, rotating between three different specimens depending upon which specimen was pumping at what appeared like a normal rate on any particular day. “An experiment” constituted one run under a given set-up using one velocity setting, one flow direction, one animal position and orientation, one laser light-sheet position, and a given camera setting and position. Once all parameters were set-up, the laser was turned-on and a 5–10 s digital movie was recorded. The set-up and flow parameters were then either left the same or changed for the next experiment (most often in a logical sequence of moving up or down the velocity scale in steps of approximately 0.5 cm/s, or at other times changing the orientation of the sponge or even changing sponges altogether, etc.).

The set-up and flow parameters were then either left the same or changed for the next experiment (most often in a logical sequence of moving up or down the velocity scale in steps of approximately 0.5 cm/s, or at other times changing the orientation of the sponge or even changing sponges altogether, etc.).

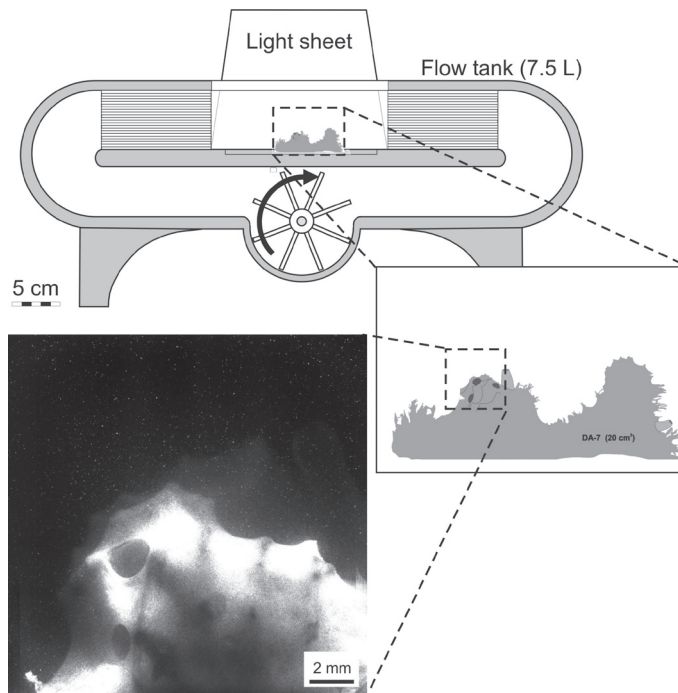


Figure 1. Schematic drawing of the 7.5 L Perspex, paddlewheel-driven flow tank, showing sponge DA7 in-place within the working section of the flow tank between two banks of flow straighteners. The laser light sheet enters the tank from above parallel to the front and rear planes of the tank. One frame from the video movie is shown in the lower left-hand corner, and dotted projection lines indicate the portion of the sponge that is in view in the video frame. Sponge drawing was traced from a photo of the sponge, and is therefore close to its actual form.

For each set-up we filmed a piece of a plastic centimeter scale placed in the focal plane next to the sponge specimen under normal light and relatively high magnification. This calibration served to compute dimensions of the specimen, its morphological features and particle velocities. For each set-up, boundary layers on all sides of the chosen specimen were calculated to make sure the specimens were well within the free-stream flow section of the tank for the flow velocities used (see Mendola *et al.* 2007b, on-line materials for a description of boundary layer calculations). Over the 3-month study 136 separate experiments were recorded at the NL facility, 129 with unidirectional and 7 with oscillating background flows.

Data analysis

After reviewing the video tapes of nearly all of the flow-tank experiments, 41 experiments deemed representative (e.g., showing a variety of morphological effects on flow around the sponge specimens) were selected for detailed data analysis. These comprised two experiments with oscillating background flow; 22 experiments with right-to-left unidirectional flow; and 19 experiments with left-to-right unidirectional flow.



For one oscillating flow experiment (CMV-1505) we tracked 800-1200 (approximately) evenly-distributed particles in each of three sequential video frames. This many particles were required to analyze the flow-fields in detail and to accurately calculate and plot vorticity within the frames. For 41 experiments chosen for less detailed analysis (included a second set of frames from CMV-1505) we reduced the time-intensive procedure of tracking 800-1200 particles in each of three video frames, and instead tracked 30-50 particles in and around four strategically-chosen digital windows on three sequential video frames (Fig. 2). The 1 mm x 1 mm digital windows were selected as representative sections of the flow-fields on either side of sponge protuberance. Close to the sponge “flanks” we identified windows C & D, and in the free-stream regions of the flow-field, windows A & B.

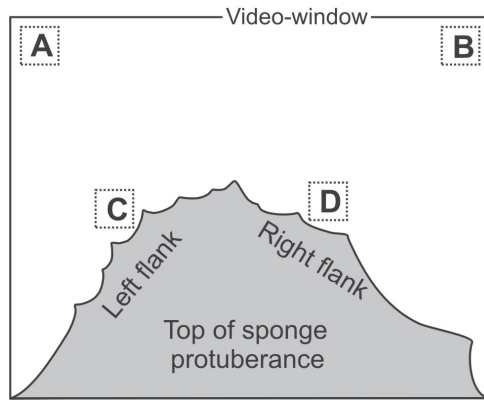


Figure 2. Schematic representation of one video frame showing the portion of the sponge protuberance in view, and the approximate locations of four scaled 1 mm x 1 mm digital windows where particles were manually tracked. Note: Entire video frame size is 15 mm x 15 mm.

Matlab sub-routines calculated and plotted individual particle velocities, streamlines, velocity contours (isotachs) and vorticity computed from the interpolated velocity vectors. This method resulted in near instantaneous 2-D velocity and vorticity distributions. Vorticity in the analysis plane $\left(\omega = \frac{\partial v}{\partial x} - \frac{\partial u}{\partial y} \right)$ was numerically approximated using the Stokes theorem

(integration was used to find the circulation around a point in continuum space):

$$\omega_{i,j} = \frac{1}{8\Delta x\Delta y} [\Delta x(u_{i-1,j-1} + 2u_{i,j-1} + u_{i+1,j-1}) + \Delta y(v_{i+1,j-1} + 2v_{i+1,j} + v_{i+1,j+1}) - \Delta x(u_{i+1,j+1} + 2u_{i,j+1} + u_{i-1,j+1}) - \Delta y(v_{i-1,j+1} + 2v_{i-1,j} + v_{i-1,j-1})], \quad (1)$$

where u , v are the velocity components in the x - and y -direction, while indexes i and j indicate the location in the computational grid.



RESULTS

Reynolds number calculations

To understand if turbulence should be expected around whole sponges and/or single protuberances, biometric measures and Reynolds number (Re) calculations were made using dimensions measured from photographs of eight sponges (Table 1). Only protuberances which were in a measurable projection on the photograph were measured. We chose 5 cm/s for the Re calculations, as this was a nominal “proximal” flow velocity measured *in situ*. (Note: “proximal” flow was recorded within 2 cm of the sponge surface and 2-4 cm from the local substratum next to individual sponges in nature; Mendola *et al.* 2007a). Five cm/s flow speed was also within the range of background flows applied in the flow-tank experiments. The results revealed Reynolds numbers that exceeded the range where turbulence could be expected due to the presence of whole sponges and/or single protuberances.

Sponge	Sponge diameter, long axis (mm)	Sponge diameter, short axis (mm)	Re at BV 5 cm/s Whole sponge	Protuberance avg. diameter (mm \pm STD)	Re at BV 5 cm/s Protuberances
C – site/ruler	127.08	113.83	5736	20.57 \pm 1.49	980
DSC-1237	127.1	78.82	4902	12.17 \pm 2.94	579
DAL – Spain lab	72.33	52.21	2965	19.01	905
C – site summer '06	76.19	55.72	3141	8.73 \pm 1.11	416
B – site #3	107.91	71.33	4267	10.03 \pm 0.97	478
DSC-338	128.62	87.64	5149	6.87 \pm 1.20	327
B – site #4	96.89	51.19	3526	7.57 \pm 1.38	360
DSC-332	79.93	60.04	3333	10.52 \pm 2.46	501

Table 1. Reynolds number calculations for whole sponges (column 4) and protuberances (column 6) at nominal background velocities encountered by *Dysidea avara* specimens in nature.

Sponge experiments

Figure 3 shows the oscillatory flow cycle from experiment CMV-1505, and the time points where individual frames were analyzed. Figs. 4 (a-f) and 5 (a-f) present PTV results from experiment CMV-1505 at the corresponding time points of the oscillatory flow cycle indicated in Fig. 3.

Given the high magnifications used in the flow tank experiments only a part of one protuberance could be in view at one time. The sponge used in experiment CMV-1505 possessed two major protuberances separated by a “valley” region (Fig. 1). In each of the panels of Figs. 4 and 5, only the left major protuberances is shown with traced black outlines. The part of the

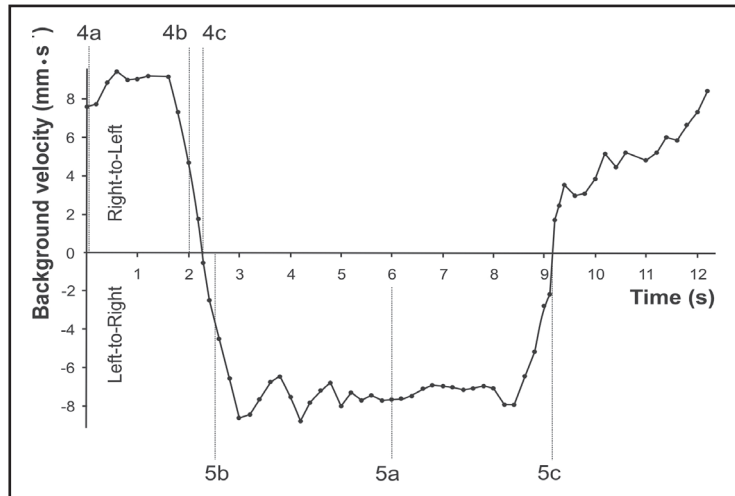


Figure 3. Oscillatory flow-cycle of experiment CMV-1505 showing time points chosen for detailed particle tracking analyses presented in Figures 4 & 5 panels a, b, c, respectively. Background velocities were measured within the reference windows (A & B) shown in the video frame in Fig. 2.

sponge that is in front of the laser-light sheet is enhanced with a photographic overlay (grey colored surface covered with small conule “bumps”). The part of the sponge that is *within and behind* the laser-light sheet is enhanced with a semi-transparent photographic overlay.

Figures 4 & 5 are constructed from PTV data analyzed from three sequential frames of the 500 fps digital movie from experiment CMV-1505, and thus represent a 0.006 s “snapshot” in time of the flow-field moving past the sponge protuberance. Panels *a*, *b* and *c* show speed contours, streamlines and velocity vectors, and panels *d*, *e*, and *f* of both figures plot vorticity.

Figure 4 – right-to-left flow direction

In Fig. 4 panel *a*, we see three discrete regions of the 2-D flow-field. Region (1), the orange-red, 60-80+ mm/s region of high velocity and mostly parallel streamlines “skimming” over the top of the sponge and deflected upwards by the protuberance. We speak of this as the region of “free-stream velocity”, which in this case is approximately 80 mm/s. Region (2) is the mid-velocity transition boundary layer (BL) located just above the surface of the sponge (light-blue to yellow isotachs). Region (3) is the blue-to-dark-blue area of low velocity flow located in the wake (*i.e.*, down-stream) of the sponge protuberance and to its left.

Also in Fig. 4 panel *a*, we see low velocity streamlines entering into two large holes on the left side of the sponge protuberance. These are functioning over-sized ostia (OSO) which are taking fluid and particles into the sponge as potential food. In Fig. 4 panel *b*, as the background velocity decreases, we see that the upper OSO is still functioning. At this





particular moment in the flow cycle (just at the transition point between flow directions in the oscillating background flow) we could not resolve the direction of particle movement at the opening of the lower OSO. (See Mendola *et al.* 2007b for an explanation of the function of over-sized ostia in *Dysidea avara*.)

In Fig. 4 panel *c*, at the near-zero velocity crossover point between the R-L and L-R flow directions the deceleration of the water mass is nearly complete. We still can see a blue-green “tongue” of 25-45 mm/s flow momentarily “lingering” above the sponge protuberance. The paddlewheel has just begun to turn in the opposite direction, so a low velocity water mass (blue isotachs) is now seen entering the field of view from the left side. Some of this water mass is colliding with the sponge protuberance glancing downward towards the bottom of the tank, where it is redirected upwards forming a low intensity substratum-induced clockwise circulating eddy.

Figure 4 – evidence of morphology-induced vorticity

Fig. 4 panel *d* shows areas of relatively high vorticity (the dark-red centered masses of fluid particles located just above the sponge protuberance and trailing downstream, to the left). The highest vorticity was found closest to the no-slip surface of the sponge where pressure gradients and shear forces are expected to be highest. Further away from the sponge vorticity decreased. As the velocity of the R-L flow diminishes (Fig. 4 panel *e*) the vortical patches are seen in much degraded states, and in Fig. 4 panel *f*, as the R-L momentum further decreases approaching the zero velocity crossover point between the R-L and L-R flow directions, the vortical patches are less concentrated and further separated from the sponge surface.

Figure 5 – left-to-right flow direction

In Fig. 5 panel *a*, the flow was reversed in the oscillation cycle and approached the sponge protuberance from the left-side. The picture is very different from that of Fig. 4 panel *a*, when the flow direction was from the right-to-left. Gone is the traveling eddy previously seen on the left-side of the protuberance. It is now replaced by a relatively large, low-velocity, morphology-mediated vortex circulating over the top of the protuberance. In Figure 5 panel *b*, as the water mass decelerates, the large eddy starts to raise and separate from the surface of the sponge. In Fig. 5 panel *c*, the eddy has become almost totally disorganized as the velocity of the water mass further decreases to the near-zero crossover point between flow directions.

In the vorticity plots (Fig. 5 panels *d*, *e*, *f*) the vertically-oriented left flank of the protuberance, with its complex morphology, has produced large, relatively non-discrete cells of increased vorticity near the sponge surface. These can be compared to the “flatter” less complex morphology and more discrete vortical cells from Fig. 4, panel *d*.

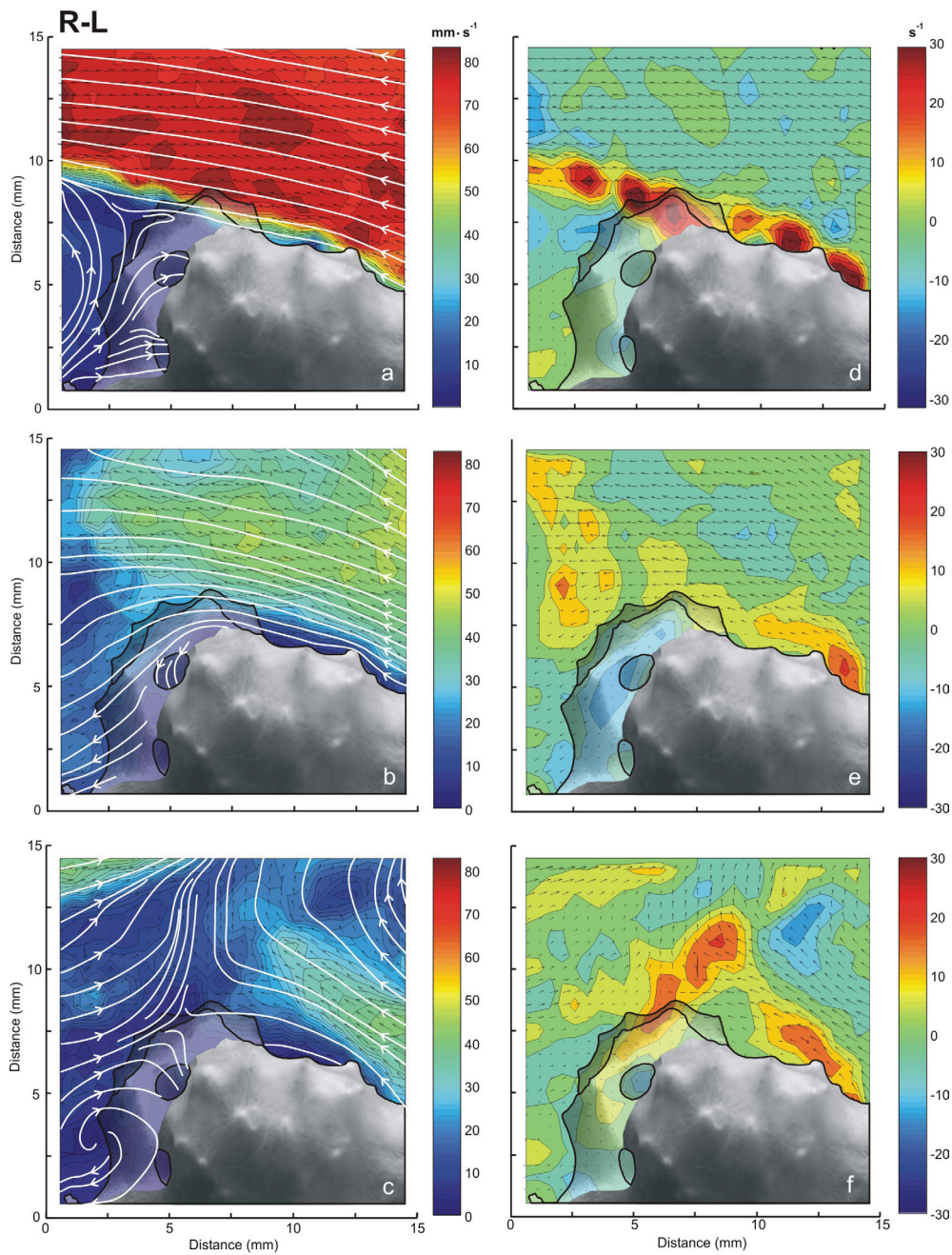


Figure 4. Panels *a*, *b*, *c* plot velocity data (speed isotachs, velocity vectors and streamlines) from 0.006 s segments of the flow-cycle, respectively, where the flow approached the sponge from the right side and moved to the left side (R-L). Panels *d*, *e*, *f*, show contour plots of vorticity and velocity vectors at the corresponding 0.006 s shown in panels *a*, *b*, *c*.





Morphology induced flow patterns

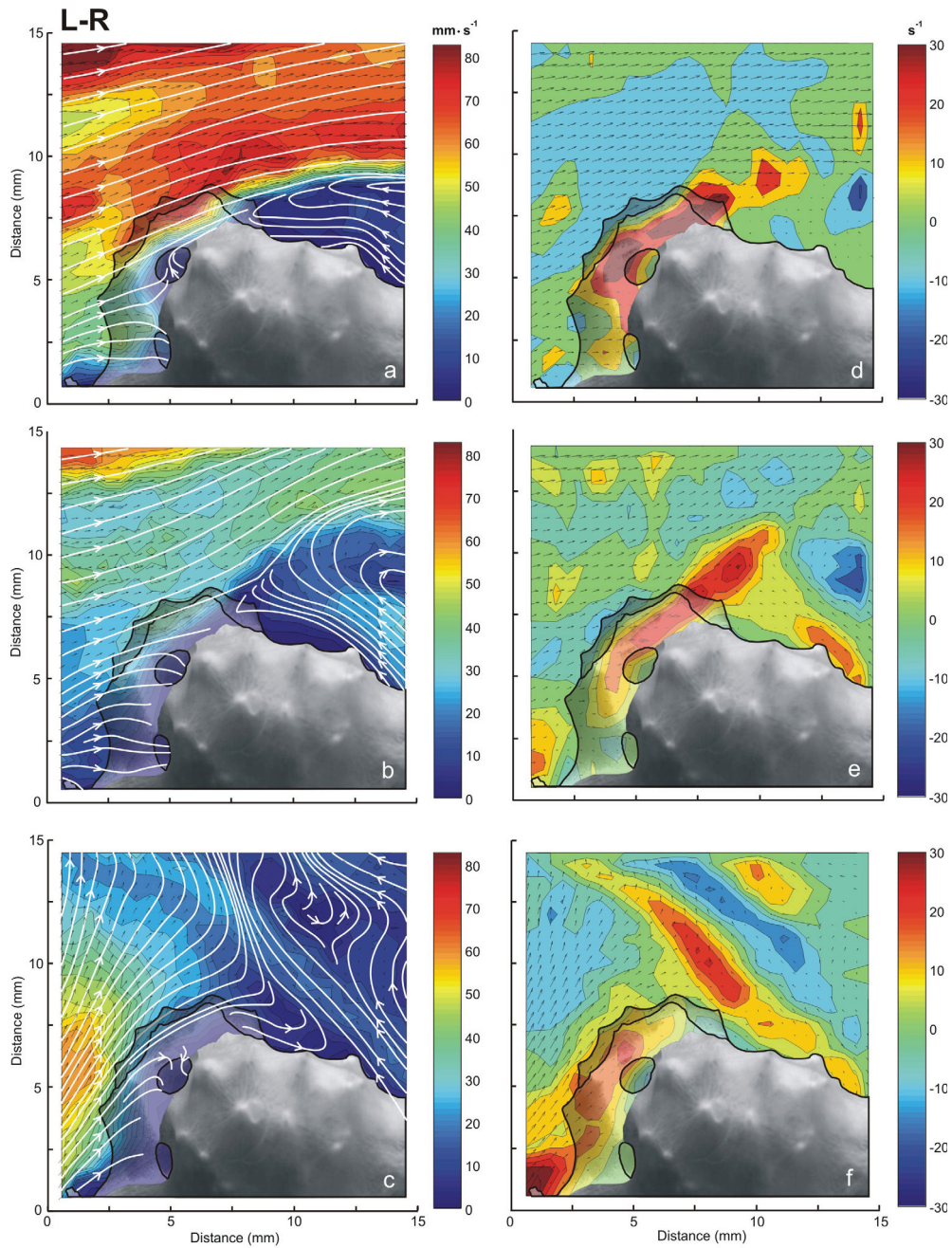


Figure 5, panels *a, b, c* plot velocity data (speed contours, vectors and streamlines) from 0.006 s segments of the flow-cycle, respectively, where the flow approached the sponge from the left side and moved to the right side (L-R). Panels *d, e, f*, contour plots of vorticity and velocity vectors at the corresponding 0.006 s shown in panels *a, b, c*.





Tables 2 & 3 present average particle speed and vorticity data from the 41 experiments analyzed. The results are highly variable: showing different flow directions and velocity amplitudes near the flanks of the sponge body (digital windows C & D, Fig. 2); two different background flow directions (L-to-R & R-to-L; ref. windows A & B, Fig. 2); and different levels of either clockwise (-) or counter-clockwise (+) vorticity near the surface of the sponge (digital windows C & D, Fig. 2).

A: R → L ⁽¹⁾						B: R → L								
C: R → L ⁽²⁾						D: R → L ⁽⁴⁾								
left flank						right flank								
> 40 mm/s		40 - 20 mm/s		< 20 mm/s ⁽⁶⁾		> 40 mm/s		40 - 20 mm/s		< 20 mm/s				
Speed (mm/s)	Vorticity (s ⁻¹)	Speed (mm/s)	Vorticity (s ⁻¹)	Speed (mm/s)	Vorticity (s ⁻¹)	Speed (mm/s)	Vorticity (s ⁻¹)	Speed (mm/s)	Vorticity (s ⁻¹)	Speed (mm/s)	Vorticity (s ⁻¹)			
43.2	-18.0	22.3	2.1	3.2	-12.1	(did not occur)	(did not occur)	(did not occur)	(did not occur)	2.5	-1.3			
62.2	-3.2	32.0	0.1	7.1	-0.2					2.6	1.1			
66.4	-7.8	36.2	2.9	8.5	0.9					2.9	1.1			
66.6	-7.7	38.2	-2.1	12.0	-0.9					3.0	-1.2			
68.8	-9.2			12.9	2.5					3.0	1.5			
84.6	28.0			13.2	2.7					3.6	-4.9			
				14.2	1.4					12.4	-10.4			
				14.4	6.4					18.1	-15.8			
c.f. Fig 2a ⁽⁷⁾		c.f. Fig 2b		c.f. Fig 2b		c.f. Fig 2b,c								

C: L → R ⁽³⁾						D: L → R ⁽⁵⁾					
> 40 mm/s		20 - 40 mm/s		< 20 mm/s		> 40 mm/s		20 - 40 mm/s		< 20 mm/s	
Speed (mm/s)	Vorticity (s ⁻¹)	Speed (mm/s)	Vorticity (s ⁻¹)	Speed (mm/s)	Vorticity (s ⁻¹)	Speed (mm/s)	Vorticity (s ⁻¹)	Speed (mm/s)	Vorticity (s ⁻¹)	Speed (mm/s)	Vorticity (s ⁻¹)
(did not occur) ⁽⁸⁾		26.8	18.6	1.3	0.6	(did not occur)		20.3	5.3	3.0	-1.2
				18.6	14.8			20.5	8.3	6.9	1.2
								27.2	18.3	10.4	3.6
		c.f. Fig 2a		c.f. Fig 2a				c.f. Fig 2b,c		c.f. Fig 2b,c	

Table 2. Particle speed and vorticity from 22 flow-tank experiments using seven different sponges (3/NL, 4/Spain) where the flow direction in the flow-tank was from **Right-to-Left**. The tables are divided into left or right flank of the sponge as shown in Figure 1. The “A, B, C, D” designations (notes 1-5) refer to the digital windows from Figure 1 where particle speed and direction determinations were made. “R → L”, e.g. notes (1, 2) indicates that particles were traveling from Right-to-Left within the designated digital windows; “L → R” (notes 3, 5) indicates particles were traveling from Left-to-Right within the designated digital windows. For the vorticity data, positive numbers indicate counter-clockwise rotating particles and negative numbers indicate clockwise rotating particles. Note 6: speed groupings of particles were divided into three ranges solely for convenience with no implied functional or other significance. Note 7: refers the reader to **Figure 4** which presents flow-fields from one representative experiment when the flow-tank flow direction was from **Right-to-Left**. Note 8: “did not occur” indicates that in this digital window, speed category and flow direction, no flow vectors were observed that matched these criteria.

A: L → R ⁽¹⁾						B: L → R					
C: L → R ⁽²⁾						D: L → R ⁽⁴⁾					
left flank						right flank					
> 40 mm/s		40 - 20 mm/s		< 20 mm/s ⁽⁶⁾		> 40 mm/s		40 - 20 mm/s		< 20 mm/s	
Speed (mm/s)	Vorticity (s ⁻¹)	Speed (mm/s)	Vorticity (s ⁻¹)	Speed (mm/s)	Vorticity (s ⁻¹)	Speed (mm/s)	Vorticity (s ⁻¹)	Speed (mm/s)	Vorticity (s ⁻¹)	Speed (mm/s)	Vorticity (s ⁻¹)
46.3	27.0	22.4	0.2	3.4	-5.0	58.8	18.4	22.1	16.9	6.5	-1.4
59.2	5.8	23.1	6.3	4.5	-1.7	59.8	30.0	27.9	8.4	6.6	1.3
63.8	11.6	23.4	-2.7	5.2	4.1	61.5	29.9	30.0	14.0	6.7	-2.4
		28.8	-2.0	5.7	-1.0	70.1	23.6	33.2	25.6	7.1	3.8
				6.9	-0.1	72.5	19.4	34.6	21.7	7.6	1.7
				7.0	8.2					9.6	-1.3
				7.1	6.5					12.9	-4.9
c.f. Fig 3a ⁽⁷⁾		c.f. Fig 3b		c.f. Fig 3c				c.f. Fig 3a,b		c.f. Fig 3b,c	
C: R → L ⁽³⁾						D: R → L ⁽⁵⁾					
> 40 mm/s		20 - 40 mm/s		< 20 mm/s		> 40 mm/s		20 - 40 mm/s		< 20 mm/s	
Speed (mm/s)	Vorticity (s ⁻¹)	Speed (mm/s)	Vorticity (s ⁻¹)	Speed (mm/s)	Vorticity (s ⁻¹)	Speed (mm/s)	Vorticity (s ⁻¹)	Speed (mm/s)	Vorticity (s ⁻¹)	Speed (mm/s)	Vorticity (s ⁻¹)
(did not occur) ⁽⁸⁾		(did not occur)		3.4	1.0	(did not occur)		(did not occur)		11.7	-1.4
				5.1	-0.7					12.1	2.6
				7.3	-0.4						
				14.2	3.2						
				15.1	0.3						
				c.f. Fig 3c						c.f. Fig 3c	

Table 3. Particle speed and vorticity from 19 flow-tank experiments using seven different sponges (3/NL, 4/Spain) where the flow direction in the flow-tank was from *Left-to-Right*. The tables are divided into left or right flank of the sponge shown in Figure 1. The “A, B, C, D” designations refer to the digital windows from Figure 1 where particle speed and direction determinations were made. “L – R” (e.g. notes 1, 2) indicates particles were traveling from Left-to-Right within the designated digital windows. “R → L” (notes 3,5) indicates that particles were traveling from Right-to-Left within the designated digital windows. For the vorticity data, positive numbers indicate counter-clockwise rotating particles and negative numbers indicate clockwise rotating particles. Note 6: speed groupings of particles were divided into three ranges solely for convenience with no implied functional or other significance. Note 7: refers the reader to **Figure 5** which presents flow-fields from one representative experiment when the flow-tank flow direction was from *Left-to-Right*. Note 8: “did not occur” indicates that in this digital window, speed category and flow direction, no flow vectors were observed that matched these criteria.

DISCUSSION

Randomness and temporal nature of flow-field patterns

Studying the data for the 41 flow tank experiments (Tables 2 & 3) we were not able to find predictable patterns, trends, or correlations between, flow direction, velocity, spin direction or degree of vorticity. The indicated “did not occur” situations (where zero particles meeting the stated criteria were found) also showed no predictable pattern of occurrence within the data set. This high degree of randomness indicates that the flow-fields produced around the 7 different sponges in the 41 different experiments were unique unto that particular sponge with that experimental set-up, and at the moment the video frames were captured. Overall, this illustrates the highly complex and variable nature of the fluid dynamics around complex-shaped 3-D



objects immersed in a laminar flow-stream of a flow tank. In the shallow sublittoral zone we studied in the Mediterranean, with its even more complex animal and substrate morphologies and topographies, and inherently turbulent boundary layer flows, we would expect the same degree of randomness and variability of flow-fields over time, if not greater.

The flow fields described from Figs. 4 and 5 were the flow fields captured at those particular moments in the flow cycle. Had we selected another series of frames along the time-axis for analysis, the flow field pictures would most certainly have looked differently from those shown for the frames analyzed. We chose to fully analyze an oscillating flow experiment (CMV-1505) given that oscillating flow regimes predominated around the sponges we studied in nature. A second reason was that each of the different time/velocity points selected for presentations as “snap-shots” of the flow cycle in the panels of Figs. 4 and 5 would then be all from the same experiment.

When analyzing the effects of protuberance morphology seen in the individual video frames selected for presentation in Figs. 4 and 5, we cannot exclude the role of the non-visible morphology, *e.g.* that part of the sponge which was upstream and out of view in the video frame; (see: Fig. 1 for schematic drawing of sponge DA7, for example). The velocity and vorticity patterns shown in the figures were most certainly not solely the result of the morphology of only the parts of the sponge shown in the video window. Given that other parts of the sponge were upstream from the protuberance shown in the video frame, these too most certainly contributed to the flow patterns captured in the “snap-shots” presented in the figure panels.

Effects of turbulence and eddies on particle motion

Marcu *et al.* (1995) present governing non-dimensional equations (2), (3) for the behavior of a small, spherical, rigid particle of diameter d , density ρ_p and velocity $\mathbf{V} = (u_p, v_p)$ moving in a dilute fluid with density ρ_f and velocity $\mathbf{U} = (u_f, v_f)$, determined by

$$\mathbf{V} = \frac{d\mathbf{x}_p}{dt}, \quad (2)$$

$$\frac{d\mathbf{V}}{dt} = \frac{1}{St} (\mathbf{U}|_{\mathbf{x}=\mathbf{x}_p} - \mathbf{V}) + \frac{1}{Fr^2} \mathbf{e}_g, \quad (3)$$

where Stokes' drag law is employed. Here \mathbf{x}_p denotes the instantaneous position of the particle, \mathbf{U} is the fluid velocity at the location \mathbf{x}_p , while \mathbf{e}_g represents the unit vector in the direction of the gravity vector's projection into the r, θ radial-azimuthal plane. The parameters are the Stokes (St) and Froude (Fr) numbers (equations 4 & 5, respectively). The core size $\delta = \sqrt{\nu/\sigma}$ of the vortex circulation Γ is determined by the balance of strain σ and viscous diffusion ν .





$$St = \frac{d^2 \rho_p \sigma \Gamma}{18 \rho_f \nu^2} \quad (4)$$

$$Fr = \frac{\sigma^{3/4} \Gamma}{\nu^{3/4} \sqrt{g}} \quad (5)$$

where g is the length of the projection of the gravitational acceleration vector \mathbf{g} (on two-dimensional particle dynamics in the r, θ plane).

Crowe *et al.* (1985) interpreted the Stokes number as the ratio of the response time of the particle $\tau_A = \rho_p d^2 / 18\mu$ to the time-scale associated with the fluid motion, reminding the reader that small values of the Stokes parameter may be regarded as describing either very light particles or a very viscous fluid, and in both cases the particle behavior is dominated by viscous forces. The relationship is relevant in our case of very small, bacterial-sized sponge food particles and low Re (Reynolds number) viscous flows close to sponge surfaces.

The Froude number expresses the relative importance of inertial to gravitational forces on particle motion. Large Froude numbers describe inertia-dominated particle motion, for which gravity is not important and the behavior of the particle is determined by the ratio between viscous and inertial forces given by the Stokes number.

Marcu *et al.* (1995) also suggested, that for very small particles weakly affected by gravity and trapped within a relatively small vortex at low Re flows, the centrifugal force acting on the particles would always be smaller than the inward radial drag force, and therefore the particles would be driven by the flow towards the center of the vortex. This suggestion applies in our case to micro-algal-sized food particles (but probably not non-motile bacteria, which are for all intent and purposes neutrally buoyant and not greatly effected by gravity) that may become trapped within a vortex formed above the sponge protuberances (*e.g.*, Fig. 5, panel *a*). The opposite is true for heavier, larger particles (*i.e.*, larger diatoms), which would characteristically move away from the center of the vortex and asymptotically approach a circular trajectory at a radius within the vortex where the balance between the centrifugal and viscous drag force would be restored. Vastistas (1989) and Kaftori *et al.* (1995a, b), also instruct that we should expect small, denser than seawater particles (*e.g.*, algal cells, small diatoms, flagellates, etc.) to be momentarily trapped within vortices formed above the sponge protuberances. After a number of flow cycles moving the same water mass back and forth over the sponge, particles could become permanently trapped either within the inter-protuberance valleys, or within the inter-conule “mini-valleys.” Once at the level of the inter-conule valleys, particles small enough to pass the ostia would be subject to the negative pressures produced by the choanocyte pumps where they could be sucked into the ostia as potential food for the sponge. Food-worthy particles that land onto the surface of the sponge that are too large to pass the ostia, are often phagocytosed directly through the pinacoderm (Simpson, 1984).



In Fig. 4, panel *a*, the low velocity eddy seen on the left-side of the sponge protuberance was (in real-time) moving away from the sponge. In a natural setting (or in the flow tank) such an eddy could re-suspend lightweight, micrometer-sized organic particles which had previously settled onto the substratum. Then on the next reversal of the flow cycle those particles could be carried back over the sponge and deposited onto the dermal membrane for possible intake into ostia as food. These observations and assumptions support the earlier discussed “wake trapping” hypothesis put forth by Abelson *et al.* (1993). This type of organic particle re-suspension from the sediment has also been demonstrated for sediment-living phoronids by Johnson (1988) and for polychaetes by Carey (1983).

In Fig. 5, panel *a*, we see flow being drawn out of the top OSO, while flow is drawn into the bottom OSO. In Fig. 5 panel *b* (only 0.002 s in real time later) flow can be seen to be drawn into both the upper and lower OSO at the same time. Also in Fig. 4 panel *a*, both OSO are drawing in water. Thus it would seem that development of multiple OSO by the sponge in different morphological regions of its body would provide multiple options for high-rate particle capture at different time points in the ambient flow cycle.

Figure 5, panels *c* & *f* show different flow features and morphology interactions (at this crossover point) than were seen at the crossover point in Fig. 4 panels *c* and *f*. Again, these differences illustrate the inherent complexity of the flow-fields surrounding and moving past any complex-shaped object on the sea floor in the shallow sublittoral, sponges included. It also illustrates possible, 3-D effects not seen in the instantaneous 2-D flow snap-shots captured in our sample figures.

McNair *et al.* (1997) and McNair (2000) studied the behavior of suspended particles sinking towards the bottom in oceans, lakes and rivers. They developed equations to calculate how long the particles took to “hit bottom” in relation to their density, size and the degree of local turbulence. Their results predict that for small negatively buoyant particles (*e.g.* fine silt, small organic particles, and/or invertebrate larvae) there is always a region near the bottom (or above a sponge) in which turbulence increases rather than decreases the mean bottom-hitting time. (Neutrally buoyant small particles such as non-motile bacterial cells, pico- and nanoplankton are exceptions to their findings.)

These findings are particularly relevant in the case of our flow tank observations, where morphology-induced turbulence and local eddies were localized above (or alongside) the sponge protuberances (for example, Fig. 5, panels *a* & *b*; and Fig. 4 panel *c*, respectively). These localized cells of increased turbulence would serve to lengthen the time that trapped food-sized particles (larger than bacteria) would be held-up in the water column above the sponge, increasing the probability that such particles would settle into the conule dominated regions (*i.e.*, within 1-2 mm of the sponge surface) where they would come under the influence of the negative pressures produced by the sponge pumps, and if small enough be taken into the ostia as potential food particles.



Possibility for conule-induced effects

The PTV methods used in this study could not resolve flow effects within 1-2 mm of the sponge surface due to light-scattering and low particle abundance at the sponge surface. Therefore, we were not able to investigate any potential effects of the mm-size conules which characteristically cover the entire surface of all *Dysidea* species, including *D. avara*. To shed more light on the possible roles for the mm-sized conules, we investigated the possibility of using computational fluid dynamic modeling (CFD) methods. With this methodology, fine-scale, 3-dimensional computational grids could be constructed to represent a portion of the surface area of a sponge arranged with different-sized conules. The sponge tissue could be modeled as a porous medium and the pumping activity of the choanocytes could be modeled with a preset pressure drop (Riisgård *et al.* 1993; Larsen and Riisgård, 1994; and Reiswig, 1974, 1975). With CFD modeling, the influence of both flow parameters and morphological parameters could be studied systematically, including the effect of varying morphological parameters on influx of fluid and micron-sized food particles into the sponge.

We speculated as to the possible functional advantages for the sponge having a body surface literally covered with 0.3-1.6 mm tall conules. One suggestion was that once μ m-sized food particles had settled to below the tops of the conules they would become trapped in the viscous environment, and thereafter be sucked into the sponge ostia by the negative pressure produced by the choanocyte pumps. Another suggestion was that pressure differences between upstream and downstream flanks of the conules, caused by flow over the conulated surface, had an additional positive effect on total influx, *i.e.*, the “dynamic pressure” effect (Vogel, 1975, pg. 286), compared to the influx produced by the choanocyte pumps alone.

We studied the distribution patterns of ostia on the sponge dermal membrane, and observed that they were grouped in clusters located between dermal fibers which radiated outward from the tips of each of the conules. The ostia were in the right places (*i.e.*, grouped in radial patterns surrounding each of the conules) to support both suggestions and allow inflow into the sponge for flow approaching the conules from any direction (such as the oscillating flow regimes recorded from the shallow sublittoral environment we studied in Spain).

Our intention for the future is to continue our studies of the interaction of flow and morphology with this sponge using a flow-tank, CFD modeling, and possibly other approaches as well.

ACKNOWLEDGEMENTS

This project was financially supported by EU project No. 017800. We thank Sander Kranenbarg, Ph.D. and ir. Mark van Turnhout (both of WU/EZO) for their help with Matlab programming.



REFERENCES CITED

- Abelson, A. T. Miloh, and Y. Loya. 1993. Flow patterns induced by substrata and body morphologies of benthic organisms, and their roles in determining availability of food particles. *Limnol. Oceanogr.* **38** (6): 1116-1124.
- Bell, J. J., and D. K. A. Barnes. 2000. The influence of bathymetry and flow regime upon the morphology of sublittoral sponge communities. *J. Mar. Biol. Assoc. U.K.* **80**: 707-718.
- Bell, J. J., D. K. A. Barnes, and C. Shaw. 2002a. Branching dynamics of two species of arborescent demosponge: the effect of flow regime and bathymetry. *J. Mar. Biol. Ass. U.K.* **82**: 279-294.
- Bell, J. J., D. K. A. Barnes, and J. R. T. Turner. 2002b. The importance of micro and macro morphological variation in the adaptation of a sublittoral demosponge to current extremes. *Mar. Biol.* **140**: 75-81.
- Carey, D. A. 1983. Particle resuspension in the benthic boundary layer induced by flow around polychaete tubes. *Can. J. Fish. Aquat. Sci.* **40** (suppl. 1): 301-308.
- Crowe, C. T., R. Gore, and T. R. Truitt. 1985. Particle dispersion by coherent structures in free shear flows. *Part. Sci. Tech.* **3**, 149-158.
- Johnson, A. S. 1988. Hydrodynamic study of the functional morphology of the benthic suspension feeder *Phoronopsis viridis* (Phoronida). *Mar. Biol.* **100**: 117-126.
- Kaftori, D., G. Hetsroni, and S. Banerjee. 1995a. Particle behavior in the turbulent boundary layer. I. Motion, deposition, and entrainment. *Phys. Fluids* **7** (5): 1095-1106.
- Kaftori, D., G. Hetsroni, and S. Banerjee. 1995a. Particle behavior in the turbulent boundary layer. II. Velocity and distribution profiles. *Phys. Fluids* **7** (5): 1107-1121.
- Larsen, P. S. and H. U. Riisgård. 1994. The sponge pump. *J. theor. Biol.* **168**: 53-63.
- Marcu, B., E. Meiburg, and P. K. Newton. 1995. Dynamics of heavy particles in a Burgers vortex. *Phys. Fluids* **7** (2): 400-410.
- McNair, J. N., J. D. Newbold, and D. D. Hart. 1997. Turbulent transport of suspended particles and dispersing benthic organisms: how long to hit bottom? *J. theor. Biol.* **188**: 29-52.
- McNair, J. N. 2000. Turbulent transport of suspended particles and dispersing benthic organisms: the hitting-time distribution for the local exchange model. *J. theor. Biol.* **202**: 231-246.
- Mendola, D., S. de Caralt, M. J. Uriz, F. van den End, J. L. van Leeuwen, and R. H. Wijffels. 2007a. (submitted). Environmental flow regimes for *Dysidea avara* sponges.
- Mendola, D., J. G. M. van den Boogaart, J. L. van Leeuwen, and R. H. Wijffels. 2007b. Re-plumbing in a Mediterranean sponge. *Biol. Lett.* **3**(6): 595-598.
- Minale, L., R. Riccio, and G. Sodano. 1974. Avarol, a novel sesquiterpenoid hydroquinone with a rearranged drimane skeleton from the sponge *Dysidea avara*. *Tet. Lett.* **38**: 3401-3404.
- Müller W. E. G., A. Maidhof, R. K. Zahn, H. C. Schröder, M. J. Gasic, D. Heidemann, A. Bernd, B. Kurelec, E. Eich, and G. Sibert. 1985. Potent antileukemic activity of the novel cytostatic agent avarone and its analogues *in vitro* and *in vivo*. *Cancer Research* **45**, 4822-4827.
- Reiswig, H. M. 1974. Water transport, respiration and energetics of three tropical marine sponges. *J. Exp. Mar. Biol. Ecol.* **14**: 231-249.
- Reiswig, H. M. 1975. The aquiferous systems of three marine demospongiae. *J. Morph.* **145**: 493-502.
- Riisgård, H. U., S. Thomassen, H. Jakobsen, J. M. Weeks, and P. S. Larsen. 1993. Suspension feeding in marine sponges *Halichondria panicea* and *Haliclona urceolus*: effects of temperature on filtration rate and energy cost of pumping. *Mar. Ecol. Prog. Ser.* **96**: 177-188.
- Simpson, T. L. 1984. *The Cell Biology of Sponges*. Springer-Verlag, Berlin.
- Sipkema, D., R. Osinga, W. Schatton, D. Mendola, J. Tramper, and R. H. Wijffels. 2005. Large-scale production of pharmaceuticals by marine sponges: sea, cell or synthesis? *Biotechnol. Bioeng.* **90**: 201-222.



Morphology induced flow patterns

- Teragawa, C. K. 1985. Mechanical function and regulation of the skeletal network in *Dysidea*. In: New Perspectives in Sponge Biology. (ed) K. Rützler. Third Internat. Conf. on Biol. of Sponges. Woods Hole, MA, USA. Smithsonian Institution Press, Washington, D.C. Pp. 252-258.
- Uriz, M. J., D. Rosell, and D. Martin. 1992. The sponge population of the Cabrera archipelago (Balearic Islands): Characteristics, distribution and abundance of the most representative species. PSZN I: *Mar. Ecol.* **113**: 101-117.
- Uriz, M. J., X. Turon, J. Galera, and J. M. Tur. 1996. New light on the cell location of avarol within the sponge *Dysidea avara* (Dendroceratida). *Cell Tissue Res.* **285**: 519-527.
- Vatistas, G. H. 1989. Analysis of fine particle concentrations in a confined vortex. *J. Hydraulic Res.* **27**: 417-427.
- Vogel, S. 1975. Flows in organisms induced by movements of the external medium. In: Scale Effects in Animal Locomotion. T. J. Pedley (ed). Academic Press, London.
- Witte, U., T. Brattegard, G. Graf, B. Springer. 1997. Particle capture and deposition by deep-sea sponges from the Norwegian-Greenland Sea. *Mar. Ecol. Prog. Ser.* **154**: 241-252.





Chapter 5

Oscular outflow rates for *Dysidea avara* sponges

Dominick Mendola ^{1,2,*}, Jos G. M. van den Boogaart²,
Sonia de Caralt ³, Johan L. van Leeuwen², René H. Wijffels¹

¹ Bioprocess Engineering Group ²Experimental Zoology Group,
Wageningen University, P.O. Box 8129, 6700 EV, Wageningen, The
Netherlands; ³CSIC Centre for Advanced Studies, Blanes (Girona) Spain

*Author for correspondence, e-mail: dominick.mendola@wur.nl

Abstract: Oscular outflow rates for *Dysidea avara* sponges were studied to better understand the volumetric pumping rate of this sponge on a daily basis. These data were to be applied to setting culture criteria for *ex situ* aquaculture in controlled environment tanks to yield sponge biomass for extraction of avarol, its valuable natural product chemical constituent. A flow tank and particle tracking velocimetry were employed to measure oscular outflow from laboratory-acclimated and freshly-collected specimens of *Dysidea avara* sponges. Both unidirectional and oscillating (0.20 Hz–0.33 Hz) background flows from near zero to 114 mm/s were tested. Oscular outflow velocities ranged from (12.7–130.4 mm/s) and volumetric outflow rates from (0.004–0.013 ml (ml sponge)^{−1}s^{−1}). Outflow velocities varied with changes in background flow speeds, but we saw no synchrony or significant patterns in our data. Some specimens stopped pumping after some minutes exposure to background flow speeds of ca. 75 mm/s, another kept pumping up to 120 mm/s, and others stopped pumping at lower background flow speeds; and at other times for no apparent reason. Flow tank results were compared to oscular outflow velocities for 21 sponges and 97 oscula in the sea, ranging from zero (no outflow) to 177 mm/s. Great variation in outflow velocity was seen from sponge-to-sponge and from multiple oscula on one sponge *in situ*. In calm seas 66% of the oscula sampled were strongly pumping whereas only 24% were strongly pumping within 1–5 days following a storm. In the flow-tank, both laboratory-acclimated and freshly-collected specimens produced outflow velocities within the ranges measured in nature. We could not detect if water flow through the aquiferous system of *D. avara* (including oscular outflow) was aided by induced water flow from the environment, as reported for other sponges and marine invertebrates. Results are supported by other studies in the Western Mediterranean, that classified *Dysidea avara* as a cryptic and fragile species, found primarily in sheltered habitats.

Key words: *Dysidea avara*, oscular flow rates, flow tank



INTRODUCTION

Dysidea avara is a cryptic species, found mostly in sheltered habitats throughout its range in the W. Mediterranean (Uriz *et al.* 1992). We studied water flow in close proximity to *D. avara* sponges within a shallow rocky coastal site in N. E. Spain (Mendola *et al.* 2007a, submitted), and corroborated the Uriz *et al.* findings. Proximal flows (recorded within 2 cm of the sponge surface and within 2-4 cm of the substratum) averaged only 2.6 cm/s in calm seas and 5.9 cm/s during infrequent storms.

The primary aim of this research was to study the relationship between oscular outflow speed and oscular volumetric outflow rate in relation to varying background flow speeds for *Dysidea avara* sponges in the controlled environment of a flow tank. The overall aim was to better understand the range and periodicity of oscular outflow rates so that better estimates of pumping rates for whole sponges could be made. Such rates could aid establishing overall feeding rates and regimens for tank-based aquaculture of this sponge, which is desired for its valuable bioactive natural products avarol and avarone (Müller *et al.* 1986, Minale *et al.* 1974, Uriz *et al.* 1996).

Other researchers have reported oscular outflow rates for a variety of sponge species, both *in situ* and in the laboratory (Table 1). Parker (1910, 1914) used a glass tube to cannulate oscula and measure outflow pressures ranging of 1.3-2.9 mm water for seven Bermuda species, and 3.5-4.0 mm water for one South Carolina, USA species. From outflow pressures, osculum and specimen dimensions supplied by Parker, we calculated an outflow rate of 0.010 ml/ml sponge·s⁻¹ for a single finger cut from a *Spinosella sororia* colony. From the outflow from that one finger of the sponge, Parker extrapolated total daily outflow to 1,575 liters for a large colony with 20 similar-sized fingers.

Bidder (1923) measured oscular outflow velocity from two tubular-shaped Mediterranean calcareous sponges held in a tank using carmine and indigo suspensions, a centimeter scale, and a timer. He found mean oscular velocity was 7.0 cm/s in still water, which was lower than the 8.5 cm/s outflow velocity he measured for a colony in the sea. He calculated the outflow rate for the in-sea specimen at 0.26 ml/s (but did not report sponge volume). From a scaled figure drawing of his laboratory specimen of *Leucandra aspera*, we estimated sponge volume at about 10 ml which results in an estimated outflow rate for this specimen of about 0.026 ml (ml sponge)⁻¹s⁻¹.

Reiswig (1971, 1974) reported oscular outflow velocities and water transport (pumping) rates for three species of Caribbean reef sponges. For a *Mycale* sp., outflow velocity was 66-91 mm/s, transport rate 0.21-0.34 ml (ml sponge)⁻¹s⁻¹; for *Verongia gigantea*, 25-168 mm/s, and 0.04-0.15 ml (ml sponge)⁻¹s⁻¹; and for *Tethya crypta* 55-182 mm/s, and 0.11-0.22 ml (ml

sponge)⁻¹s⁻¹. Transport rates for the *Mycale* sp. remained rather constant over periods of days and were pretty much independent of sponge size. Water transport rates from *V. gigantea* were much more variable responding to changes in environmental conditions, with reduced activity seen for larger individuals. For *T. crypta*, water transport was found to respond to a 10-15 day cycle with about 5-day “resting periods” in between. Peaked activity was in the middle of the cycle, diminishing on either side. Pumping activity in *Tethya crypta* was not found to be related to animal volume. Oscular outflow was not reported in relation to local ambient flow velocity.

Reiswig (1975) collected live *Haliclona permollis* specimens from embayments in central California, and returned them to the laboratory, where he used slow shutter speed photographs of particles being ejected from the oscula to estimate axial velocity leaving the osculum at 89 mm/s (n = 11), and a pumping rate of 0.314 ml/s (equiv. to 27.2 L over a 24 hr period).

Vogel (1974, 1977) used a pair of thermistors to simultaneously measure oscular outflow velocities and background flow speeds for eight sponge species at sites on Bermuda. Active oscular outflow velocities varied from 7.5-22.0 cm/s depending on species with no particular correlation between species, size or habitat. Volumetric outflow per unit volume of sponge was estimated in the range of 0.20-0.40 ml (ml sponge)⁻¹s⁻¹ (similar to Reiswig’s results). Some specimens were anesthetized *in situ* by holding a plastic bag of freshwater over the sponge for a few minutes. Following anesthesia, oscular outflow velocity increased linearly with increasing background current velocity, demonstrating environmentally-induced flow through the inactivated specimens proportional to background current speed.

Riisgård *et al.* (1993) cut one ml-size branches from the North Sea sponge *Haliclona urceolus*, and measured pumping rate directly using an ingenious balanced-level pumping chamber and laser-floating mirror projecting technique. Three measures of pumping rate ranged from 0.048-0.100 ml (ml sponge)⁻¹s⁻¹. Outflow velocities were in the order of 54 mm/s.

Our group reported outflow rates for three specimens of *Dysidea avara* sponges held in a flow tank (Mendola *et al.* 2007b). Oscular outflow rates were between 13 mm³/s and 108 mm³/s. From sponge volumes and number of oscula, pumping rates of 0.003-0.010 ml (ml sponge)⁻¹s⁻¹ were calculated. Schläppy *et al.* 2007 (working with specimens of *D. avara* from our laboratory) used particle tracking velocimetry to calculate a pumping rate of 0.004 ml (ml sponge)⁻¹s⁻¹ (corroborating our calculations with a completely different set-up). When compared to the outflow rates reported previously by other authors with other species (Table 1) these rates are quite low, suggesting there was either a handling or tank effect that artificially depressed outflow rates, or that *D. avara* is naturally a low output rate sponge.



Source	Species	Oscular outflow speed (mm/s)	Pumping rate ml (ml sponge) ⁻¹ s ⁻¹
Parker (1910), (1914)	<i>Spinosella sororia</i>	4	0.01
Bidder (1923)	<i>Leucandra aspera</i>	70-85	0.026
Reiswig (1971, 1974)	<i>Mycale</i> sp.	66-91	0.21-0.34
	<i>Verongia gigantea</i>	25-168	0.04-0.15
	<i>Tethya crypta</i>	55-182	0.11-0.22
Reiswig (1975)	<i>Haliclona permollis</i>	85-92	0.13
Vogel (1977)	(8 species – grouped)	75-220	0.2-0.4
Rilsgård <i>et al.</i> (1993)	<i>Haliclona urceolus</i>	54	0.048, 0.06, 0.1
Mendola <i>et al.</i> (2007b)	<i>Dysidea avara</i> DA2	8.7-88.0	0.008
	<i>Dysidea avara</i> DA4	58-110	0.03-0.01
	<i>Dysidea avara</i> DA7	35-130	0.01
Schläppy <i>et al.</i> (2007)	<i>Dysidea avara</i> DA2	0.5-14	0.004

Table 1. Oscular outflow speeds and pumping rates for sponges from literature sources.

METHODS AND MATERIALS

A 7.5 liter-capacity Perspex flow-tank was built for low-speed flow tracing experiments with live sponges. The vertical recirculating water stream was circulated by a DC motor-driven paddlewheel connected to a regulated DC power supply, reversing relay and timer. This arrangement allowed for unidirectional or bidirectional flows over a pre-set oscillating frequency range of 0.1-1.0 Hz. The working section of the flow-tank (18 cm x 12 cm x 6 cm) was isolated by two banks of flow-straighteners made from commercially available formed blocks of polypropylene straws, each with internal diameter of 5.7 mm. The upper flow limit for maintaining laminar flow within in the working section was determined to be approximately 15 cm/s, however even non-laminar flows at higher velocities could also be attained (see Mendola *et al.* 2007b, online materials, for a full description of the flow tank set-up).

Nine, small-size (15-50 ml) *Dysidea avara* specimens were collected at 9-12 m depth on pieces native rock from the L'Escala region in N.E. Spain, and transported to The Netherlands (NL). Specimens were maintained in a 550 liter aquarium with biofiltration over a period of 3-months. Sponges were fed twice daily with marine broths made from fish and shrimps, and/or manufactured shellfish diets (INVE, Belgium CAR-1 & SELCO), and 3-4 times per week with cultured micro-algae (*Phaeodactylum tricornutum*, *Nannochloropsis* sp.): total starting concentrations 2×10^5 to 3×10^5 particles/ml. Not all specimens returned to the NL were used for oscular outflow experiments; only three sponges that showed consistent pumping activity were used.

Prior to commencing oscular-outflow experiments the flow-tank was filled with 30 µm sand-filtered seawater taken from the sponge holding tank. The flow-tank was seeded with

either cultured microalgae (*Nanochloropsis* sp., 3-4 μm dia. or *Isochrysis galbana*, 6-8 μm sickle-shaped rods) or pre-soaked 0.5-6.0 μm dia. hollow glass beads (J. J. Bos, NL) to attain a particle density of *ca.* 100,000 particles/ml. The particles were required to reflect laser light for tracing particle paths over, into (only with over-sized ostia; see below) and out of (oscula) of the live sponge specimens. A laser light sheet (0.5 mm width) was projected downward into the flow-tank from an Excel 2300 laser solidly mounted and affixed to a cement wall above and just behind the tank. The high-speed (50-500 fps) photography set-up employed a Redlake® MotionPro 10,000 digital camera, Nikon® 105/1:2.8 lens and 50 mm extension ring. Images of the plume of ejected glass particles from the sponge osculum were captured onto a PC using Redlake's Midas Player® software and analyzed using Matlab® with embedded sub-routines which plotted individual particle velocities, streamlines, velocity contours (isotachs) and vorticity.

Oscular outflow (pumping rate) experiments were run periodically over a 3-month period rotating between three different test animals depending upon which sponge was pumping at a normal rate on any particular day. The chosen test specimen was gently lowered into place into the flow-tank always kept underwater inside a small beaker (where sponge volume was estimated). Once set-up, oscular outflow experiments were run in linear succession for varying periods of time depending on sponge pumping response and the aim for each series of experiments. One specimen was generally used for either a morning or an afternoon session, but on occasion a strongly-pumping sponge was used for both morning and afternoon sessions on the same day.

One experiment equated to one flow-tank run under a given set-up: *i.e.*, one velocity setting, one flow-direction, one animal position, one laser light-sheet position and one camera setting and position. Once all parameters were set-up, the laser was turned-on and a 5-10 second digital movie was recorded onto the computer storage buffer. Each 5-10 s movie was given a sponge- and time-coded number ("DAL 1303" for example) and designated as "one experiment." When testing a sponge for oscular outflow response a series of experiments (8-10; *e.g.*, DAL 1303-1320) were run in succession at different background flow speeds.

Particle density in the flow tank was checked between runs and made-up if necessary to approximately 100,000 particles/ml. For each set-up a calibration run was made, wherein a piece of plastic centimeter scale was placed vertically next to the sponge specimen and a short video series recorded under normal light at relatively high magnification. The calibration provided the distance scale from which dimensions of the specimen (including oscular diameter) and particle flow velocity (in the x-y plane of the light sheet) could be calculated. Over a 3-month study, 136 (5-10 second duration) oscular outflow experiments were performed at the NL facility.

A second experimental set-up was installed for a 1-week period near the collection site in Spain. Of 12 freshly-collected sponges, seven were pumping sufficiently to be used as subjects



for oscular outflow experiments. However, not all movies from all sponges were analyzed or reported due to time constraints. We conducted 194 (5-10 second duration) oscular outflow experiments in Spain to test for any difference in behavior and/or performance between freshly-collected and laboratory-reared sponges. In this set of experiments a larger flow tank (20L) was used and only glass beads (no algae) were used for flow tracing. Unfiltered natural seawater at ambient temperature/salinity was used for the Spain set-ups.

Oscular outflow speed was measured using particle tracking velocimetry (PTV). Individual particles ejected out of the osculum in the exhalant water stream were tracked in subsequent video frames. Background flow speed was also measured using the PTV method. A region (or regions) sufficiently away from the sponge body and upstream in the flow tank was (were) chosen for tracking particles for calculating background speed. At the minimum, 10 particles were tracked for any one experiment to determine mean background flow speeds.

Outflow rates were calculated from measured oscular diameters, and the assumption that the instantaneous outflow velocity profile was a paraboloid with a circular base equal to the area of the osculum opening. With the camera lens magnifications used, and the accuracy of the scale calibration, we were able to read oscular diameter accurately to one decimal place (*i.e.* 0.1 mm).

A sub-routine was written in Matlab which calculated outflow rates for each particle tracked (*i.e.*, clicked with the computer mouse) leaving the osculum from subsequent video frames. For each outflow rate determination usually 10-20 particles with the tallest trajectories (and only those from the center 1/3 of the osculum opening) were tracked just above the osculum just after them leaving the osculum. This convention eliminated the slower-exiting particles nearer to the walls of the exhalant canal leading to the exit osculum. Detailed methods can be found in: Mendola *et al.* (2007b), online materials. For some specimens outflows from 2, 3 or more oscula were tracked and a simple average outflow rate derived. The average was then multiplied by the total number of oscula showing on the sponge to arrive at whole sponge pumping rate. For other experiments, only outflow from one osculum was tracked, so that one osculum rate was multiplied by the total number of oscula showing on the sponge to obtain whole sponge pumping rates.

In situ oscular outflow speeds were measured during two 1-week field trips to our coastal sampling site in N.E. Spain, in July and October, 2006. In total 21 sponges and outflow speeds from 97 oscula were obtained at three depths (4.5, 8.8 and 14.3 m). Outflow velocity measurements were made using a diver-operated, heated thermistor flow sensor and recorder. The thermistor was placed max. 3 mm above an osculum using a firmly fixed tripod. Never less than 6 replicate outflow speed measurements were made (range 6-21) from each osculum, spaced approximately 2 seconds apart. Background flow speeds were also recorded within 2 cm of the sponge surface and 2-4 cm above the local substratum. On average 11 background flow speed replicates spaced approximately 2 seconds apart were recorded for one sponge

(replicate range: 3-36). Outflow speeds from multiple oscula on each sponge were made (range: 2-14 oscula per sponge). For a given sponge sampled all oscular outflow speeds and proximal flow speeds were recorded within 10-15 minutes of each other.

Oscular diameters for sponges *in situ* were accurately measured from close-up photographs where a scalable object was in the plane of focus of the camera. Maximum diameters (length and width) plus tissue depth (height) were made for sponges *in situ* using a caliper with a sharpened depth pin. Water samples were taken in very close proximity to the same sponges for which oscular outflow was measured. Water samples were collected *in situ* using a 2 L Niskin bottle, and quantified for pico- and nanoplankton (four groups) plus heterotrophic bacteria numbers using flow cytometry following methods of Ribes *et al.* (1999).

RESULTS

Figure 1 shows a typical outflow plume exiting from the osculum of a sponge against a background of light-reflecting glass beads in the flow tank. The flow in the tank was moving from right to the left in the picture at 70 mm/s. The plume is being deflected downstream by the force of the water mass which is moving due to rotation of the paddlewheel of the flow tank. At the magnification used for this photo, the ejected plume is seen to be mostly devoid of beads indicating that the sponge has retained a high percentage of beads as “pseudo-food” in its choanocyte chambers. Under higher magnification a sufficient number of beads were found in the plume to adequately estimate outflow speed. (Table 2).



Figure 1. Still photo frame from laser-illuminated video sequence showing a portion of *Dysidea avara* specimen DA7. The osculum outflow plume (bending downstream) is visible against a field of light-reflecting glass beads dispersed in the flow-tank. The plume appears devoid of particles indicating the sponge was retaining most of the beads it ingested leaving few in the plume (not visible at this magnification). Background flow speed was 70 mm/s. Scale: osculum opening is 1.05 mm diameter.

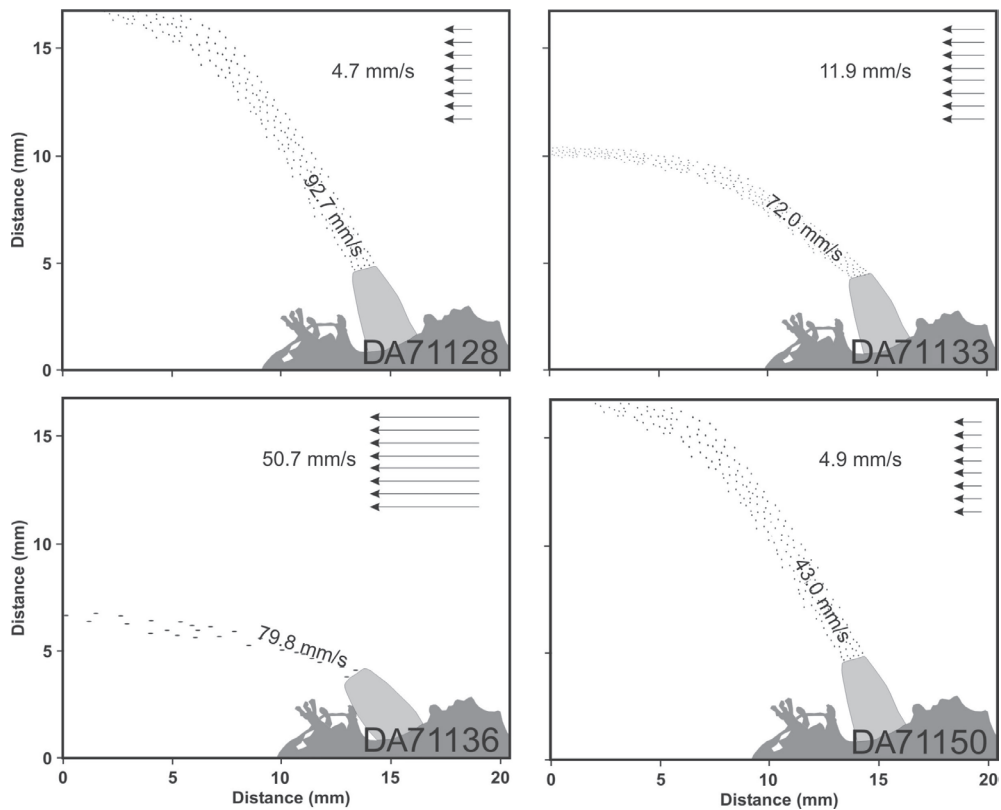


Figure 2. Outline drawing of an oscular outflow & background flow speed series with sponge DA7. Background flow was unidirectional throughout the series flowing right-to-left over the sponge. The osculum can be seen bending down-stream under the force of the highest background velocity flow of 50.7 mm/s, lower left frame. Outflow velocities (measured in the center of the jet) are imprinted onto the outflow plumes in each frame. Clock times are shown next to sponge number in each frame; total elapsed time for series was 22 minutes.

Figure 2 presents graphic results of a series of experiments with one of two oscula on sponge DA7; illustrating significantly reduced oscular outflow velocities over a relatively short time span (22 minutes). Background flow speeds were cycled from low to high, then back to low in four steps. The results show that after 22 minutes of continuous pumping (when background flow speed was returned to about the same speed as at the start of the series) oscular outflow velocity was considerably lower (43.0 mm/s) than at the start (92.7 mm/s). Outflow rates for the four time frames were as follows: 11:28 a.m., 0.007 ml (ml sponge)⁻¹s⁻¹; 11:33 a.m., 0.006 ml (ml sponge)⁻¹s⁻¹; 11:36 a.m., 0.006 ml (ml sponge)⁻¹s⁻¹; and 11:50 a.m., 0.003 ml (ml sponge)⁻¹s⁻¹ (ave. 0.006 ml (ml sponge)⁻¹s⁻¹). (Note: all outflow rates reported include an unknown amount of inter-cellular bound free water which may be inducted into the aquiferous system during pumping and exhaled out of the oscula.)



Oscular outflow in relation to background flow speed

Figure 3 shows oscular outflow results at different background speeds for five sponges. The six different series of experiments represent some examples of trends in oscular outflow rates against different background speeds. Each of the sponge specimens used in the series of experiments featured in panels a, b, and c attained outflow rates that were much higher (maximal rates 148–226 mm³/s) than any of the sponges featured in panels d, e, and f (maximal rates 30–82 mm³/s). Except where indicated in the foregoing descriptions, glass beads were used as flow tracking particles.

In panel (a) background flow speed was never greater than 24 mm/s (equal to calm season proximal flows, 5–14-m depths at the field study site). Oscular outflow remained generally stable at a high outflow rate (ave. 209.9 mm³/s \pm 9.4 mm³/s STD). A very small up-turn in oscular outflow rate (18.3 mm³/s) from the measure 2 minutes prior was coincident with the highest background flow speed applied (24 mm/s).

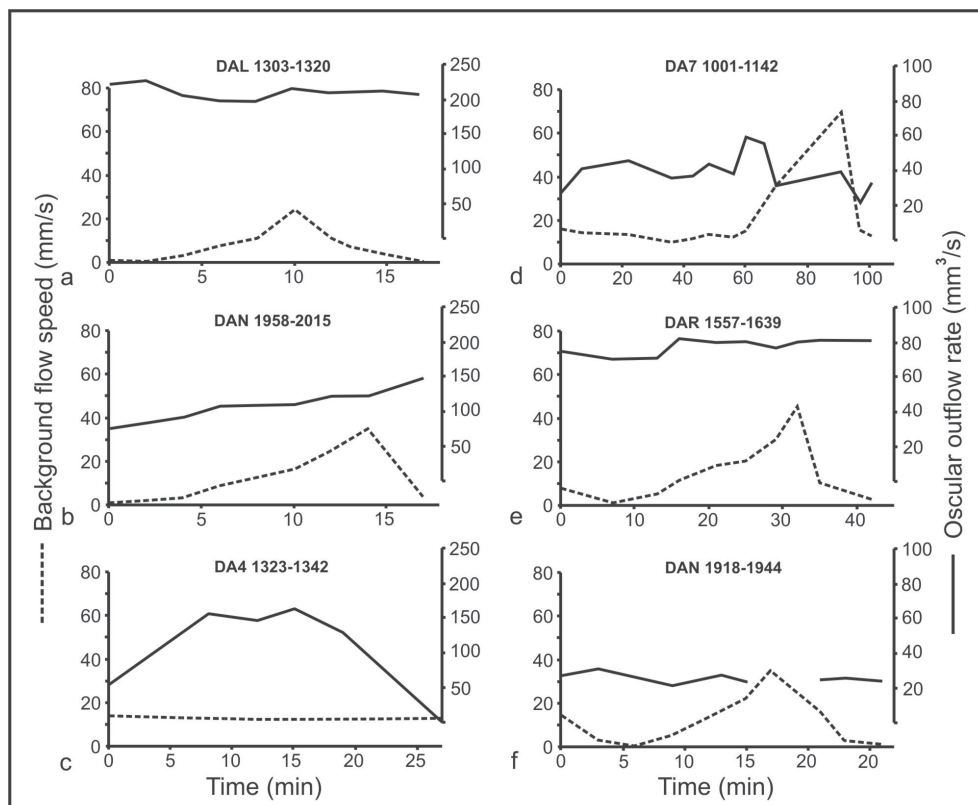


Figure 3. Representative results for oscular outflow vs. background flow speed for 5 sponges and 6 series of experiments (approx. 60 individual experiments represented).



In the 17 minute series of experiments presented in panel (b), it seemed that for the first 14 minutes (6 measures) oscular outflow was responding to increasing background flow, however, when background flow speed was reduced precipitously (from 35 mm/s to 3.8 mm/s) outflow still increased.

In the series seen in panel (c) the sponge began to pump and increased outflow rate to 163 mm³/s. At the 15th minute measurement the sponge reached its peak outflow rate, then 4 minutes later pumping rate had dropped and the sponge had stopped pumping altogether at the 27th minute measure.

At the start of the series shown in panel (d) only natural algae was dosed into the flow tank for use in flow tracing. For 43 minutes the sponge pumped at an average rate of 37.3 mm³/s, and filtered natural algae cells. Background flow speed averaged 13 mm/s during this period. After 43 minutes glass beads were added to the flow-tank to mix with any remaining algal cells. During the remaining 53 minutes of the series, the background speed was first increased to 70 mm/s and then reduced to 13 mm/s. The sponge first seemed to respond to the initial increase in background speed by increasing outflow rate, but after 6 minutes of higher pumping rate, outflow rate dropped again to below average for this series of experiments.

In panel (e), a sharp increase in background flow speed elicited no clear response in oscular outflow speed, which remained fairly constant at a relatively low average outflow rate of 77.9 mm³/s (± 4.3 mm³/s STD) throughout the 42 minute series.

A gap is seen in the outflow series shown in Fig. 3 panel (f) coincident with the highest background flow speed administered in this series (35 mm/s). The gap occurred because we were not able to find enough particles being emitted from the osculum during that period to make an accurate estimate of outflow (*i.e.* the sponge was retaining most of the glass particles as “pseudo-food”). Studying the video frames closely revealed that at two minutes before the gap was detected the highly elastic osculum membrane was fully distended by the pressure of the out-flowing water. The membrane shape could very aptly be described as a nozzle. The opening was smaller in diameter than the mid-section, which bulged outward somewhat due to the internal water pressure. When we manually moved through the video frames of the gap period using the slider tool, the osculum membrane was seen to “flutter” and become less distended. At four minutes after the gap measurement the membrane was again fully distended. The opening diameter of the osculum before the gap was 2.0 mm. It reduced to 1.5 mm diameter during the gap (a 44% reduction in area for the oscular opening), and four minutes afterwards it was back to 2.0 mm diameter. The smaller diameter during the gap period, coupled with the observed “flutter” indicated a reduced pumping level during the gap. On a proportional basis to the reduced area of the oscular opening (and using the calculated outflow volume from two minutes before the gap) outflow during the gap would have been maximally 13.3 mm³/s.

Figure 4 shows results from one oscillating flow experiment with sponge DA7, comparing oscular outflow rate from one of the two oscula showing on this sponge, to oscillating

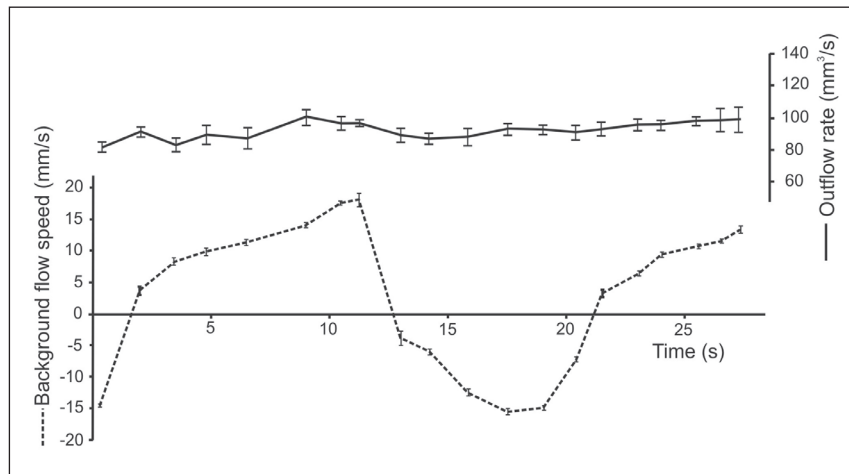


Figure 4. Oscular outflow rate in relation to an oscillating background flow for *Dysidea avara* sponge DA7 (sponge volume, 20 ml).

background flow speeds of approximately +17 mm/s, -15 mm/s maximum range. The average pumping rate was $92.2 \text{ mm}^3/\text{s} \pm 5.34 \text{ mm}^3/\text{s}$ STD.

Table 2 presents the summary of oscular outflow for six sponges tested in the flow-tank arranged in descending order of sponge size. Pumping rate of the osculum tested is

Sponge/Exp. I.D.	Est. Sponge Volume ml	Avg. Oscular Outflow Velocity mm/s \pm STD	Pumping Rate ml (ml sponge) ⁻¹ s ⁻¹	Pumping Rate liters/day whole sponge
DAN-1918-Spain	120	15.3 ± 1.6	0.008	82.94
DAR-1557-Spain	80	33.6 ± 1.8	0.008	54.14
DAL-1303-Spain	60	94.3 ± 4.2	0.011	57.89
DA2-1542-NL	30	26.0 ± 31.4	0.008	20.74
DA7-1001-NL	20	78.0 ± 9.8	0.010	17.28
DA7-Oscil-NL	20	119.8 ± 6.9	0.009	15.84
DA7-1112-NL	20	77.4 ± 22.0	0.008	14.11
DA7-1317-NL	20	75.1 ± 7.6	0.008	13.54
DA7-1049-NL	20	73.3 ± 15.6	0.004	6.91
DA4-1323-NL	15	82.4 ± 41.0	0.013	16.63
DA4-1440-NL	15	69.0 ± 28.0	0.004	4.54
Average \pm STD			0.008 \pm 0.003	

Table 2. Estimated volume, average oscular outflow velocity, pumping rate per ml sponge mass per second, and extrapolated pumping rate for the whole sponge on a daily basis are presented for six *Dysidea avara* sponges. Notes: DA7-Oscil-NL indicates an oscillating flow-cycle experiment conducted in The Netherlands laboratory; DAN-1918-Spain, indicates sponge DAN experiments started at 19:18 hrs in Spain temporary laboratory, etc.



extrapolated to pumping rate for the whole sponge on a liters per day basis (column 5) using the estimated sponge volumes from column 2, and the number of oscula on that particular sponge (100% of the oscula were presumed to be pumping). Pumping rate in ml of water pumped by one ml of sponge mass per second is listed in column 4; (not all experiments conducted with all sponges are shown).

Oscular outflow from wild sponges in situ

Table 3 gives the results of *in situ* mean oscular outflow velocity measurements for 21 sponges and 97 oscula in relation to mean background flow speeds. The July recording period was during calm weather and flat seas, and the mean background flow speed over four consecutive sampling days was $27.3 \text{ mm/s} \pm 13.3 \text{ STD}$. The October recording period (5 consecutive days) commenced 1 day after a wind-storm had abated (where surface waves had been 1-2 m on 7-10 second intervals). However, the range of mean background flows for the October period was a low $16.4 \text{ mm/s} \pm 7.3 \text{ STD}$, differing significantly ($P = 0.009$) from the July period.

	4.5 m		8.8 m		14.3 m		<i>n</i> = (units)
	July	Oct.	July	Oct.	July	Oct.	
No. Sponges	2	4	5	3	3	4	21
No. Oscula	4	21	14	28	11	19	97
Mean Oscular Outflow Velocity \pm STD	19.4 ± 5.8	4.2 ± 1.0	74.3 ± 9.7	19.0 ± 5.0	25.6 ± 7.2	6.0 ± 1.6	(mm/s)
Mean Local Background Flow Speed \pm STD	17.2 ± 8.0	3.6 ± 1.1	27.3 ± 13.3	16.4 ± 7.3	18.4 ± 4.6	7.4 ± 0.80	(mm/s)
Strongly-flowing Oscula	3	1	12	17	4	1	38
Marginally-flowing Oscula	0	20	2	10	7	18	57
Not-flowing Oscula	1	0	0	1	0	0	2
% Strongly-flowing Oscula	75%	5%	86%	61%	36%	5%	66% July 24% Oct
% Moderately-flowing Oscula	0%	95%	14%	36%	63%	95%	26% July 75% Oct
% Oscula Not flowing	25%	0%	0%	4%	0%	0%	8% July 1% Oct

Table 3. Mean oscular outflow velocities, background flow speeds, and oscula flow-strength ratios for *Dysidea avara* sponges at three depths *in situ*; July and October, 2006, Cala Illa Mateua, L'Escala, Girona, Spain.



For one large sponge in the field (sponge B-3 at the 8.8 m sheltered “mini-cave” site in October) oscular outflow velocities were obtained for 14 of 38 total oscula within 15 minutes. This sponge produced the highest oscular outflow velocity measured in this study (17.7 cm/s; July). From *in situ* caliper measurements we estimated its volume of 576 cm³. From close-up scaled photographs we measured oscular diameter for nine oscula and arrived at an average of 7.7 mm. Outflow rate calculations using these dimensions yielded 0.05 ml/ml sponge·s⁻¹. The extrapolated whole sponge rate on a per day basis was 2,388 L per day.

A result from the *in situ* oscular outflow studies (data not shown) showed in July (when the weather and seas were calm) that oscular outflow speeds for pumping sponges at the protected 8.8 m mini-cave site were significantly higher (single factor anova, $P = 0.006$) than for sponges at the 4.5 m site, and the deeper 14.3 m site (single factor anova $P = 0.006$). Oscular outflow velocities for the July 8.8 m sponges were also significantly higher (single factor anova, $P = < 0.001$) than for any depth-group from the October sampling. For the July 8.8 m site sponges, 134 separate oscular outflow velocity measurements were recorded for oscula that were flowing at a velocity in excess of the mean background flow speed; 37 of those (28%) were in the range 9.7-17.7 cm/s.

DISCUSSION

Oscular outflow velocities and rates

Whole sponge pumping rate from the flow-tank studies (Table 2, column 5) was positively correlated with sponge volume ($r^2 = 0.94$, $P = < 0.0001$); *i.e.*, larger sponges pumped more water per day than did smaller sponges. If we were to add the one *in situ* result for the large B-3 sponge to the flow-tank results it would raise the correlation coefficient to 0.97. This sponge was the largest *Dysidea avara* found in our field investigations in Spain, but even its 1,172 L/day outflow was still a factor of about 20 lower than the 23,000 L/day we calculated from data reported by Reiswig (1974) for a *Mycale* sponge from a deep Jamaican reef.

Back-dividing each of the whole sponge pumping rates (Table 2) by the sponge volume and calculating the average, we obtained a rather constant pumping rate for *Dysidea avara* of 0.008 ml (ml sponge)⁻¹s⁻¹ \pm 0.003 STD. This average pumping rate is considerably lower than reported for: three Caribbean sponges (0.04-0.34 ml (ml sponge)⁻¹s⁻¹, Reiswig, 1974); North Sea *Haliclona* cuttings (0.07 \pm 0.03 ml (ml sponge)⁻¹s⁻¹, Riisgård *et al.* 1993); a California *Haliclona* (0.13 ml (ml sponge)⁻¹s⁻¹, Reiswig, 1975); and eight Bermuda species (0.2-0.4 ml (ml sponge)⁻¹s⁻¹, Vogel, 1977). Results from this study are two times lower than that measured for the calcareous Mediterranean sponge *Leucandra aspera* (Bidder, 1923), and equal to rates obtained in the laboratory for *Spinoseella sororia* a common Bermuda finger sponge (Parker 1910, 1914). The current results are also somewhat different from previously



reported results by our group for *Dysidea avara* sponges DA2, DA4 and DA7 (Mendola *et al.* 2007b). These same three sponges were also subjects in this study (Table 1).

The Caribbean sponges were all considerably larger than the *Dysidea avara* specimens we tested in the flow tank, however, the North Sea *Haliclona* cuttings were much smaller; (sponge volumes were not reported in the Bermuda study). Given the whole sponge size/ outflow rate positive correlation, it is not surprising that outflow rates for the relatively small-sized *Dysidea avara* sponges in this study were consistently lower than those reported by Reiswig (1974) or Vogel (1977) for larger sponges. However, comparing our results to those obtained for the 1 ml-size *Haliclona urceolus* branches reported by Riisgård *et al.* (1993) our results are a factor of 10 lower. This disagreement between results for very different-sized sponges is difficult to explain. Performing comparative oscular outflow measurements in our experimental set-up with other sponge species using *Dysidea avara* as controls would be needed to be able to compare pumping rates unambiguously.

The results of the 22 minute, 4-measure outflow series shown in Fig. 2, illustrates the subject sponge either became fed-up with glass beads and then slowed its pumping rate (indicating possible satiation), or possibly a “tank effect” or other disturbance contributed to the outflow reduction witnessed. We plotted oscular outflow rate against background flow speed, and found no response of outflow rate to the steep increase in background flow speed applied before the 11:36 measurement (lower left frame Fig. 2), ruling out high flow, *per se*, as the cause for the decline in outflow rate recorded at the end of the experiment. The exact cause of the slow-down in pumping rate was not determined, nor were experiments conducted to further investigate the most probable cause, due to the need for problematic controls (*e.g.*, same-size sponge with similar history of pumping rates, not fed), etc., and extensive SEM work to try and detect evidence of satiation, both of which were outside the scope of this research.

The largest sponge tested in the flow tank (DAN, est. volume 120 ml) would have been classified as a medium-sized sponge within the population of *Dysidea avara* at the field study site. The size of our flow tank could not accommodate sponges much larger (*i.e.* taller) than DAN. With a larger flow-tank it would be interesting to measure outflow rates from larger specimens to look for a possible peak in oscular outflow with size (as was reported for the large Caribbean sponge *Verongia gigantean* reported by Reiswig, 1974). Another alternative could be a plateau in outflow rate above a certain sponge size.

From our experience over the 3-month period when 136 separate outflow experiments were conducted, we came to recognize that the *Dysidea avara* captive sponge specimens varied considerably in their “performance” (*i.e.* pumping rates) from day-to-day, sometimes as much as 7.5x. When any one specimen was pumping at its best, we recorded maximal outflow rates in the higher range reported in Fig. 3 (148-226 mm³/s) when not at its best its output could be in the lower reported range (30-82 mm³/s). The range of variability

encompassed what we believe is “the normal range” for *D. avara* specimens of this size range, which included the specimens freshly collected for the runs conducted at the temporary laboratory set-up in Spain.

Comparative pumping and food sources – temperate vs. tropical sponges

When comparing oscular outflow rates between sponges from differing habitats it is important to keep in mind that sponges are pumping water through their bodies primarily to feed themselves, and in a food particle rich environment less pumping is required (to ingest a given quantity of calories, for example) than in a particle poor environment. Water samples taken in close proximity to the sponges from which we obtained oscular outflow measurements *in situ* showed high concentrations of combined total pico- and nanoplankton, and heterotrophic bacteria (3.1×10^6 and 3.2×10^6 cells/ml, respectively). These planktonic fractions are known to make-up the majority of particles filtered by *Dysidea avara* sponges, accounting for 85% of its total ingested organic carbon. The remaining 15% comes from larger-sized particulate fractions, revealing that this sponge receives virtually none of its organic carbon needs from dissolved organic matter (DOM), and in fact is a net DOC producer (Ribes *et al.* 1999), and is virtually free of bacterial symbionts (Turon *et al.* 1997).

In contrast to the nutrient rich coastal waters of the Mediterranean where *Dysidea avara* is found, deep, oligotrophic tropical coral reef waters (Caribbean reefs included) are known for their much lower total particle concentrations (*ca.* 10^4 – 10^5 /ml), and low levels of total particulate organic carbon content (58–71 μg POC/L; Reiswig, 1981). Such particle-poor environments may obviate higher pumping rates for coral reef-dwelling sponges to meet their total caloric needs. Yahel *et al.* (2003) showed that for one Red Sea sponge, (*Theonella swinhoei*) symbionts accounts for up to two-thirds of the entire sponge biomass, and the sponge-symbiont association is an efficient user of dissolved organic matter (DOM) from the water column. The exact mechanisms for the DOM removal is yet to be elucidated, but the implication is that symbiont-bearing sponges may obtain at least a portion of their nutritional needs through symbiont pathways, and therefore (we speculate) would require higher pumping rates to “mine” the relatively “low grade ore” of DOM.

Flow-through augmentation from “free energy” from the environment

Jorgensen (1966) presents data and calculations that suggest that the energy contained in the food particles filtered by a sponge from its surrounding medium barely meets the energy requirements of its pumping apparatus. He further suggests, that given that sponges are a highly successful group of active suspension feeders inhabiting diverse environments from the seas, oceans and many freshwaters of the planet, as a group they must have evolved and adapted mechanisms for energy conservation and/or utilization of the “free energy” of the water mass moving passing them.



From an evolutionary perspective it can be stated, that for a filter-feeding aquatic organism, any mechanism that can reduce the energy costs of moving water past or through its filtering apparatus should be favored by natural selection. This supposition has led marine researchers to look for, and describe what they concluded were energy saving devices and behaviors in: sponges (Vogel, 1974, 1975); ascidians (Knott *et al.* 2004; and Young and Braithwaite, 1980); and sea scallops (Hartnoll, 1967); among others. Vogel, (1974, 1975, 1977) and Vogel and Bretz (1972) discuss three mechanisms for utilization of induced flow by active suspension feeders: (1) dynamic force, (2) the Bernoulli effect, and (3) viscous entrainment. Vogel (1978) also makes an elaborate case for one-way valves in sponges (based on experimental evidence from both field and model work) that he suggests aid sponges in assuring one-way flow through their aquiferous systems while allowing induced flow from the environment.

From our results we cannot conclude that pumping rate in *Dysidea avara* directly responds to abrupt or even gradual increases in background flow speed. This is best illustrated in the oscillating background flow example presented in Fig. 4. These observations led us to conclude that *Dysidea avara* has not evolved morphological adaptations to take significant advantage of any of the environmental flow induction mechanisms proposed by Vogel, nor did we find evidence for true one-way valves in *Dysidea avara*. By contrast, we found that this sponge controls the rate of water movement through its aquiferous system by controlling its pumping action. Examples from Fig. 3 illustrate this behavior, where sharp rises in background flow speed did not produce concomitant rises in oscular outflow rates.

“Shut-off” oscular outflow response

A characteristic behavior of flow tank specimens was what we termed “shut-off”, where sponges first slowed then stopped pumping at increased background flow speeds, or other applied experiment conditions. For all specimens tested the response was different and variable from experiment to experiment. For a number of specimens, at or about 75 mm/s (applied for longer than a few minutes) oscular membranes began to bend over against the increasing force of the background flow, outflow rate slowed and then stopped, *i.e.*, “shut-off”. Still for other specimens “shut-off” did not occur until the background flow speed was at 100 mm/s, and for one case and experiment with sponge DA4, shut-off did not occur until the background flow speed was 120 mm/s.

Shut-off also occurred for reasons other than high background flow, for example, we observed shut-off coincidentally after a particular specimen had been moved around the tank a number of times during an experimental series. On a few occasions we observed un-expected shut-off following administration of a feeding stimulant (shrimp extract) that was often administered to stimulate the sponge to pump at a higher rate. At other times the stimulant had an immediate effect on the sponge and it would resume pumping immediately,

sometimes at a considerably higher rate than before it had shut-down. At still other times specimens were known to shut-off with no correlation to any experimental manipulation, or otherwise detectable cause. Usually, but not in all cases after a sponge had shut-off, we could stimulate it to start pumping again by exchanging most or all of the water in the flow tank with fresh water from the community sponge holding tank.

Oscular shut-off behavior was also observed with *Dysidea avara* sponges in the sea, and found to occur in about the same range of background flow speeds (8-13 cm/s; unpublished observations). Again, not all oscula on any one sponge *in situ* were flowing at the same rates at the same time. During calm weather more oscula were found to be flowing at a higher rate than following a stormy period (Table 3). In a strong surging sea we observed that oscula protected by virtue of their position on the sponge (*e.g.*, those located on the side of the sponge away from the prevailing flow direction close to a rock face, or to another sponge or organism) were often open and flowing, whereas others facing the full force of such flows were closed. During strong storms we observed that nearly all of the oscula on all sponges were shut-down (also reported for Caribbean reef sponges by Reiswig, 1971). Following a storm oscula opened again as the waves subsided, which could take just a few hours for short-duration squalls, or days in the case of stronger persistent storms (Table 3, and unpublished data).

CONCLUSIONS

It is important for the reader to know that only a relatively small portion of all of the outflow experiments conducted are reported. The time required for analyzing each series of experiments was significant, and therefore, we chose to find and present representative examples of different responses of specimens to different treatments to illustrate the range of responses and some trends observed in the data set. We concluded that analyzing more data, *per se*, would not have changed the trends represented in the outflow series shown in Fig. 3, namely that *Dysidea avara* regulates its outflow through its pumping activity, and does not change its outflow rate to any appreciable degree as a response to abrupt or even gradual changes in background flow speeds within its normal environmental flow range. As flow speeds raise above its normal operating range (*e.g.*, during periods of storms and rough seas) the sponge slows, then shuts-down its outflow, closes its oscula and simply waits until conditions and local background flow speeds return to within its normal operating range to resume pumping.

The results of our research (both from the flow tank and the field studies) allow us to recommend to *Dysidea avara* aquaculturists, that background flow speed applied in culture tanks should not eclipse 8-10 cm/s for anything but momentary periods at the peaks of an oscillating flow regime. This moderate range of ambient flow speeds should prevent *en*



masse “shut-down” of the sponges’ internal pumps, and allow the sponges to pump water continuously (notwithstanding normal endogenous rhythms) to maximize feeding, growth, biomass and natural product production.

ACKNOWLEDGEMENTS

This study was financially supported by EU Project No. 017800. We thank Sander Kranenbarg, Ph.D. and ir. Mark van Turnhout (both of WU/EZO) for their help with Matlab programming. We thank M. Ribes of CSIC, Barcelona, for advise and help with flow cytometry.

REFERENCES CITED

- Bidder, G. P. 1923. The relation of the form of a sponge to its currents. *Quart. J. Microscop. Soc.* **67**: 292-323.
- Hartnoll, R. G. 1967. An investigation of the movement of the scallop, *Pecten maximus*. *Helgolander Wiss. Meeresunter.* **15**, 523-533.
- Jorgensen, C. B. 1966. The Biology of Suspension Feeding. Pergamon Press, New York.
- Larsen, P. S. and H. U. Riisgård. 1994. The sponge pump. *J. theor. Biol.* **168**:53-63.
- Knott, N. A., A. R. Davis, and W. A. Buttemer. 2004. Passive flow through an unstalked intertidal ascidian: orientation and morphology enhance suspension feeding in *Pyura stolonifera*. *Biol. Bull.* **207**: 217-224.
- Mendola, D., S. de Caralt, M. J. Uriz, F. van den End, J. L. van Leeuwen, and R. H. Wijffels. 2007a. (submitted). Environmental flow regimes for *Dysidea avara* sponges.
- Mendola, D., J. G. M. van den Boogaart, J. L. van Leeuwen, and R. H. Wijffels. 2007b. Re-plumbing in a Mediterranean sponge. *Biol. Lett.* **3**(6): 595-598.
- Minale, L., R. Riccio, and G. Sodano. 1974. Avarol, a novel sesquiterpenoid hydroquinone with a rearranged drimane skeleton from the sponge *Dysidea avara*. *Tet. Lett.* **38**: 3401-3404.
- Müller W. E. G., A. Maidhof, R. K. Zahn, H. C. Schröder, M. J. Gasic, D. Heidemann, A. Bernd, B. Kurelec, E. Eich, and G. Sibert. 1985. Potent antileukemic activity of the novel cytostatic agent avarone and its analogues *in vitro* and *in vivo*. *Cancer Research* **45**: 4822-4827.
- Parker, G. H. 1910. The reaction of sponges with a consideration of the origin of the nervous system. *J. exp. Zool.* **8**: 3-41.
- Parker, G. H., 1914. On the strength of the volume of water currents produced by sponges. *J. exp. Zool.* **16**: 443-446.
- Reiswig, H. M. 1971. *In situ* pumping activities of tropical Demospongiae. *Mar. Biol.* **9**: 38-50.
- Reiswig, H. M. 1974. Water transport, respiration and energetics of three tropical marine sponges. *J. Exp. Mar. Biol. Ecol.* **14**: 231-249.
- Reiswig, H. M. 1975. The aquiferous system of three marine Demospongiae. *J. Morph.* **145**(4): 493-502.
- Reiswig, H. M. 1981. Particulate organic carbon of bottom boundary layer and submarine canyon cavern waters of tropical coral reefs. *Mar. Ecol. Prog. Ser.* **5**: 129-133.
- Ribes, M., R. Coma and J-M. Gili. 1999. Natural diet and grazing rate of the temperate sponge *Dysidea avara* (Demospongiae, Dendroceratida) throughout an annual cycle. *Mar. Ecol. Prog. Ser.* **176**: 179-190.
- Riisgård, H. U., S. Thomassen, H. Jakobsen, J. M. Weeks, and P. S. Larsen. 1993. Suspension feeding in marine sponges *Halichondria panicea* and *Haliclona urceolus*: effects of temperature on filtration rate and energy cost of pumping. *Mar. Ecol. Prog. Ser.* **96**: 177-188.



- Schläppy, M-L, F. Hoffman, H. Røy, R. H. Wijffels, D. Mendola, M. Sidri, and D. de Beer. 2007. Oxygen dynamics and flow patterns of *Dysidea avara* (Porifera: Demospongiae). *J. Mar. Biol. Ass. U.K.* **87**: 1677-1682.
- Turon, X., J. Galera, and M. J. Uriz. 1997. Clearance rates and aquiferous systems in two sponges with contrasting life history strategies. *J. Exp. Zool.* **278**: 22-36.
- Uriz, M. J., D. Rosell, and D. Martin. 1992. The sponge population of the Cabrera archipelago (Balearic Islands): Characteristics, distribution and abundance of the most representative species. PSZN I: *Mar. Ecol.* **113**: 101-117.
- Uriz, M. J., X. Turon, J. Galera, and J. M. Tur. 1996. New light on the cell location of avarol within the sponge *Dysidea avara* (Dendroceratida). *Cell Tissue Res.* **285**: 519-527.
- Vogel, S. 1974. Current-induced flow through the sponge *Halichondria*. *Biol. Bull.* **147**: 443-456.
- Vogel, S. 1975. Flow in organisms induced by movements of the external medium. In: Scale Effects in Animal Locomotion. T. J. Pedley (ed). Academic Press. London. Pp. 285-297.
- Vogel, S. 1977. Current-induced flow through living sponges in nature. *Proc. Natl. Acad. Sci.* **74** (5): 2069-2071.
- Vogel, S. 1978. Evidence for one-way valves in the water-flow system of sponges. *J. exp. Biol.* **76**: 137-148.
- Vogel, S., and W. L. Bretz, 1972. Interfacial organisms: passive ventilation in the velocity gradients near surfaces. *Science.* **175**: 210-211.
- Yahel, G., J. H. Sharp, D. Marie, C. Häse, and A. Genin. 2003. In situ feeding and element removal in the symbiont-bearing sponge *Theonella swinhoei*: Bulk DOC is the major source for carbon. *Limnol. Oceanogr.* **48**(1): 141-149.
- Young, C. M., and L. F. Braithwaite. 1980. Orientation and current-induced flow in the stalked ascidian *Stela montereyensis*. *Biol. Bull.* **159**: 428-440.



Chapter 6

Re-plumbing in a Mediterranean sponge

D. Mendola^{1, 2, *}, J. G. M. van den Boogaart²,
J. L. van Leeuwen², R. H. Wijffels¹

¹ Bioprocess Engineering Group ²Experimental Zoology Group,
Wageningen University, P.O. Box 8129, 6700 EV, Wageningen,
The Netherlands. *Author for correspondence:
email: dominick.mendola@wur.nl

Abstract: Observations are reported for *Dysidea avara* sponges where once-functioning oscula (outlets) are converted through internal re-plumbing into functioning over-sized (1.5-2.5 mm dia.) ostia (inlets). Flow-tank studies employed high-speed photography and particle tracking of laser-illuminated 0.5-6.0 μm diameter glass beads to trace particles streaming into over-sized ostia. A fluorescein dye/glass bead uptake experiment showed that an over-sized ostium was connected (through internal structures) to the lone osculum. Beginning 30 seconds after uptake and continuing over a 20 minute period dye streamed from the osculum, but no beads emerged. Scanning electron microscopy revealed beads were deposited only on the inhalant side of particle filtering choanocyte chambers and not on the exhalant side, suggesting internal re-plumbing had occurred. Functioning over-sized ostia were also found on freshly-collected specimens in the field, making it highly unlikely that formation of over-sized ostia was only an artifact of sponges being held in a laboratory tank.

Key words: sponges; over-sized ostia, replumbing



INTRODUCTION

Sponges filter bacteria, micro-algae and other small particles from ambient water as food. Water is drawn-in by flagellar motion through thousands of 5-50 μm ostia (size is species-dependent). Inflow passes through inhalant canals to particle-filtering choanocyte chambers, then out through exhalant canals to millimeter-sized (or larger) surface openings called oscula (Bergquist 1978).

Dysidea avara (Schmidt) is a spongin-supported demosponge (Order Dictyoceratida) found in low-flow cryptic habitats of the rocky sublittoral of the middle and western Mediterranean basins (Uriz *et al.* 1992). Normal-sized ostia range from 27-31 μm diameter grouped in clusters of 15-20. Cluster groups are located between dermal reticulations radiating from the tips of conules formed by the uplifting of the surface membrane by major skeletal fibers (Teragawa 1985). Oscula range from 1-10 mm diameter, are generally found on elevated and conulated protuberances, and have raised cylindrical membranes which open/close to control outflow rate (Fig. 3, Electronic Supplementary Materials - ESM).

Remodeling in sponges is the process by which individuals change body forms (including the positions of ostia and oscula) in response to changes in environmental factors (Simpson 1984). Here we report evidence that *Dysidea avara* is able to convert oscula into functioning over-sized ostia (OSO; 1.5-2.5 mm dia) by internal re-plumbing, *i.e.*, old exhalant canals are converted to new inhalant canals, and *visa versa*.

METHODS AND MATERIALS

Nine, small-size (15-50 cm^3) *Dysidea avara* specimens were collected at 9-12 m depth on pieces of native rock from the L'Escala region in N.E. Spain. Specimens were transported to The Netherlands and maintained in a 550 liter aquarium with biofiltration. Over the entire 3-month period of this study, sponges were fed 2x/day with marine broths made from fish and shrimps, and/or manufactured shellfish diets (INVE, Belgium CAR-1), and 3-4x/week with cultured micro-algae (*Phaeodactylum tricornutum*, *Nannochloropsis* sp.): starting concentrations 2-3 $\times 10^5$ particles/ml.

In/out-flow velocities, flow rates, and local background velocities (LBV) were derived using particle tracking velocimetry (PTV) in a 7.5 liter flow-tank (Fig. 4, ESM). A mixture of 0.5-6.0 μm dia. hollow glass beads (J.J.Bos, NL) was seeded into the flow-tank (*ca.* 100,000 particles/ml) to reflect laser light and trace flow streamlines entering OSO and exiting oscula. A laser light sheet (0.5 mm width) was projected inside the flow-tank from an Excel 2300 laser. High-speed photography (50-500 fps) employed a Redlake® digital camera, Nikon® 105/1:2.8 lens and 50 mm extension ring. Images were captured onto a PC using Redlake's Midas Player® and analyzed using Matlab® sub-routines. We estimated the accuracy of determination of outflow rates at $\pm 8\%$, and inflow rates at $\pm 14\%$ (see methods addendum



in ESM). Flow-tank experiments in Spain were conducted in an indoor laboratory 150 m from the collection site. Local seawater and ambient conditions were used.

To trace flow into and out of specimens and to test for particle retention, a fluorescein dye (Aldrich F2456, 95%) plus glass bead uptake experiment was performed. A 15 cm³ specimen with one osculum and 3 OSO was selected (DA-7, Table 1 ESM). The tip of a 0.9 mm-bore hypodermic needle was positioned close to OSO-1. Glass beads were mixed into a fluorescein dye/seawater solution (approx. 1×10^6 beads/ml) and loaded into a syringe attached to the needle. Beginning at t_0 , and spaced 2-3 minutes apart, 3 small increments of dye/bead suspension were carefully expelled out of the needle directly in front of OSO-1. The video camera, laser (and normal light) were used to visualize and record movies of the fluorescein dye and glass beads being sucked into the OSO and exiting the osculum.

Specimen fixation and SEM methods followed Johnston and Hildemann (1982). After fixation the entire specimen was frozen in 100% ethanol/liquid nitrogen and cryofractured. The first fracture was on the centerline of the filmed OSO-1 structure and in-line with the osculum; and the second by splitting one of the first halves on the centerline of one of the 2 remaining OSO. One part from the second fracturing broke into two which resulted in four pieces. While still in 100% ethanol excess materials were trimmed-away. The four pieces were dried in a critical-point dryer (Balzers) then glued onto sample holders using conductive carbon cement. Each sample was sputter-coated with 20 nm platinum, and viewed using a field emission scanning electron microscope at 4 kV (JEOL 6300 F, Tokyo, Japan).

RESULTS

Morphological changes and flow rates

Within days of introduction into the 550 L aquarium, 6 of 9 specimens resorbed most of their oscular membranes but not all of them. For 3 sponges where oscular membranes had been resorbed 1.5-2.5 mm circular or oval holes remained. Pinacoderm grew to cover over some holes and in other cases holes remained uncovered. These 3 sponges maintained some holes for their entire 3-months in the aquarium. Within days to weeks new oscula developed elsewhere on their body surfaces.

After 4 weeks in the 550 L aquarium flow-tank studies commenced with the 3 specimens with large holes on their surfaces. A total of 49 inflow (into OSO) and 93 outflow (from oscula) PTV experiments were performed (Table 1, ESM). For one sponge with residual holes (sponge DA-7) three holes had been converted into functioning over-sized ostia (OSO), *i.e.*, beads were seen being drawn into the OSO. Figure 1a shows the three OSO on the surface of DA-7. Figure 1b shows PTV-derived streamlines and flow speed distributions around this sponge and into the OSO. Spatially-averaged input velocities were: 7.2 ± 2.7 mm/s for OSO-1 and 10.7 ± 1.5 mm/s for OSO-2 (*see details of velocity and flow-rate calculations in*

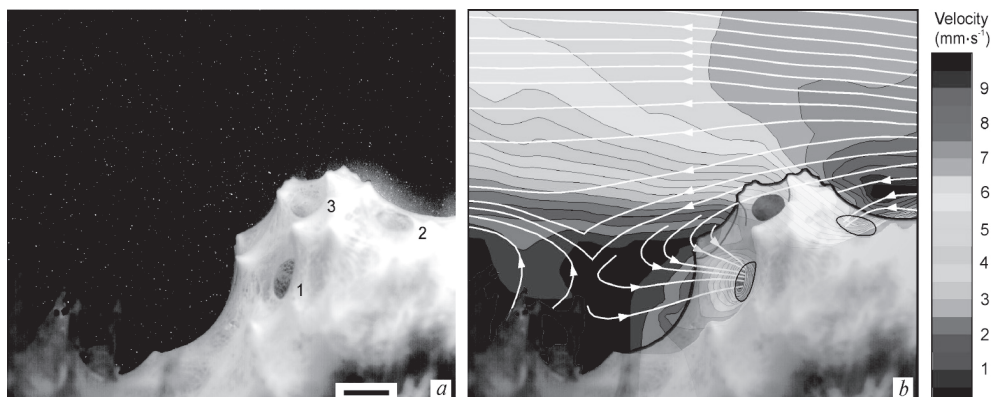


Figure 1. (a) Normal light photograph of *Dysidea avara* sponge showing three over-sized ostia (1, 2, 3) superimposed onto a high-speed video image showing laser-illuminated glass beads in the background; (b) shows computed speed distributions (colors) and (white) streamlines around sponge which is superimposed semi-transparently onto calculated speed distributions. Inflow is visible only for ostia 1 & 2, given that ostium 3 was not illuminated by the laser light-sheet. Scale bar = 2 mm. [movie in ESM shows beads entering over-sized ostia.]

ESM). Local background velocities (LBV) upstream of the sponge averaged 7 mm/s, whereas velocities in the lee of the protuberance with the OSO were reduced by morphology-induced drag to 1-4 mm/s (fig. 1b).

Calculated spatially-average inflow rates were: 18.3 mm³/s (OSO-1) and 19.4 mm³/s (OSO-2). Beads had been seen entering OSO-3, therefore it was assigned the average inflow rate of the two filmed ostia. Therefore, the combined inflow rate of the 3 OSO was estimated at 55-60 mm³/s. Less than an hour earlier we had measured outflow rate for the osculum located on the same protuberance at 108.4 mm³/s. We assumed local ostia served the local osculum, therefore the 3 OSO contributed approximately 50% of the oscular outflow. Concurrently the sponge possessed two oscula, the second was on the other protuberance. Its outflow rate was 96.5 mm³/s. Therefore the 3 OSO contributed *ca.* 28% of total flow rate through the sponge. In keeping with the principle of continuity the remaining 72% was provided by fields of normal-sized ostia.

Large surface holes were observed on many *Dysidea avara* sponges *in situ* in Spain. Of 12 specimens collected for flow-tank studies 7 were pumping sufficiently to allow recording oscular outflow movies. Two of the 7 were checked for over-sized ostia and inflow of particles. On one sponge (DA-R, ESM Table 1) we found and filmed one functioning OSO. Calculated spatially-average inflow velocity was 1.7 ± 0.4 mm/s, average inflow rate 5.7 mm³/s, and LBV 0.5 mm/s.

Fluorescein dye/glass bead uptake experiment (Fig. 2a)

Three releases of fluorescein dye/bead solution (each approx. 25 μ l) were performed over a 10 minute period. Less than 30 seconds elapsed between the first release and when





dye began exiting the osculum indicating a functional connection to OSO-1. We estimated 10% of each release (2.5 μ l) escaped the suction of OSO-1. These portions were carried downstream by the background flow (LBV = 2.9 mm/s) and diluted into the 7.5 liters of 0.2 μ m filtered seawater in the flow-tank (dilution, approximately 1 bead/ml). Given this high dilution factor it is not surprising that neither dye or beads were observed being sucked into normal-sized ostia.

The spatially-averaged inflow velocity was 1.3 ± 0.2 mm/s, and inflow rate was 5.5 mm³/s. Approximately 20 minutes into the experiment the camera was focused onto outflow from the osculum. Two 10 second movies were recorded, one using laser illumination the other normal light. No glass beads were filmed within the green dye plume exiting the osculum.

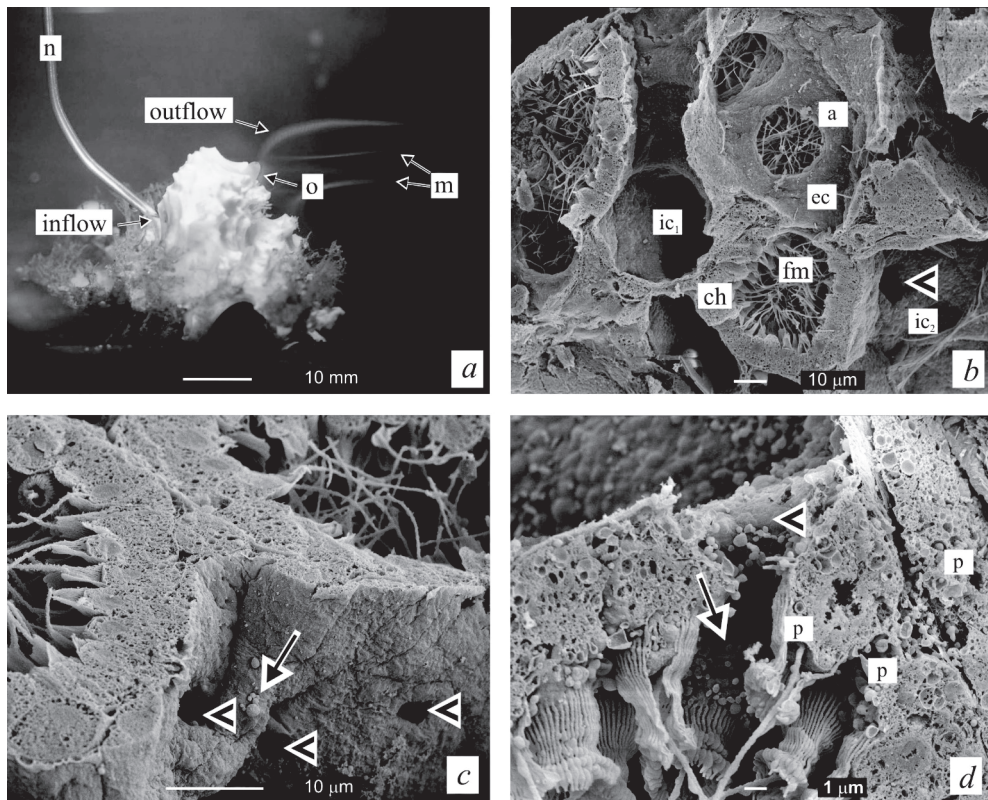


Figure 2. (a) fluorescein dye experiment. Normal light digital photograph of sponge DA-7 as fluorescein dye began to exit the osculum; (b) SEM digital image of internal anatomy of sponge DA-7; (c) inhalant canal and prosopyles (inlets to choanocyte chambers); [see enlarged image of beads in ESM Fig 2(c)]; (d) glass beads deposited on inhalant side of choanocyte chamber. Note: partially torn prosopyle (artefact of cryofracture) with glass beads deposited onto the prosopyle wall and at the base (inhalant side) of choanocyte collars; **a** = apopyle (exit of choanocyte chamber); **ch** typical cryofractured choanocyte chamber showing mass of tangled flagella; **ec** exhalant canal; **fm** flagellar mass; **ic₁** inhalant canal; **ic₂** inhalant canal leading to prosopyle; **m** streams of dye that escaped the suction of the ostium; **n** hypodermic needle; **o** osculum; **p** phagosomes with ingested glass beads; (**<**) prosopyle openings which lead into the choanocyte chambers; (**→**) glass beads.





This indicated that the OSO was connected *via* internal structures to the only osculum, and glass beads were being completely retained within the sponge. Since after 20 minutes no glass beads had been seen exiting the osculum the experiment was terminated and the sponge fixed for scanning electron microscopy (SEM).

SEM images

We made an oblique cut across the inhalant canal leading directly from OSO-1 down into the sponge. Although no SEM pictures were made of the entire canal a few glass beads were seen and imaged. Glass beads were deposited on internal structures of only those pieces produced from cryofracturing across OSO-1 (where beads were administered) and then only on the prosopyle (inlet) side of the choanocyte chambers and not on the apopyle (outlet) side. This suggests that the sponge re-plumbed some of its inhalant canals to connect with OSO-1 and at least some of its choanocyte chambers (figs. 2 c, d: →). No glass beads were observed within the masses of tangled flagellae of any of 7 choanocyte chambers imaged (Fig 2b).

DISCUSSION

Remodeling in sponges (*i.e.*, subtle or radical changes in body form) is a well studied phenomenon triggered by environmental changes including temperature, salinity, other stressors, or age and reproductive imperative (Fell *et al.* 1989; Van de Vyver and Willenz, 1975; Cerrano *et al.* 2001). We subjected *Dysidea avara* sponges to the cumulative stress of collection, long distance transportation, and introduction to an artificial environment. Shortly thereafter they underwent external and internal remodeling and produced functioning OSO from resorbed oscula. We also showed the existence of functioning OSO in freshly-collected individuals making it highly unlikely that such structures developed purely as a consequence of collection, transport and culture stress. We hypothesize that such structures are formed opportunistically in response to environmental triggers as a mechanism for increasing food particle ingestion rates.

Based on results of our fluorescein dye/glass bead uptake experiment we concluded that it was highly improbable that more than a few of the glass beads deposited within the choanocyte chambers and inhalant canals imaged entered the sponge through normal-sized ostia, given the extremely low density of stray beads in the tank coupled with the short time period of the experiment, and the fact that only choanocyte chambers in-line with the osculum and OSO were imaged. Glass beads were also seen within phagosomes of choanocytes (Fig. 2d; **p**) indicating ingestion had occurred during the 20 minute experiment [supported by findings of Turon *et al.* (1996) who fed latex beads to *Dysidea avara*, and Leys and Eerkes-Medrano (2006) who fed latex beads to a syconoid calcareous sponge].

Although we cannot fully exclude that some of our quantifications of inflow and outflow might have been influenced by friction boundary layers (FBLs) generated in the flow-tank,



calculations showed that all velocity measurements were made well outside the calculated FBLs.

This work opens the door for more thorough follow-on studies designed to identify the exact triggers for OSO formation and test their quantitative effect on filtration rate in *Dysidea avara* – and possibly other sponges as well.

This paper was published as:

Mendola, D., J. G. M. van den Boogaart, J. L. van Leeuwen, and R. H. Wijffels. 2007. Re-plumbing in a Mediterranean sponge. *Biol. Lett.* 3(6): 595-598.

Note: the following supplementary materials were placed on-line to support the electronic version of this paper which was published online on 16 August, 2007, as: Mendola, D., J. G. M. van den Boogaart, J. L. van Leeuwen, and R. H. Wijffels. Re-plumbing in a Mediterranean sponge. *Biol. Lett.* doi: 10.1098/rsbl.2007.0357.

Electronic Supplementary Materials (ESM – online only)

M-1. Movie (.mov) sequence of glass flow-tracer beads entering over-sized ostia of specimen DA-7 [from Figure 1(a)]

ESM Fig. 2c, enlargement (.jpg). Enlargement of cluster of glass beads seen in Fig 2c

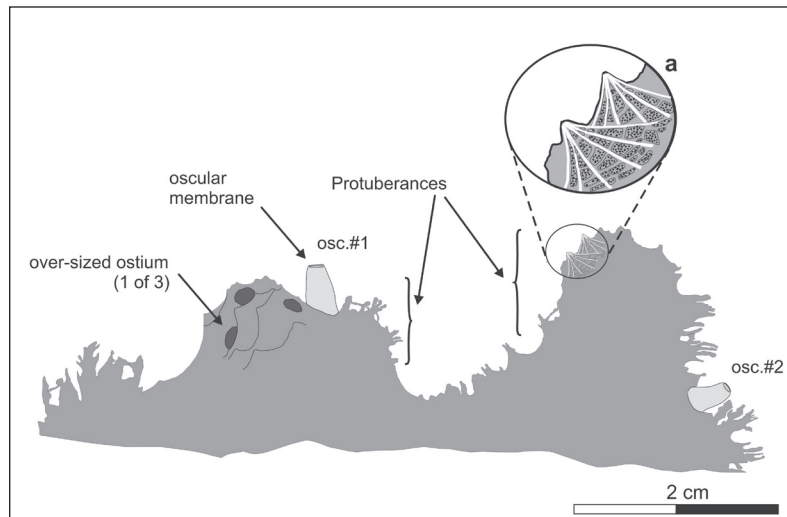


Figure 3. Scaled cartoon depicting the profile of sponge DA-7 (traced from photograph) showing the positions of its two oscula and three over-sized ostia on its two major protuberances. Enlarged detail shows two typical conules with radiating dermal reticulations and clusters of normal-sized (30 µm dia.) ostia.





METHODS ADDENDUM

Flow-tank and filming set-up

The Perspex plastic flow-tank has a total internal volume of approximately 7.5 L (Fig. 4). The rectangular working section measures 18 cm (length) x 12 cm (width) x 6 cm (height). Flow velocity, direction and directional periodicity can be varied through a DC-motor driven paddle wheel and controller. The upper flow limit (for maintaining laminarity within in the working section) is about 15 cm/s, however higher, non-laminar flows can be attained. Flow is straightened using two stacks of thin-walled polypropylene straws placed on either side of the working section (straw inner diameter is 5.7 mm). At background velocities used in the reported experiments, a sponge of 3 cm high and 3 cm deep is well inside the friction boundary layers generated at the side walls of the working section.

Flow calculations

To calculate velocity vectors, individual particles were tracked manually using a custom software routine written in Matlab®. Standard PIV and PTV software could not be used for accurate velocity measurements close to the sponges because of light reflected and dispersed

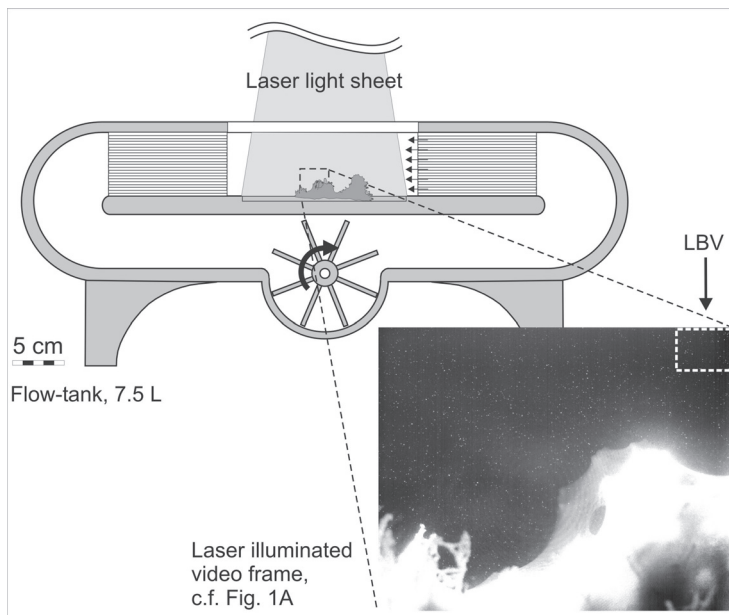


Figure 4. Scale drawing of a side elevation of the recirculating flow-tank used in the reported experiments. Sponge DA7 is depicted in profile sitting in the working section of the tank, between the two bundles of flow-straightening straws. Flow in this cartoon is uni-directional generated by the motor-driven paddlewheel. The laser light sheet is depicted illuminating a section of the sponge which bears the over-sized inlet structures (same video frame as in Fig. 1A, see also M-1). LBV is the area in the movie frame where “local background velocity” was determined.





by the sponge, which introduced errors. The custom designed software allowed for zooming and contrast enhancement for each individual movie frame. This made it possible to follow a selected particle no matter how much (or how little) light it reflected. The software calculated the centre of area of an indicated particle to the sub-pixel level, thus eliminating user inaccuracy in cursor placement. Velocity is calculated by the covered distance of a particle over two subsequent film frames.

Primary Assumption (see Figure 5)

Based on fluid mechanical principals governing low Reynolds number flow in pipes, we have assumed a perfect paraboloid-shaped velocity profile of the jet exiting the osculum. The paraboloid outflow shape is derived when we take into consideration friction generated at the walls of the cylindrical [pipe] of the osculum, which slows the outflow at the walls, ultimately leading to the paraboloid shape at the exit. For an over-sized inlet structure we assumed a cylindrical velocity profile at the entrance of the opening.

Oscular outflow rates

To calculate oscular outflow rates, velocity vectors of individual glass beads seen being ejected out of an osculum were determined at points just above the lip of the osculum. Given that *D. avara* oscular membranes are very smooth and flexible they always took a tubular shape with a circular opening when the sponge was pumping. Re-stating our primary assumption, the instantaneous outflow velocity profile was assumed to resemble a paraboloid with a circular base. A series of circular paraboloids were fitted through the oscular opening (points 1 and 3, Fig. 4) and a point (e.g., point 2) on the oscular span indicating the position of the vector of a traced particle (i.e., its velocity). Because particle paths deflect due to background flow, only the velocity component perpendicular to the oscular opening was considered (generally > 90% of the true vector). The maximum of the series of paraboloids was used to calculate the flow rate as the integral of the outflow velocities over the outlet surface.

Over-sized ostia inflow rates

In contrast with the outflow rate calculations, a cylinder (instead of a paraboloid) was fitted to the ostial opening for calculating inflow

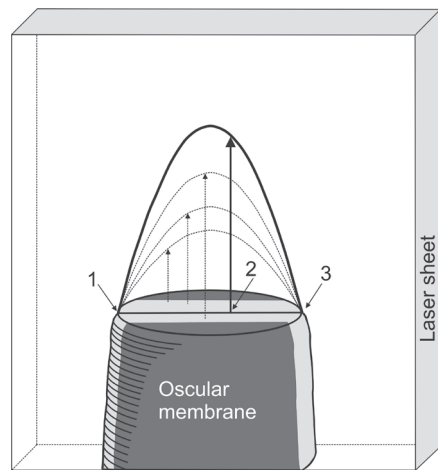


Figure 5. Cartoon depicting *Dysidea avara* oscular membrane and family of paraboloid shapes and velocity vectors (e.g., 2) used for deriving volume outflow from oscula. Note: illuminated area crossing the osculum diameter (1,3) produced by the laser light sheet.



rates. The height of the cylinder was calculated as the spatial average velocity of all particles entering the over-sized ostium in 0.25 s (100 movie frames). Subsequently, the inflow rate was calculated as the average inflow velocity times the ostial inlet surface. Local background velocity (LBV) was calculated from the spatial average velocity in an up-stream corner in the field of view as indicated in Fig. 3.

Error analysis

Three types of errors influenced the calculations: The first was caused by the accuracy of indicating the diameter of an osculum and/or an over-sized ostium. These errors were empirically determined to be maximally $\pm 7.5\%$ for oscular diameters, and $\pm 1.0\%$ for over-sized ostia diameters. The smaller estimated error for the over-sized ostia was possible because these structures generally showed sharper edges than did oscula.

The second type of error occurs when we assume the shape of over-sized ostium to be a perfect circle, whereas it may be somewhat elliptical in shape. We estimate this type of error to be maximally $\pm 12.5\%$.

The third type of error is caused by the software, when the centre of area of an indicated particle is calculated (after the threshold level is manually set). If the threshold level is set at a slightly different value, the computer may calculate another centre of area for the same particle on the same frame. This type of error was empirically determined to be maximally $\pm 0.5\%$.





specimen no. & profile (not drawn to scale)	sponge volume (cm ³)	no. of oscula	no. of over- sized ostia	no. of exp.		range of observed inflow rates (mm ³ /s)	range of observed outflow rates (mm ³ /s)	no. of dye / bead experiments
				inflow	outflow			
DA-2 	30	4	>5	0	4	-	0 ^{*5} -66.9	0
DA-4 	15	3	>10	0	15	-	13.0-50.1	0
DA-7 	20/15 ^{*1}	2 / 1 ^{*2}	3 / 3 ^{*3}	46	71	6.3-26.9	0 ^{*5} -108.4	1
DA-R 	80	>3	>3	3	3	0 ^{*4} -5.7	8.5-10.3	0

Table 1. Specimen numbers and profiles with relevant anatomical facts; plus listings of experiments performed and ranges of calculated inflow and outflow rates.





Notes, 1, 2, 3 – During the first series of experiments (Sept., 2006) Sponge DA-7 had a volume of 20 cm³. Three months later (Dec. 2006) DA-7 had reduced its volume to 15 cm³ by resorbing most of one of its two protuberances (the one that did not possess the 3 over-sized ostia), and closing the osculum on that protuberance. It also repositioned the three over-sized ostia on its major protuberance.

Note 4 – For sponge DA-R two different over-sized ostia were filmed; one of the two did not show inflow.

Note 5 – All four sponges were subjects of experiments conducted with varying ranges of background (LBV) velocities. For DA-2, DA-4 and DA-7 background flow velocities ranged between 0 and 120 mm/s. DA-R backgrounds ranged between 0 and 35 mm/s. At relatively high background velocities (*i.e.*, beginning at approx. 75 mm/s) DA-2 and DA-7 stopped pumping (e.g., oscular outflow rate = 0 mm³/s). DA-4 did not stop pumping, even when background velocity was raised to 120 mm/s (the highest level tested in these experiments).

ACKNOWLEDGEMENTS

We acknowledge support from EU project 017800, and Ulrike Müller, Ph.D. and Henk Schipper (both of WU/EZO) for help with the manuscript and SEM respectively.

REFERENCES CITED

- Bergquist, P. R. 1978. *Sponges*, Hutchinson, London.
- Cerrano, C., G. Magnino, A. Sará, G. Bavestrello, and E. Gaino. 2001. Necrosis in a population of *Petrosia ficiformis* (Porifera, Demospongiae) in relation with environmental stress. *Ital. J. Zool.* **68**(2): 131-136.
- Fell, P. E., P. Knight, and W. Rieders. 1989. Low-salinity tolerance of and salinity-induced dormancy in the estuarine sponge *Microciona prolifera* (Ellis et Solander) under long-term laboratory culture. *J. Exp. Mar. Biol. Ecol.* **133**: 195-211.
- Johnston, I. S., and W. H. Hildemann. 1982. Cellular organization in the marine demosponge *Callyspongia diffusa*. *Mar. Biol.* **67**: 1-7.
- Leys, S. P., and D. I. Eerkes-Medrano. 2006. Feeding in a calcareous sponge: particle uptake by pseudopodia. *Biol. Bull.* **211**: 157-171.
- Simpson, T. L. 1984. *The Cell Biology of Sponges*. Springer, New York. Pgs. 517-526.
- Teragawa, C. K. 1985. Mechanical function and regulation of the skeletal network in *Dysidea*. In: New Perspectives in Sponge Biology. K. Rützler (ed). Third Internat. Conf. on Biol. of Sponges. Woods Hole, MA, Smithsonian Institution Press, Washington, D.C.
- Turon, X, J. Galera, and M. J. Uriz. 1997. Clearance rates and aquiferous systems in two sponges with contrasting life-history strategies. *J. Exp. Zool.* **278**: 22-36.
- Uriz, M. J., D. Rosell, and D. Martin. 1992. The sponge population of the Cabrera archipelago (Balearic Islands): Characteristics, distribution and abundance of the most representative species. *PSZN I: Mar. Ecol.* **113**: 101-117.
- Van de Vyver, G., and P. H. Willenz. 1975. An experimental study of the life-cycle of the fresh-water sponge *Ephydatia fluviatilis* in its natural surroundings. Wilhelm Roux's *Archives of Develop. Biol.* **177**: 41-52.





Chapter 7

General Discussion and Conclusions



INTRODUCTION

Aquaculture of marine sponges for their natural product chemical constituents was first proposed in the mid 1980s. In the early 1990s, the New Zealand National Institute of Water and Atmospheric Research (NIWA) in collaboration with the University of Canterbury and the National Cancer Institute, USA, began the first in-sea aquaculture trials with a deep-water *Lissodendoryx* species they affectionately named “Yellow Slimy.” This sponge was one of two sponges known at that time to contain trace amounts (0.3 mg/kg) of the antitumor compound halichondrin B (Hart *et al.* 2000). The initial in-sea culture trials were successful with some trials producing remarkably fast growth (Munro *et al.* 1999). However, scale-up projections showed a daunting 1,000-5,000 tonnes of sponge per annum would be required to support future commercial drug sales. Even for a relatively fast growing sponge such an undertaking would be an immense in-sea effort, costing undoubtedly millions of dollars to set-up and millions per year to operate. Could such an effort be cost effective? Paramount to answering that question would be to know the projected future selling price of the drug. But final drug prices cannot be reliably estimated until very late in human clinical trials. The risk of spending millions of dollars on aquaculture ahead of a confirmed need was not justified, and consequently the natural product did not advance to human clinical trials. In the interim a complex synthetic analogue, E7389 (a novel tubulin inhibitor) was developed (Choi *et al.* 2003), which is currently in Phase II/III human trials for advanced breast cancer by the Japanese pharmaceutical company Eisai. It is expected that a new drug application (NDA) will be filed with the FDA (USA) for treatment of breast cancer in the first qtr. 2008 (D. Newman, pers. comm.).

Key to the decision to invest large sums in sponge aquaculture is knowledge of competing technologies that could supplant aquaculture before the investment is recouped. If the sponge is known to contain the desired compound in high yield, then sponge aquaculture could be a sustainable source of supply. However, if biosynthetic evidence exists that points to a possible microbial (symbiont) source, or a shared sponge-symbiont biosynthesis, then there is a chance aquaculture could be rendered obsolete in the future by development of an economical microbial fermentation (Garson, 1994; Faulkner *et al.* 1999; Taylor *et al.* 2007). In the case of halichondrin B, other congeners were discovered in diverse phylogenetic groups of sponges from distant areas of the world ocean, implicating a common symbiont source. However a microbial source has yet to be discovered and completion of the synthesis of the analogue has reduced the impetus to continue the search.

Today, marine biotechnology has progressed to a level of technological sophistication where culture of a chemistry-producing putative sponge symbiont apart from the host is a goal that most marine biotechnologists believe will be reached soon, at least for some cases (Hill *et al.* 2005). Also under development is sponge cell culture, which shows great



promise for facile and cost effective production of sponge-derived natural products in the future (Rinkevich, 2005). Both of these advancing technologies are strong competition for sponge natural product aquaculture (Wijffels, 2007).

So what role, if any, does aquaculture of sponges play in the rapidly advancing field of marine biotechnology? For some sponge products the chemical yield is high enough that aquaculture of the source organism could be cost effective. Most notably in this category is avarol from *Dysidea avara*, with a yield up to 3 g/kg fresh weight sponge (10,000 times the yield of the aforementioned halichondrin B). Currently there is no cost effective competing technology for production of avarol, and therefore aquaculture of *Dysidea avara* sponges, either “*in situ*” (in the sea) or “*ex situ*” (in tanks) could be a sustainable alternative to wild collections. Sipkema *et al.* (2005) analyzed the technical and economic feasibility for eight competing methods for producing avarol. Aquaculture was deemed the most feasible and cost-effective methodology, yielding a projected 14.4 €/patient-need per year cost for treatment of psoriasis. During the past five years, some limited in-sea aquaculture trials of *Dysidea avara* have been conducted both in the Greek Isles and in Turkey (R. Osinga, pers. comm.), but to-date no systematic study of the culture requirements for the sponge have been performed.

Sponges are very sensitive to pollutants in the water column, and in recent years the traditional Mediterranean bath sponge beds have suffered from the effects of increased levels of pollutants, and the secondary effects of disease. With coastal areas suitable for sponge aquaculture becoming increasing polluted, and/or deemed off-limits to aquaculture due to competing uses (and with world weather and sea conditions becoming increasing problematic) controlled environment culture of sponges in tanks has been proposed as an alternative to in-sea aquaculture (Mendola *et al.* 2006). Some “*ex situ*” culture trials in controlled environment tanks and bioreactors with have been performed by our group with *D. avara* (Sipkema *et al.* 2006) but growth to-date has been anything but progressive.

Water flow is literally the “life source” for sponges; it brings their food and dissolved oxygen and carries away their metabolic wastes. So understanding the basic water flow requirements for a sponge is first order for establishing a reliable culture protocol. This need led to the thesis project presented in the foregoing chapters, and its results and findings will undoubtedly be taken into consideration by current and future *Dysidea avara* sponge “Pharmers.” It remains to be seen if sponge aquaculture for natural products will become an economic enterprise, or remain only a concept supplanted by more cost effective biotechnologies.

FUTURE DIRECTIONS FOR SPONGE FLOW RESEARCH

Many interesting and possibly important questions were generated during the course of the investigations for this thesis that could not be addressed for various reasons. Either such questions were outside the scope of the planned research, they would have required



fabrication of new equipment, or simply they would require additional time not available within the time-frame of this thesis project. Some of these questions and possibilities for future sponge flow research are outlined below.

Morphology and flow

The field research (Chapter 3) identified three morphotypes of *Dysidea avara* that predominated at three depths and flow ranges within a study site on the N. E. Spanish coast. Future research could look further into the morphotype question using a well-designed morphological index to compare differences between sponges from differing flow regimes and habitats. Transplant experiments could be designed that move sponges from one flow regime to another and document (with stereo photography) any morphological changes. Sponges could be brought into the laboratory and subjected to various controlled flow regimes and monitored for morphological changes under close observation.

A morphology vs. flow experiment was conceived but not undertaken, which was keyed to a known behavior of *Dysidea* sponges of transporting grains of sand, shell debris, and discarded sponge spicules into their major skeletal fibers as means of stiffening their spongin-only fibrous skeletons (Teragawa, 1986). The hypothesis suggested that sponges in higher flow environments would incorporate more skeletal stiffening grains than those in lower-flow environments. The experimental design would involve nothing more than collecting a statistically valid number of sufficiently-sized explants from large (older) sponges from high, medium and low flow environments, followed by a careful digestion of the organic materials and careful weighing of the remaining inorganic fractions to see if the high-flow group had significantly higher amounts of inorganic “ballast.”

Oscular outflow in-the-sea

With the multi-oscule *Dysidea avara* and one thermistor probe, measuring all or even a majority of all oscula on any one sponge specimen simultaneously (or even near-simultaneously) was not possible. Consequently, we never measured more than 40% of the oscula present on any one sponge at one time due to always limited dive time. We saw distinct differences between outflow speeds and percentage of oscula pumping at any one time. With a six, or eight-channel (or more) long-term recording thermistor flow sensor such a task would be more easily accomplished and hopefully yield a more realistic measure of the total outflow from an individual sponge at one time. With an extended battery pack the instrument could be left *in situ* for extended periods to gain an understanding of the outflow magnitude and periodicity over time.

Flow tank studies

To save costs, the flow tank used in this research (Chapters 4, 5, and 6 was designed and built for relatively small *Dysidea avara* specimens (up to about 150 cc volume), therefore it was



a relatively small unit (7.5 L cap.). It produced laminar flow within its working section only up to approximately 13 cm/s. If a larger flow tank could be afforded and built larger-sized sponges could be accommodated and higher flow speeds could be attained. This would allow a better understanding of the relationship of sponge size to oscular outflow rates and a wider variety of flow treatments to be applied.

The tank also was fabricated with input-output ports, with the concept in-mind to recirculate the water through a multi-stage biofilter. It was envisioned that a particular specimen would be held for days to weeks to study various aspects of morphological response (such as general remodeling and conule height changes) to various programmed changes in flow regime. Such experiments were never set-up due to time constraints, but remain an interesting possibility for future studies.

Computational fluid dynamic modeling studies

The flow-tank studies reported in Chapter 4 revealed many interesting effects of larger-scale sponge morphology on local flow-fields surrounding sponges. We speculated as to what effects could be attributed to the mm-sized conules which cover the entire surface of all species of the genus *Dysidea*. From our *in situ* work we knew that the sponges from the lower-flow, deeper station possessed taller processes and more “spiky” conules than did the sponges from the higher-flow, near surface station, so we speculated that the taller conules presented some functional advantage for the deeper-dwelling sponges.

Given that the PTV methods could not resolve flow effects close to the sponges (due to light scattering and low particle abundance), it was suggested that computational flow dynamic methods could be employed to study possible effects of the mm-sized conules. We initiated some exploratory work, developed some computational grids, and ran a series of preliminary simulations in Fluent™ to investigate flow around patterns of conules of two sizes (0.4 mm and 0.8 mm).

Biometric measurements

We made conule height and inter-conule spacing measurements from photographs of *Dysidea avara* sponges in the wild, and calculated velocities for a Reynolds number $Re = 40$, given that below this Re we would not expect turbulence to be formed at the level of the conules. Table 1 shows the results of these measurements and calculations. The derived velocities were well above what we would expect for the normal flow range in nature, so turbulence production close to the sponge surface was ruled-out as a possible function of the mm-sized conules.

Summary methods – computational fluid dynamic modeling studies

The CFD modeling space was designed as a 3-D rectangular “tank” measuring 16 mm x 10 mm x 4 mm (length x width x height). A field of 13 conules was mathematically constructed onto



Sponge	Average distance between conules (mm)	Velocity (cm/s) at Re = 40	Average height of conules (mm \pm STD)	Velocity (cm/s) at Re = 40
C – site/ruler	5.60 \pm 1.26	0.75	1.61 \pm 0.47	2.65
DSC-1237	3.69 \pm 1.03	1.15	0.85 \pm 0.41	4.95
DAL – Spain lab	3.68 \pm 1.35	1.15	0.69 \pm 0.38	6.05
C – site summer '06	3.04 \pm 0.83	1.40	0.97 \pm 0.34	4.35
B – site #3	2.91 \pm 0.94	1.45	0.51 \pm 0.22	8.40
DSC-347	2.70 \pm 0.93	1.60	0.56 \pm 0.27	7.55
DSC-338	2.50 \pm 0.88	1.70	0.42 \pm 0.21	10.15
B – site #4	1.81 \pm 0.60	2.35	0.30 \pm 0.13	14.25
DSC-332	1.57 \pm 0.54	2.70	0.94 \pm 0.36	8.40

Table 1. Biometric measurements of conule spacing and conule heights for *Dysidea avara* sponges, and calculations of velocities at which Reynolds number (Re) equals 40 for each of the two biometric measures: inter-conule spacing and conule height.

a 7.854 mm x 7.854 mm section on the flat bottom of the tank. Inflow into the computational space was modeled as a parabolic boundary layer with a no-slip condition prescribed on the tank bottom (including the conulated surface) and no-shear conditions for the lateral walls and the top. We specified a uniformly-distributed porosity of 30% for the simulated dermal membrane and internal sponge tissue (porosity was estimated from observations and photographs of *Dysidea avara* specimens taken *in situ*, and from the literature for other demosponges).

A smaller computational box (the sponge pumping space) was mathematically attached beneath the main fluid grid-box. The pumping space was divided horizontally into two sub-spaces, each with a vertical thickness of 1 mm. At the boundary between the two sub-spaces a pressure jump Δp of $(24 - c v)$ Pa (Larsen and Riisgård, 1994) simulated the parallel pumping action of the sponge choanocyte chambers, where c is a constant ($c = 6,000 \text{ kgs}^{-1}\text{m}^{-2}$) and v is the physical flow speed through the pumping surface. At the bottom margin of the lower sub-space a uniform pressure of 5 Pa was defined. Pressure losses and intra-canal water velocities within the aquiferous system were in agreement with data from literature (Riisgård *et al.* 1993). The pressure differential over the entire pumping surface ranged from 12 - 15 Pa at resultant flow velocities in the porous medium of 2 mm/s and 0.3 mm/s, respectively.

In the computation of the external flow, we numerically approximated the Navier-Stokes equations for incompressible fluid flow. In the porous medium the Darcy equation was used (thus convective acceleration and diffusion were ignored). The pressure drop through the porous medium was assumed to be proportional to fluid velocity, and accordingly, Fluent[™] computed the pressure field in 3-D.



Preliminary results – CFD simulations for modeled sponge conules

The conule simulations (Fig. 1) produced high pressures on the flow-facing flanks of the modeled conules, and reduced (negative) pressures on the leeward flanks, with amplitudes depending on free-stream velocity and conule size. For the simulation series free-stream velocities of differing magnitudes (1-100 cm/s) were prescribed at the top of the modeled tank. The results consistently produced laminar flow at the level of the conules for every free-stream velocity tested. These results were supported by our Re calculations for live sponges *in situ* (Table 1) which produced velocities in the range of 26-100 mm/s for conules from sponges in the sea that were within the size range of the modeled conules. Again, these resultant velocities were below the level where turbulence would be expected.

Influx simulations

Preliminary influx results (Fig. 2) compared influx *i.e.*, water moving through the ostial pores of the modeled sponge, for a flat sponge model (without conules) to a similar model with either 0.4 mm or 0.8 mm conules. Also modeled were the effects of increasing the surface area of the sponge pump for both conule heights (Fig. 2; “increased pump”) and increasing the volume of the computational tank (Fig. 2; 1.4x “wide tank”). These variations were simulated as a means of testing the model for sensitivity to these two parameters.

The results showed that the influx was maximized at a background velocity of 16 cm/s (for a conule height of 0.4 mm) and 17 cm/s (for a conule height of 0.8 mm; see “flat pump” curves), while it diminished at lower and higher background velocities. Overall the 0.8 mm

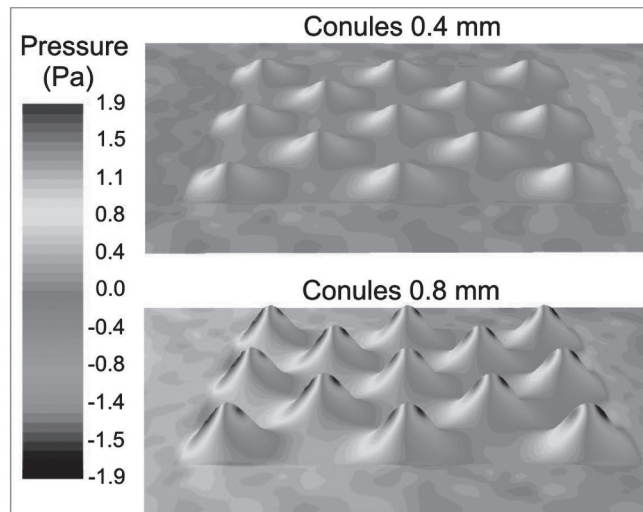


Figure 1. 3-D pressure landscapes of 13 conules of two sizes, each arranged onto simulated 7.854 mm x 7.854 mm pieces of a 30%-perforated, flat sponge dermal membrane. The model was designed to mimic similar portions of live *Dysidea avara* dermal membrane surfaces, which are not (in general) as flat as the simulated dermal surfaces.



conules were shown to be more advantageous for improving influx than the 0.4 mm conules (about 2% improvement at the peak performance). When compared to the flat sponge with no conules, the 0.4 mm conules produced a 2% improvement in influx rate, and the 0.8 mm conules produced a 4% increase. Both improvements are considered biologically significant, given that sponges are known to pump on a high duty cycle per day, and many days, or even weeks and months in succession (depending on species and environment), except when the effects of storms reach their habitats when they sometimes shut-down to protect from having their ostia plugged with sediment.

The causal factors for the improvements in influx rate due to the conules are related to the relative pressure distributions around the conules as seen in Fig. 1. At lower velocities, influx is increased via dynamic pressure on the upstream flanks of the conules, while on the leeward flanks under lower pressure some smaller amount of influx occurs. At higher velocities, influx increases on the upstream flanks, but decreases on the leeward flanks (due to lower pressures developed as water moves faster over the conules) to a point where flux direction is reversed to *efflux* on the leeward flanks lowering overall net influx into the sponge. The pressure effects for the taller conules were greater than for the shorter conules.

We speculated that sponges found in lower flow micro-habitats would benefit from having

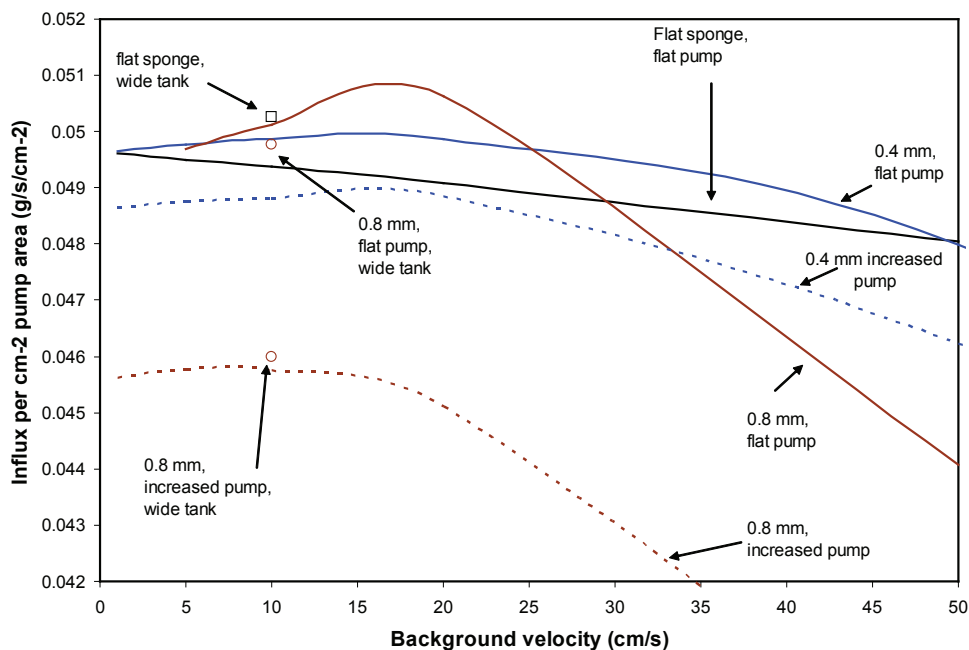


Figure 2. Results of influx models for a hypothetical flat sponge provided with 30% porosity of its total surface area (including conules). The flat sponge model is without conules. The increased pump model increases the pumping area in proportion to the increased surface area provided by the conules. The wider tank model uses a width of 14 mm, a 40 % increase compared to the standard tank model.





taller, more branched protuberances and taller conules. Such a more vertically-oriented “spiky” body plan with larger conules would increase local pressure differences around the sponge causing light-weight food particles to become trapped within the influence of sponge protuberances and thereafter settle-out of the water column. An oscillating flow regime would aid the process by increasing the number of “collision events” of particles and sponge parts, to enhance and compliment particle trapping by the sponge morphology.

These speculations were supported by our *in situ* observations of *Dysidea avara* body plans at a coastal site in Spain where an oscillating flow regime prevails. Sponges monitored at a 14.3 m depth low-flow station showed a consistently taller, more branched body form with taller conules than did specimens from a 4.5 m depth higher-flow station where the sponges were more globular in shape and with smaller conules. Close observation of sponges at the 14.3 m depth station revealed deposits of particulate organic matter trapped between and at the bases of the branches of the “spiky” finger-like protuberances, supporting our speculations.

Future possibilities for the CFD modeling studies

Future CFD modeling studies might include varying the computational tank set-up to simulate forced flow between protuberances with conules. In that type of simulation the form of the input flow stream would be changed from a parabolic boundary layer profile to parallel, plug-flow profile. Other simulations could include modeling parts of protuberances or groups of protuberances with conules of varying heights and inter-conule spacing. In place of the flat surface sponge model, a curved surface model better resembling the actual surfaces of live *Dysidea* sponges could be developed, with and without conules. The actual shape of the individual conules could also be improved in future studies to better resemble the shape of natural conules (*e.g.*, more “pointed” at the top, and with re-curved flanks).

It would also be interesting to attempt modeling flow through the sponge’s aquiferous system, especially to study flow past modeled choanocytes and flow through choanocyte chambers (for which we have excellent, scaled scanning electron micrographs). Such studies would help us to better understand the possible causal factors for the choanocyte pump “shut-down” phenomenon that occurs in this sponge at relatively low ambient background velocities.

GENERAL CONCLUSIONS

From the results of our field investigations we concluded that *Dysidea avara* sponges would best be cultured in a low-speed oscillating flow regime. From flow tank studies we concluded that the overall form of the sponge, *i.e.*, its morphology, including the forms of its surface protuberances and conules all contribute to increased mixing at the sponge surface. We speculated as to how morphology-induced mixing could help trap food particles by



increasing the collision events between particles and the sponge contributing to increased food particle influx. The sponge operates at a fairly constant pump pressure, except when ambient flow speeds approach the 7-13 cm/s range, when the sponge begins to shut down. The ambient speed range for shut-down determined in the flow tank studies varied from specimen-to-specimen depending upon size, condition and experiment-related factors. Shut-down behavior was also observed in the sea, when storms and high flow rates triggered the behavior. We speculated that shut-down is caused by either reduced efficiency of the flagellar pumping apparatus, or *en masse* shut-down of the pumps. Pump shut-down is followed immediately by the physical collapse of the thin, fragile membranes which surround each of its exhalant oscula, which prior to shut-down were held open and distended by the force of the exiting flow-stream.

We measured oscular outflow from 97 oscula on 21 sponges in calm seas and found 66% of oscula were strongly flowing. Following a stormy period that proportion reduced to only 24%. Oscula closure during storms for deep Caribbean reef sponges was linked to higher sediment loads in the water column causing clogging of sponge aquiferous systems (Reiswig, 1974); the same could be true for *D. avara*, although we made no sediment load measurements either before or after storms.

The average pumping rates derived for *Dysidea avara* (0.008 ml/ml sponge·s⁻¹ based on single oscula measurements) are generally lower than those reported in the literature for other sponges. This fact could be explainable on the basis of the positive correlation found between sponge size and outflow rate (also found for *Tethya crypta* sponges on a Caribbean reef by Reiswig, 1974). In this context, it could be speculated that since *Dysidea avara* is found primarily in low flow environments with generally high food particle diversity and abundance (Ribes *et al.* 1999) it requires less pumping to obtain sufficient food for meeting its metabolic requirements than a sponge found in a particle poor environment (such as a sponge resident on an oligotrophic tropical reef).

As stated in the introduction, the overall goal of this research was to be able to specify an optimal flow regime for culturing *Dysidea avara* sponges in tanks, and/or on racks in the sea. With the results obtained from the field and flow-tank work we can, with a high degree of confidence, prescribe suitable flow regimes for tank and/or in-sea cultures. For tank cultures we would prescribe an oscillating flow regime with a periodicity of 0.25 Hz and peak velocities of about ± 10 cm/s. For in-sea culture, flow-field mapping during different seasons of the year using a recording velocimeter should precede site selection. Preference should be given to diver-accessible, storm-protected sites in the 15-20 m depth horizon where yearly averaged flow speeds range from 5-10 cm/s at the level of the sponge culture racks.





PERSONAL COMMUNICATION CITED

David J. Newman, D. Phil., Chief, Natural Products Branch, Developmental Therapeutics Program, National Cancer Institute, USA.

REFERENCES CITED

- Choi, H. W., D. Demeke, F. A. Kang, Y. Kishi, K. Nakajima, P. Nowak, Z. K. Wan, and C. Y. Xie. 2003. Synthetic studies on the marine natural product halichondrins. *Pure Appl. Chem.* **75**:1-17.
- Faulkner, D. J., M. K. Harper, C. E. Solomon, and E. W. Schmidt. 1999. Localisation of bioactive metabolites in marine sponges. *Mem. Qld. Mus.* **44**: 167-173.
- Garson, M. J. 1994. The biosynthesis of sponge secondary metabolites: Why it is important. Van Soest, R. W. M., T. M. G. van Kempen, J-C Braekman (eds). *Sponges in Time and Space*. Proceedings of the 4th Internat. Porifera Congress, Amsterdam.
- Hart, J. B., R. E. Lill, S. J. H. Hickford, J. W. Blunt, and M. H. G. Munro. 2000. The Halichondrins: Chemistry, Biology, Supply and Delivery. In: Fusitani, N. (ed) *Drugs from the Sea*. Karger, Basel. Pp. 134-143.
- Hill, R. T., O. Peraud, M. T. Hamann, and N. Kasanah. Nov. 2005. Manzamine-producing actinomycetes. U. S. patent application 20050244938.
- Larsen, P. S., and H. U. Riisgård. 1994. The sponge pump. *J. theor. Biol.* **168**: 53-63.
- Mendola, D., S. A. Naranjo Lozano, A. R. Duckworth, and R. Osinga. 2006. The Promise of Aquaculture for Delivering Sustainable Supplies of New Drugs from the Sea: Examples from in-Sea and Tank-Based Invertebrate Culture Projects from Around the World. Proksch, P., W. E. G. Müller (eds). *Frontiers in Marine Biotechnology*. Horizon Bioscience, Wymondham.
- Munro, M. H. G., J. W. Blunt, E. J. Dumdei, A. J. H. Hickford, R. E. Lill, S. Li, C. N. Battershill, and A. R. Duckworth. 1999. The discovery and development of marine compounds with pharmaceutical potential. *J. Biotechnol.* **70**: 15-25.
- Reiswig, H. W. 1974. Water transport, respiration and energetics of three tropical marine sponges. *J. exp. mar. Biol. Ecol.* **14**: 231-249.
- Ribes, M., R. Coma, and J-M. Gili. 1999. Natural diet and grazing rate of the temperate sponge *Dysidea avara* (Demospongiae, Dendroceratida) throughout an annual cycle. *Mar. Ecol. Prog. Ser.* **176**: 179-190.
- Rinkevich, B. 2005. Marine invertebrate cell cultures: new millenium trends. *Mar. Biotechnol.* **7**: 429-439.
- Riisgård, H. U., S. Thomassen, H. Jakobsen, J. M. Weeks, and P. S. Larsen. 1993. Suspension feeding in marine sponges *Halichondria panicea* and *Haliclona urceolus*: effects of temperature on filtration rate and energy cost of pumping. *Mar. Ecol. Prog. Ser.* **96**: 177-188.
- Sipkema, D., N. A. M. Yosef, M. Adamczewski, R. Osinga, D. Mendola, J. Tramper, and R. H. Wijffels. 2006. Hypothesized kinetic models for describing growth of globular and encrusting demosponges. *Marine Biotechnol.* **8**: 40-51.
- Sipkema, D., R. Osinga, W. Schatton, D. Mendola, J. Tramper, and R. H. Wijffels. 2005. Large-scale production of pharmaceuticals by marine sponges: sea, cell or synthesis? *Biotechnol. Bioeng.* **90**: 201-222.
- Taylor, M. W., R. Radax, D. Steger, and M. Wagner. 2007. Sponge-associated microorganisms: evolution, ecology and biotechnological potential. *Micro. Molec. Biol. Rev.* **71**(2): 295-347.
- Teragawa, C. K. 1986. Particle transport and incorporation during skeleton formation in a keratose sponge: *Dysidea etheria*. *Biol. Bull.* **170**: 321-334.
- Wijffels, R. H. 2008. Potential of sponges and microalgae for marine biotechnology. *Trends Biotechnol.* **26**(1): 26-31.





| Summary

The principal aim of this research was to understand the optimal water flow requirements for the marine sponge *Dysidea avara*, so that flow parameters could be set for *ex situ* culture in tanks, or *in situ* culture in the sea. The ultimate goal was to help insure the success of large-scale aquaculture of this sponge for obtaining biomass for extraction of its valuable terpenoid natural product avarol.



Process development and economics of aquaculture for natural product chemicals

In Chapter 2, results from two successful in-sea aquaculture feasibility projects and one partially successful *ex situ* tank culture project were presented. The steps involved in full process development for each of the three examples (a bryozoan, an ascidian, and a sponge) and their attendant costs and economics were detailed. Results showed that in-sea aquaculture for the bryozoan and the ascidian for their anti-cancer natural products could be profitable at the projected market prices for the drugs. However, for the case history example presented for sponge culture in controlled environment tanks, the results were less positive or conclusive. Slow growth and low chemical yields, followed by the drug being dropped by the pharmaceutical company sponsor, left aquaculture of the source sponge redundant.

In-sea investigations of ambient flow regimes – Chapter 3

From the results of our field investigations on the N.E. coast of Spain, we learned that *Dysidea avara* inhabits primarily low flow habitats protected by rock cover or depth. Proximal flow speeds recorded within 2-4 cm of specimens at three depths were mostly oscillatory in form and averaged only 1.6 cm/s in calm seas, 5.9 cm/s during infrequent storms, and 2.6 cm/s over all seasons, depths and sea conditions.

Sponge morphologies at the three depths differed. Near-surface (4.5 m) forms were globular, without tall processes – but with large oscula. Mid-depth (8.8 m) sponges had tall, thick protuberances each topped with a large osculum. Deeper (14.3 m) forms had tall, thin, heavily-conulated “spiky” tree-shaped protuberances with narrow basal attachments and small oscula not placed at the upper tips of the protuberances. We speculated that the variation in morphotypes were responses to diminishing proximal flows with depth.

Flow tank studies of morphological effects on flow patterns close to sponges – Chapter 4

The field observations were applied to the design a recirculating flow tank, which was used together with particle tracking velocimetry (PTV) and laser-illuminated high speed photograph to reconstruct near instantaneous flow fields around live specimens. We sought to better understand how the morphology in this sponge interacts with flow passing close to its surfaces, to gain a better overall understanding of how flow in nature helps to sculpt the body forms we encountered in the field, and how body forms, in turn, effect food particle capture in this species.

Flow results showed induced mixing at the sponge surface due to the complex surface morphology, with a high degree of variation between experiments. Regions of increased vorticity and larger-scale vortices were formed, changing and moving from moment to moment over the sponge surfaces. We speculated on how morphology-induced mixing could



help trap food particles by increasing the collision events between particles and the sponge, contributing to increased food particle influx. We also discussed how the morphology in this species reflects the prevailing flow regimes recorded at each of the three depth stations in the field study.

Modeling work

Computational fluid dynamic simulations were initiated to model the effects of mm-scale conules on fine-scale flow over the sponge surface, and to study how varying the size, spacing and other aspects of the conules effected influx into the sponge. Preliminary results for two fields of 13 conules (0.4 and 0.8 mm tall) set on separate modeled pieces of flat sponge showed increased pressures on the leading flanks of the conules and reduced pressures on their leeward flanks increasing in magnitude with conule height. Influx simulations showed sensitivity to conule height, the total area over which the pumping pressure was applied, and degree of blocking in the computational “tank.” Future simulations are planned to test other conule spacing and heights, the combined effects of conule spacing and height, and the spacing between conulated sponge protuberances in various orientations.

Oscular outflow in-the-sea and in the flow tank – Chapter 5

The flow tank and PTV methods were also used to visualize and calculate outflow velocities and rates from individual sponge oscula in relation to varying background velocities. Oscular outflow velocities ranged from (12.7–130.4 mm/s) and volumetric flow rates from 0.004–0.013 ml/ml sponge/s (includes any inducted inter-cellular free water). Outflow velocities varied with changes in background flow speeds, but no synchrony or significant patterns were seen. Sponges were shown to first slow down then cease pumping activity altogether when background flows reached the surprisingly low range of 7.5–12 cm/s (depending on the individual tested and experiment). Shut-down occurred for other reason than elevated background flows, and sometimes sponges shut-down for no apparent reason. A similar shut-down response in the same background flow speed range was also seen in the field with wild sponges.

During storms when current speeds were elevated and when there was a significant amount of sediment in the water column, most oscula on most sponges were closed. In calm weather 66% of oscula were open and flowing strongly; 25% were moderately flowing, and 8% were not flowing at all. Measurements taken from 1–5 days following a storm showed only 24% of oscula were strongly flowing, 75% moderately flowing, and only 1% not flowing at all.

Both the 3-month laboratory-acclimated sponges and the freshly-collected specimens produced outflow velocities in the flow-tank that was within the range measured for sponges *in situ*. A wide range (1.1–17.7 cm/s) in oscular outflow velocities were recorded for wild sponges. One large specimen *in situ* produced an estimated daily outflow rate of 1,172 L/day.



Calculated average outflow rates averaged $0.008 \text{ ml (ml sponge)}^{-1}\text{s}^{-1}$, which was somewhat lower than that reported in the literature for other sponge species.

We also sought to detect if flow through the aquiferous systems of the flow-tank specimens was enhanced by induction from ambient flow (as had been demonstrated for other sponge species and other benthic invertebrates). Flow-tank results showed relatively “flat” outflow curves over time, and we did not detect any evidence of induced flow through this sponge.

Over-sized ostia – a new discovery for *Dysidea avara* – Chapter 6

The flow tank and PTV tools were also applied to investigate unusual dermal membrane openings termed “over-sized ostia” (OSO), which we observed in our laboratory-held sponges. As the sponges remodeled their body forms to adjust to the new tank environment (*a well documented process for sponges in general*) they converted some oscula (outlets) into functioning over-sized (*i.e.*, 1.5-2.5 mm dia.) inlets through internal re-plumbing of their inhalant-exhalant canals. With PTV we recorded tracer beads being taken into the OSO at high rates. Functioning OSO were also found on freshly-collected specimens brought into a flow-tank set-up in Spain, supporting the conclusion that development of OSO was not purely a response to specimens being held in tanks for extended periods. The full adaptive significance for *D. avara* forming and using the oversized inlets remains speculative pending future investigations. Based on our estimates of increased influx per unit sponge surface area, however, we theorized that the over-sized inlet structures allowed the sponge to exploit food resources at an increased rate.

General Discussion and Conclusions

In the General Discussion and Conclusions Chapter, the role of aquaculture for future production of sponge natural products is discussed in the context of competing technologies. Given that current evidence for avarol biosynthesis implicates the sponge as the true source and not a microbial symbiont, aquaculture of *Dysidea avara* to yield the natural product is projected as the only viable large-scale production technology for the near-term.

I discuss some interesting un-answered questions generated during the thesis project and possible future directions for sponge flow research. I also discuss and present the very interesting and insightful preliminary results obtained from computational flow dynamic modeling simulations of the effects of mm-sized surface “bumps” called conules, on flow over and influx into modeled ostial fields placed onto a simulated piece of sponge surface. I suggest future directions for continuing this very useful methodology to help us better elucidate the effects of specific morphology features on flow close to the sponge surface.

The General Conclusions recommend the most appropriate range and form for aquaculture flow regimes derived from the thesis results (*i.e.*, maximum magnitude 7-10 cm/s, in an oscillating flow cycle). Key results from the individual chapters are discussed, and an overall recommendation for locating an in-sea *Dysidea avara* “aquapharm” is given.



| Samenvatting

De belangrijkste doelstelling van dit onderzoek was het begrijpen van het effect van de uitwendige vloeistofstroomsnelheid op de voedselfilterfunctie van de mariene spons *Dysidea avara*. Deze kennis is van belang om de hydrodynamische condities te kunnen ontwerpen voor de kweek van sponzen in zowel *ex situ* kweektanks als voor het *in situ* kweken van deze sponzen in de zee. Het uiteindelijke doel was grootschalige aquacultuur van deze spons mogelijk te maken. Uit de geproduceerde sponsbiomassa kan avarol geëxtraheerd worden, een medicinaal waardevolle terpenoïde die door deze spons geproduceerd wordt.



Procesontwikkeling en economie van aquacultuur van bioactieve componenten uit mariene invertebraten

In Hoofdstuk 2 zijn de resultaten van haalbaarheidsstudies van aquacultuur voor productie van bioactieve componenten beschreven. Het betreffen een tweetal succesvolle projecten voor productie in zee en een project, met gedeeltelijk positief resultaat, voor de productie in *ex situ* tanks. De stappen die nodig zijn voor de ontwikkeling van het volledige proces worden voor deze 3 voorbeelden beschreven (een mosdiertje (Bryozoa), een zakpijp (Ascidiacea) en een spons (Porifera)). Tevens wordt een kostenberekening gegeven en wordt de economische haalbaarheid beschreven. Resultaten laten zien dat aquacultuur in de zee van zowel de bryozoa als de ascidia voor de productie van bioactieve stoffen met een activiteit tegen kanker een winstgevend proces kan opleveren met de aangenomen marktprijzen voor de te ontwikkelen medicijnen. Voor de productie van bioactieve stoffen met behulp van sponzen in *ex situ* kweeksystemen waren de resultaten minder positief. Ten gevolge van de trage groei van sponzen en de lage productopbrengst was de economische haalbaarheid onvoldoende en is dit proces destijds niet verder ontwikkeld.

Vloeistofstroomsnelheden rond sponzen in zee – Hoofdstuk 3

Onze veldexperimenten aan de noordoostelijke Spaanse kust lieten zien dat *Dysidea avara* met name voorkomt op plaatsen waar de stroomsnelheid laag is: op ondiepe plaatsen in de beschutting van kleine grotten in de rotsen of op grotere diepte. De snelheid van de oscillerende stroming, gemeten op enkele cm's afstand van de sponzen op 3 verschillende dieptes, was gemiddeld 1.6 cm/s bij rustige zee, 5.9 cm/s bij stormachtig weer en 2,6 cm/s over alle seizoenen, diepten en weersomstandigheden.

De morfologie van de sponzen was verschillend op elke diepte. Vlakbij het wateroppervlak (4.5 meter) was de spons globulair, zonder grote uitstekende delen, maar met grote oscula (de uitstroomopeningen). Op een diepte van 8.8 meter hadden de sponzen grote uitsteeksels met op de top van ieder uitsteeksel een groot osculum. Op een diepte van 14.3 meter hadden de sponzen lange dunne uitsteeksels. Het oppervlakte van de spons bevatte stekelachtige structuren. De oscula zijn klein en zijn niet gesitueerd op de top van de uitsteeksels.

Wij denken dat de verschillende morfologie van de sponzen gerelateerd is aan de stroomsnelheid van water. Hoe dieper de spons, hoe lager de vloeistofstroomsnelheid is waaraan de spons wordt blootgesteld.

Studies in stromingstanks naar de morfologische effecten op stromingspatronen dichtbij sponzen – Hoofdstuk 4

De waarnemingen die wij gedaan hebben in het veld werden toegepast voor het ontwerpen van een stromingstank met recirculatie. Deze stromingstank werd gebruikt in combinatie met particle tracking velocimetry (PTV) en middels laser belichting snelle beeld fotografie om



stromingssnelheden rond objecten te kunnen reconstrueren en te analyseren. Wij wilden de interactie tussen de morfologie van de spons en de stroming waaraan de spons blootgesteld werd beter begrijpen. De stroming vlak bij het oppervlak kon op die manier in beeld gebracht worden. Uiteindelijk zijn we geïnteresseerd in hoe de lichaamsvorm de spons helpt deeltjes uit het water beter op te nemen.

De resultaten lieten zien dat menging vlakbij het oppervlak in het algemeen geïnduceerd werd door de complexe morfologie van het oppervlak van de spons. Er was echter een enorme variatie in waarnemingen. Er waren regionen met een toename in vortciteit (een maat voor de locale rotatie) en de grote wervels die gevormd werden verplaatsten zich continu over het oppervlak van de spons. Wij speculeerden wat de rol van deze morfologisch geïnduceerde wervels in het vergemakkelijken van deeltjesopname van de spons zou kunnen zijn. Door de aanwezigheid van wervels zal het aantal botsingen tussen deeltjes en deeltjes en spons toenemen en op deze manier zal de deeltjesopnamesnelheid toenemen. Tevens zou de locatieafhankelijke morfologie van deze sponssoort de opname van deeltjes op de 3 verschillende dieptes op de plaats waar wij sponzen in de natuur bestudeerd hebben kunnen verbeteren.

Modelleren

Computational fluid dynamics berekeningen werden gestart om het effect van de mm-schaal conulen op lokale stroming over en door het sponsoppervlak te kunnen voorspellen. Met behulp van dergelijke modellen kunnen we onderzoeken wat het effect is op de instroomsnelheid van water met voedingsdeeltjes van bijvoorbeeld variaties in de grootte van de conulen en de afstand tussen de conulen. De eerste resultaten van deze berekeningen lieten zien voor een veld van 13 conulen (0.4 en 0.8 mm hoog) geplaatst op verschillende gemodelleerde stukken spons waarbij de spons voorgesteld werd als een plat oppervlak, dat de druk bij de flank van de conule die aangestroomd werd hoger was dan aan de benedenwindse zijde van de conule. Dit effect werd groter naarmate de conulen hoger waren. Berekening van de flux de spons in liet vervolgens zien dat ook hier de hoogte van de conulen een effect had. In de toekomst zullen wij het aantal simulaties uitbreiden en verschillende combinaties van hoogten van conules en de afstand tussen de conules doorrekenen. Tevens zullen we kijken naar het effect van de oriëntatie van de spons op de stromingsrichting van de omgeving.

Uitstroomsnelheid van de oscula in de natuur en in stromingstanks – Hoofdstuk 5

De stromingstank en PTV werden ook gebruikt om uitstroming via de oscula te visualiseren en daaruit uitstroomsnelheden te berekenen. Uitstroomsnelheden werden bepaald bij verschillende sponzen en bij verschillende omgevingsstroomsnelheden waaraan de sponzen blootgesteld werden. De uitstroomsnelheid uit de oscula varieerde van 0.004-0.013 ml (ml spons)⁻¹s⁻¹. De uitstroomsnelheid varieerde met veranderingen in de stroomsnelheid van



het water om de spons heen; er werd echter geen duidelijk verband waargenomen tussen de uitstroomsnelheid en de stroomsnelheid waaraan de sponzen blootgesteld werden. Bij toename van de stroomsnelheid rond sponzen leek er een afname van pompsnelheid te zijn en bleek het pompen zelfs volledig te stoppen bij reeds vrij lage omgevingsstroomsnelheden in de range van 7.5-12 cm/s (afhankelijk van het geteste individu). Een vergelijkbare afsluitrespons werd waargenomen bij vergelijkbare omgevingsstroomsnelheden bij sponzen in de natuur.

Gedurende stormachtig weer werd er een toename van omgevingsstroomsnelheid rond de sponzen waargenomen. Onder die omstandigheden wordt er eveneens vrij veel sediment in suspensie gebracht. Gedurende dergelijke omstandigheden sluiten sponzen een groot aantal van hun oscula. Onder rustige weersomstandigheden bleken 66% van de oscula geopend te zijn en sterk te pompen, 26% van de oscula pompten enigszins en 8% pompte niet. Slechts 24% van de oscula pompten goed 1-5 dagen na een storm, 75% pompte enigszins en 1% in het geheel niet.

De sponzen die gedurende 3 maanden geacclimatiseerd waren aan de omstandigheden in de tanks in het laboratorium en de vers geoogste sponzen hadden vergelijkbare uitstroomsnelheden. De variatie in uitstroomsnelheden in sponzen uit de natuur varieerde (1.1-17.7 cm/s). Een groot exemplaar had *in situ* een geschatte uitstroomsnelheid van 1,172 L/dag. De gemiddelde pompsnelheid in de sponzen was $0.008 \text{ ml (ml spons)}^{-1}\text{s}^{-1}$ (gerekend inclusief het inwendige vrije water in de spons). Dit is iets lager dan beschreven is in de literatuur voor andere spons soorten.

Voor andere soorten had men tevens waargenomen dat de pompsnelheid toenam bij toename van de stroomsnelheid in de omgeving. Wij konden dit niet waarnemen voor *Dysidea avara*; er is geen bewijs geleverd dat uitsroming uit de oscula geïnduceerd werd door de stroomsnelheid van het water om de spons.

Overgedimensioneerde ostia –een nieuwe ontdekking bij *Dysidea avara* – **Hoofdstuk 6**

De stromingstank en PTV werden ook gebruikt om opvallende openingen in het membraanoppervlak te bestuderen, welke we “Overgedimensioneerde Ostia” noemden (OSO). Deze openingen werden voor het eerst waargenomen in de sponzen die in aquaria in het laboratorium gehouden werden.. Sponzen die vanuit de natuur in de aquaria gebracht werden pasten hun lichaamsvorm aan aan de nieuw opgelegde omstandigheden in de tank. Dit is een proces dat op zich bekend is bij sponzen. De sponzen vormden een aantal van hun oscula (uitstroomopeningen) om in functionerende overgedimensioneerde (*i.e.*, 1.5-2.5 mm diameter) instroomopeningen. Tevens werd in de spons het kanalenstelsel op zo’n manier veranderd dat uitstroomkanalen veranderden in instroomkanalen. Met behulp van PTV konden wij glasbolletjes gebruikt als tracers volgen en aantonen dat die opgenomen werden



in de OSO's met hoge snelheid. Functionerende OSO's werden vervolgens ook gevonden in sponzen in de natuur. Na oogsten van deze exemplaren en experimenten in stromingstanks ter plaatste kon ook voor deze sponzen aangetoond worden dat de OSO's functioneerden als instroomopeningen. De ontwikkeling van OSO's is derhalve niet zozeer een fenomeen dat specifiek is voor sponzen die gehouden worden in tanks, maar komt blijkbaar ook in de natuur voor. Op dit moment kunnen we slechts speculeren over het belang van de vorming van OSO's voor *D. avara*. Gebaseerd op schattingen van een toename van de ingaande flux per hoeveelheid sponsoppervlak, denken wij dat OSO's sponzen in staat stellen sneller voedseldeeltjes op te nemen.

Algemene Discussie en Conclusies

In de algemene discussie en conclusie wordt de rol van aquacultuur voor de toekomstige productie van bioactieve stoffen uit sponzen besproken en vergeleken met alternatieve productietechnieken. Voor zover bekend vindt de biosynthese van avarol plaats in de spons en niet in een met de spons in symbiose levend microorganisme. Als gevolg hiervan wordt aquacultuur van *Dysidea avara* als enige realistische optie gezien voor de grootschalige productie van avarol op korte termijn.

Een aantal interessante niet beantwoorde vragen op het gebied van vloeistofstroming rond sponzen zijn naar voren gekomen tijdens dit onderzoek die interessant zijn om in de toekomst verder te onderzoeken. Mijn onderzoek heeft laten zien dat kleine (orde mm) stekelige objecten op het sponsoppervlak, "conulen", belangrijk zijn voor de hydrodynamica van de spons. Met behulp van Computational Flow Dynamics technieken laat ik zien dat deze conules de stroming over het sponsoppervlak en de opname van deeltjes door de spons beïnvloeden. Het zou interessant zijn meer gedetailleerd naar dit fenomeen te kijken om nog beter te begrijpen wat de functie is van specifieke morfologische eigenschappen voor de spons.

In de algemene conclusie wordt aanbevolen wat de meest geschikte vloeistofstroomsnelheid rond sponzen dient te zijn voor het kweken van sponzen (*i.e.* maximaal in de orde van 7-10 cm/s, in een oscillerende stromingscyclus). De belangrijkste resultaten van de individuele hoofdstukken worden besproken en een algemene aanbeveling voor het lokaliseren mariene kweken van *D. avara* in een "aquapharm" wordt gegeven.



Acknowledgements

I would like to thank all my colleagues, friends, and family who have helped me realize the completion of my Ph.D. studies. First, I would like to thank my wife Kristi and our daughter Mia for having the courage to stay back in California while I moved to The Netherlands to undertake the two year journey. Without your personal sacrifices, unwavering support and faith in me it would not have been possible for “...*Daddy to go back to school...*”

At Wageningen, I extend a most hearty *dank u wel* to Ronald Osinga, colleague and friend, for thinking of me for the EU CRAFT project; and to Prof. René Wijffels who worked hard to convince the university directorate that this “aging American” would be the best choice for the position. René, I owe you a tremendous debt of gratitude for taking me into your group and supporting me all the way through this thesis project. To my EZO colleagues, Prof. Johan van Leeuwen and Jos van den Boogaart, a special thanks for your forever cheerful, collegial attitudes, tireless tutoring, and consummate model of academic professionalism. Jos, I want to especially thank you for your amazingly selfless work in support of my thesis. To Iosune and Sonia, you both made an indelible impression upon me of the warmth, sincerity and gracious hospitality that is truly the essence of everything great about Spain, the Spanish people, and especially Catalans!

To the “*Merrie Band of PRE-Colleagues*” on the sixth floor of the Biotechnion, I thank each and everyone of you for the fun, collegial togetherness, encouraging support and friendships we forged during my time at Wageningen. I will especially miss “Wit’s Koffie Zit” times which really helped me to get through all those months away from home. To Fred van den End, I will miss your uplifting, joking-jovial Dutch ways, your great attitude, solid work ethic and your friendship. To Marcel and Dorien Janssen, I thank you both so much for your friendship and concern for my well being throughout my time in Wageningen. To Prof. Hans Tramper, I extend my most sincere thanks for your invaluable guidance and unwavering support. To Joyce, Hedy, and Nelleke, I thank each of you for all the times you helped me get through those little administrative wrinkles (in Dutch) that I did not understand.

To Marzia Sidri, “the *true* Italian...” on the sixth floor, I thank you for your loving friendship and encouragement. You, Jorge and all “*Los Wageningeros*” provided a latin-style family for me in Wageningen, that helped replace our large Italian family parties at home.

I also want to thank Jan Theunissen and his crew in the ontwikkelwerkplaats AFSG, especially Hans de R., Hans M. and André, for the professional workmanship you put into the beautiful one-off pieces of equipment used to generate the data for my thesis project.

To all I mentioned here, and to those that I did not specifically mention by name, I could not have done it without your collective friendship and support. I will be forever grateful for the wonderful experiences we shared together during my time in beautiful Wageningen.

Hartelijke Groet



Training and Supervision – VLAG Graduate School

Discipline Specific Courses

- Control of Cellular Processes and Cell Differentiation (MOB-30306, 2005)

Optionals / Meetings /Workshops

- EU Project No. 017800; Final Project Meeting (Oral Presentation): 3-6 Oct. 2007, Bremen, Germany.
- University of Stuttgart, Biologisches Institut/Zoologie (Invited Lecture): 19 June, 2007, Stuttgart, Germany.
- 8th International Marine Biotechnology Conference (Oral Presentation): 11-16 March, 2007, Eilat, Israel.
- Marine Bioprocessing Laboratory Techniques (Oral Presentation): Dec. 2006, Polish Univ. Food/Bioprocessing students and professors; practicum, WUR/PRE.
- Marine Bioprocessing Laboratory Techniques (Oral Presentation): Nov. 2006, Dutch high school teachers; practicum, WUR/PRE.
- EU Project No. 017800 Annual Progress Meeting (Oral Presentation): 2-4 Nov. 2006, Tallinn, Estonia.
- Flow Dynamics for Marine Sponges (Workshop - Oral Presentation): 10 Oct. 2006, Wageningen University, PRE & EZO groups and University of Amsterdam, Department of Computer Sciences.
- Wageningen University, Process Engineering Brainstorm Week: 12-15 Dec. 2005
- Wageningen University, Process Engineering Ph.D. Thesis Proposal – Oct. 2005
- EU Project No. 017800 kickoff meeting (Oral Presentation): 11-13 Nov. 2005, Mainz, Germany.
- Marine Biotechnology Basics and Applications Conference (Oral Presentation): 25 Feb-1 March, 2003. Wageningen University PRE, Univ. of Huelva, Spain, Dept. of Chemical and Process Engineering; Univ. of Sheffield, U.K. Dept. of Chemical and Process Engineering. Matalascanas, Spain.
- World Aquaculture Society Annual Meeting (Oral Presentation): 1-5 March, 2004, Honolulu, Hawaii, USA .
- President's U. S. Commission on Ocean Policy, Marine Biotechnology Panel (Oral Presentation): 18-19 April, 2002. San Pedro, California, USA.
- World Aquaculture Society Annual Meeting: 27-31 January, 2002, San Diego, California, USA.
- 4th Asia-Pacific Marine Biotechnology Conference (Oral Presentation): 23-26 April, 2001. Univ. of Hawaii, Honolulu, Hawaii, USA.
- New Directions in Marine Biotechnology (workshop): 14-16 Nov., 2001. *MarBEC* - Univ. Hawaii, and BioSTAR - Univ. Calif. Berkeley. Bodega Bay, California, USA.
- Marine Biotechnology in the Twenty-First Century: Problems, Promise, and Products (workshop): Nov. 5-6, 2001. Ocean Studies Board, National Research Council, Washington, D.C., USA.
- Marine Natural Products Gordon Research Conference (Oral Presentation): 27 Feb.-3 March, 2000, Ventura, California, USA.



Biography

Dominick Mendola was born on 23 March, 1943 in Carmel, California USA. He attended public grade schools in San Diego, California, then Point Loma High School, receiving his Diploma in 1960 with Academic Distinction. He attended San Diego State University, graduating in 1967 with a B.S. degree in zoology with emphasis in marine invertebrate biology. He entered the graduate school of Biology at SDSU in aquatic ecology, and was promoted to candidate for the M.S. degree in 1971. He first worked professionally for 4 years as an engineering aid, then 5 years as Development Engineer at the University of California San Diego, Scripps Institution of Oceanography, Marine Physical Laboratory. There, he conducted physical chemistry experiments, built oceanographic instrumentation, and went to sea each year as scientific crew on marine acoustical cruises. In 1973 he co-founded Solar Aquafarms, Inc., a pioneering company specializing in the design, engineering and implementation of greenhouse-covered, closed-circuit, ecologically-based fish and shrimp aquaculture, and wastewater reclamation systems. From 1981-1983 he worked as a fish and shrimp farm design/engineering consultant in Mexico and Central and South America. From 1983-1986 Mr. Mendola served as consultant then Vice President of Operations for a shrimp farming company located on the island of Molokai, Hawaii. From 1987-1988 he worked as a shrimp farming consultant for the USAID in El Salvador. From 1990-2004, Mr. Mendola co-founded, was President then CEO of CalBioMarine Technologies, Inc., which developed aquaculture-based systems for *in situ* and *ex situ* production of marine invertebrates for their bioactive natural products. Following CalBioMarine, Mr. Mendola worked as a consultant for a San Francisco, California medical biotechnology company to supply raw materials for their marine invertebrate-derive personalized immunotherapy against cancer. In Sept. 2005, he entered Wageningen University as a Senior Researcher in Bioprocess Engineering, where he conducted research on the importance of water flow for the culture of the avarol-producing Mediterranean demosponge, *Dysidea avara*, which led to the completion of the Ph.D. thesis research presented in this booklet. Mr. Mendola is married, the father of four wonderful daughters, and a grandfather to six individually-gifted grandchildren.

Cover Art

The front cover shows a magnified portion of a *Dysidea avara* sponge against an “outer space” field of light-reflecting micron-sized glass beads used for tracing flow in the flow-tank. The back cover images of the “Blue Planet” earth and the M1 galaxy (notice flow features) were obtained with permission from the NASA/USA website. Cover design and artwork by Jos G. M. van den Boogaart, WUR/EZO.